UNIVERSITY OF STRATHCLYDE

DEPARTMENT OF ELECTRONICS AND ELECTRICAL ENGINEERING

COMMUNICATION BASED LOSS-OF-MAINS PROTECTION METHOD BY FREQUENCY CORRELATION

AHMED ADNAN MAKKI

A thesis presented in fulfilment of
the requirements of the degree of
Master of Philosophy

June 2015

ACKNOWLEDGEMENTS

I wish to gratefully acknowledge the technical and financial support of the University of Strathclyde that allowed me to carry out this research. I would also like to express my appreciation to my supervisor Dr Adam Dyśko and Professor Graeme Burt for their professional advice and guidance throughout out this research. Finally, I would like to thank my parents for their great love, guidance and support. Without them I would not have been able to get this far, and they are the reason behind my patience and hard work. No matter what happens, I know that they are always standing by my side to share my happiness and accompany me with my every achievement.

DECLORATION OF AUTHOR'S RIGHT

This thesis is the result of the author's original research. It has been composed by the author and has not been previously submitted for examination which has led to the award of a degree.

Signed: _____ Date: _____

ABSTRACT

Due to the increasing penetration of distributed generation (DGs) in the distribution network in high numbers and proportions, and its conspicuous impact on power system stability. This occurs during a wide system disturbance in the power system, the DGs will start to disconnect from the main source in large proportions. This will further affect the power system stability and causes damages to its components and DGs. This thesis investigates in the reliability, security, and efficiency of satellite and internet communications, specifically for loss of mains (LOM) protection and exploring the strengths, the weaknesses, the feasibility of each type of communications, and the requirements of communication system components. By using communications network to send Phasor Measurement Unit (PMU) data to DGs protection equipment that are connected at remote areas all over UK, the LOM protection can be improved, obtain synchronization, precision, and coordination among power protection components. Satellite communication is chosen as it makes a better communication method when it comes to the installation, construction, urban disruption, time saving, and the installation and annual cost on every participant. However, the high latency issue is approached and solved by making a few changes in the communication protocol format and the data requirements to reduce the effect of latency to a level that can be tolerated.

This thesis presents the development of a novel LOM protection method based on communication and frequency correlation. The stability and sensitivity assessment will show that this method is highly secure and reliable. It can also withstand a communication delay of 120ms without causing any nuisance tripping, and have a relay response to LOM operation of a maximum of 1s. The thesis also presents a novel method in time delay estimation that has been developed for power system applications. This method is called the Linear Trajectory Path (LTP) and its performance fulfils the LOM synchronisation requirements by succeeding in determining the time delay between the two data streams within the tolerated estimation error of $\pm$100ms.

ABBREVIATIONS

A/D Analogue to Digital converter

AR Auto Re-closer

ARQ Automatic Repeat Request

AVR Automatic Voltage Regulator

BER Bit Error Rate

BW Bandwidth

CB Circuit Breaker

CEM Convergence Evaluation Method

CFC Communication Based LOM Protection Method by Frequency Correlation

CLD Communication Loss Detection Method

D/A Digital to Analogue converter

DEE Delay Estimation Error

DFT Discrete Fourier Transform

DG Distributed Generation

FEC Forward Error Correction

FFT Fast Fourier Transform

F_l Local Power Frequency

F_r Remote Power Frequency

GPS Global Position System

IP Internet Protocol

LDPC Low Density Parity Check

LOM Loss of Mains

LS	Load Switching
LTP	Linear Trajectory Path Time Delay Estimation Method
MEW	Measurement Estimation Window
NDZ	Non Detection Zone
OF	Over-Frequency
OV	Over-Voltage
PAD	Accumulated Phase Angle Drift
PCC	Point of Common Coupling
PMU	Phasor Measurement Unit
QEF	Queasy Error Free
ROCOF	Rate of Change of Frequency Method
S/N	Signal to Noise ratio
TCP	Transmission Communication Protocol
TDE	Time Delay Estimation
UDP	User Data Protocol
UF	Under-Frequency
UTC	Universal Time Coordination
UV	Under-Voltage
VEA	Variance Elimination Assessment
VPAD	Voltage Accumulated Phase Angle Drift
VPN	Virtual Private Network
VSAT	Very Small Aperture Terminal

TABLE OF CONTENTS

TABLE OF TABLES

TABLES OF FIGURES

CHAPTER 1: INTODUCTION

1.1 Power System Protection

Power system protection is the process of making the production, transmission, and consumption of electrical energy as safe as possible from the effects of failures and events that place the power system and human lives at risk. It is cost prohibitive to make power systems completely reliable and safe. Protective relays are designed to protect power system network power generation, load, monitoring and protection equipment and limit injury caused by electrical failures. The faster a faulted system element can be detected, isolated, and de-energized, the lower the probability that anyone will encounter hazardous voltages. The challenge for protective relays is to extract information from the voltage and current instrumentation that indicates whether the equipment is operating correctly or not. Although different faults require different fault detection algorithms, the instrumentation remains the same, namely voltages and currents. Properly operating relay systems isolate only the portions on the network directly involved with the fault. If relays operate too quickly or fail to operate, the fault-affected area expands and some circuits are de-energized. Parts of the power system can become isolated from the rest of the network. A large mismatch between generation and load can put an islanded network in risk of getting damaged because of losing the generation control that holds frequency and voltage within acceptable limits. Without generation control, the isolated systems will eventually be tripped off by other relays. Widespread outages caused by cascading voltage or frequency excursions require many work hours to restore power, which is costly from both a labour, time and a loss of revenue. Good relay selectivity is a key to reducing the number of outages and faster relaying minimizes the duration of power dips. The cost of protection must be justified by the value of potential losses from decreased revenue or damaged equipment. The cost of nuisance tripping (tripping when not needed) is very high, especially when greater demand is placed on power systems, and also if the protection relay did not detect the fault (called protection blinding) this would cause a lots of damage of generators, equipment and

cause injuries. Proper protection requires a balance between speed and security, based on the needs of the system.

1.2 Distributed Generation (DG)

The Distributed Generation (DGs) can be classified as inverter based DGs and rotational based DGs. The rotational based DGs include synchronous, asynchronous, and doubly fed induction generators, and the inverter based DGs include static and electronic DGs. Distributed generation offer deregulation of power production, increased system reliability of the network, peak demand reduction, and significant reduction in power system's lines losses, especially when DG power matches the load. The DGs connected to the power network in UK are classified according to the Distribution Code (DC) as five types [1]: synchronous generators (SG), fixed speed induction generators (FSIG), doubly fed induction generators (DFIG), series converter connected generators and transformer based generators.

1.2.1 Distributed Generation and auto-reclose scheme

In overhead power distribution around 80-95% of the faults are of brief nature and last from few cycles to seconds. That is why re-closers are designed to open and close three times and if the fault is not cleared it opens for the fourth time and never reclose automatically, it has to be closed manually on site or remotely by the power system administrators when the fault is cleared. The re-closer should coordinate with other protection devices located upstream towards the source where the fuse should be in position either on the low voltage side or on the high voltage side; furthermore, the re-closer should coordinate with the protection equipment located downstream towards the load where relays positioned. Thereby, when designing and installing re-closers, there must be consideration for some elements:

1. System voltage, Short circuit level, and Maximum load current.
2. The sensitivity of operation for earth faults.
3. The minimum of short circuit current, that lies within the area of protection.

There is an automatic high reclose without any deliberate delay, and there is a deliberately delayed reclose to allow fault arcs and ionized air to dissipate and to coordinate with other protective devices. The coordination between the fuses, re-closers, and relays is set up for and these elements could cause potential damage to

the power system equipment, damage to DGs, lots of outage & maintenance time and economical losses. Usually, the power from the main feeder and the DG supply the load, however, when the DG is disconnected from the mains, and the DG and the local load become islanded, at this moment the DG has to supply the local load in full. Usually, the DG supply the load with active power which means that the power factor equal to one and the phase angle is zero. Nevertheless, when the DG islands and the load become greater than the power supplies by DG, the generator will speed up to cover the load level which leads to the frequency to fall. The generator frequency controller will reinstate the frequency to its nominal level, which leads to a change in the phase angle of the power delivered by the DG to the local load, and this power will be active & reactive. Now, the phase angle difference between the island and the rest of the power system has shifted and not zero anymore. It has to be phase synchronized in order to reclose otherwise reclosing without synchronization or not reclose for more than 2s will cause an impact on both the power system and the DG and cause a lots of damages, replacements, maintenance to both sides [2, 3, and 4].

1.2.2 Impact of grid connected DGs on voltage sag

The synchronous and induction generators have a significant impact on the voltage sag magnitude and duration. With synchronous generators the voltage drop increases and the voltage dip duration prolongs and decreases its dip magnitude, while synchronous generators with PI controllers have less impact on the voltage sag compared to other types of synchronous generators. With induction generators the voltage sag magnitude is the highest followed by synchronous generators with power factor control [5].

1.2.3 Tripping Time delay

The delayed reclosing time depends on the voltage level, and the circuit breaker (CB) category. At 400kV the reclosing delay is 0.3-0.4s, at 132kV its 0.4-0.6s and at 11kV it is around 10s. The first two are mainly for power transmission, while the third voltage level is for distributing power directly to the loads, this may give enough time to allow fault arcs and ionized air to dissipate, the protective devices to coordinate with other and make sure of full synchronization before re-closing. The

relay trip signal sent the CB is estimated to be a maximum of 50msec, while the CB operation time is usually a maximum of 150msec (from 150msec for old oil CB to 50msec for the latest vacuum or SF6 switchgear) [6, 7, and 8].

1.2.4 Loss of Mains event

Loss of mains (LOM) (also called islanding) refers to a condition where a Distributed Generator and the local load connected to it get isolated from the main power grid and facility runs on its own alternative power source when energy is not coming from a power grid. Such a power source can also feed energy back into the grid. Islanding can either happen as the result of a power black-out or be set up intentionally [6].

1.2.5 DGs Protection

In order to find out the weaknesses or malfunction, that cause false tripping, and work to develop a combined method that makes the LOM protection reliable. There are two groups of protection methods, active and passive methods. Passive methods make use of the local voltages and currents Phasor to measure the power frequency or phase angle to determine whether there is a fault or everything is working normally. Active methods interact with the power system operation and make small alteration to the power system [9]. Hence causes changes in the system's parameters, since this type of methods only implemented in inverter based protection for generation with power rates of less than 50kW.

1.2.6 Non-Detection Zone (NDZ)

Most LOM protection algorithms fails to detect LOM at low power imbalances, and the range of power imbalance where LOM cannot be detected is called the Non-Detection Zone (NDZ). Making the relay's settings very sensitive will lead to false tripping and effect the power system stability; and making the settings less sensitive will cause a delay of LOM detection or detection blinding, which will be damaging to the DG, load and the power network. In addition, the non-detection zone (NDZ) problem mostly affects the reliability of the passive methods. All passive methods have NDZs (Active methods do not/or have a very small NDZ); the ROCOF and VS relay have NDZ as well, especially when the power of the DG is equal or very close to the local load. The NDZ reduces the probability of the passive relays detecting

LOM and effect the reliability of the protection system, because if the islanding continues for more than 2s [10], it would make lots of damage as it was explained before. In [9] the analysis for the NDZs at ROCOF relay showed that ROCOF relay has a NDZ of ±5% of real power imbalance, while the VS relay showed a NDZ of +15% to -10% for real power imbalance.

1.2.7 Transmission and Distribution Network

The main power stations are connected to the transmission system which operates as a fully interconnected to the system within Scotland, England and wales. The grid operates at 275kV and 400kV. The 132kV network in Scotland is also classed as part of the transmission system but this is not the case in England and wales. The distribution system operates at nominal voltages of 66kV, 33kV, and 22kV (EHV), 11kV and 6.6kV (HV) and 400 volts and 230V (LV). The 132kV network in England and Wales is also classed as part of the distribution system but this is not the case in Scotland. The Distribution Code (DC) covers the distribution systems of the DNOs which are defined so as to include equipment at 33kV and below in Scotland and 132kV and below in England and Wales [1, 10].

1.3 Research Motivation

Distributed Generation (DGs) could bring about unwanted operation of protective devices in the power system, on the other hand, the protection relays may never detect the fault and/or not operate properly, and this makes the power system protection less reliable. The power system protection equipment and devices are designed, set, and installed based on radial network with unidirectional current flow, when the DGs started to penetrate the power system in large proportions the network became bidirectional (multidirectional current flow) and this will causes a loss in coordination between the system's protective devices. The DGs will increase or decrease the fault current and cause false tripping of protection devices, protection blinding, and out of phase reclose. When loss of mains (LOM) occurs, if it is not detected quickly it would bring about more instability to the power system and damage the DG and the power system components. Upgrading the power distribution network (including the power lines' buses) is very expensive, time consuming, increase outages and not practical since the DGs are continuing to penetrate the

power network. The renewable energy based DGs have low system inertia and variable output power, supply the network with variable current levels and increasing its share of the power generation capacity of the power network. Some of the LOM protection methods available are limited to DG capacities lower than 50kW and/or complicated to implement and expensive and others would not satisfy both stability and reliability requirements. There are several researches suggested that in order to improve the reliability of the protection system by internet based LOM methods, and the authors [11] suggested the utilization of satellite communications could be used in wide proportions of power system protection applications. The tests results in [11] demonstrated clear improvement of stability of the LOM protection, however, the sensitivity level of LOM protection remained the same. Hence, practical issues relating to the reliability and latency of satellite communication channels for power system protection applications.

1.4 Research objectives

The objectives of this research can be outlined by four points:

1- Investigate the reliability and security of satellite and internet communication networks in LOM protection and determine the communication requirements.
2- Developing a reliable and stable LOM protection method
3- Developing a delay estimation method to replace the Global Positioning System (GPS) for economic reason, and this developed method should be with a level of accuracy that leads to a reliable and secure LOM protection operation that avoids nuisance tripping, protection blinding, and does not have any NDZ.
4- Developing a technique that detects corrupt data and loss of link events.

1.5 Research Contributions

The research contribution is mainly based on developing a novel clock free time delay estimation method, and a method developed from the delay estimation method to detect corrupt, high error data and loss of link event these two methods are designed for all power system applications that do not require a real time data measurements. The contributions and their novelty are outlined in two points:

1- The author has developed a novel communication type LOM protection method based on frequency correlation by using data convergence and accumulative sum of frequency difference. This method is very sensitive and stable, and enforces security and reliability to the system. The knowledge of the data requirements of the LOM protection, data measurements, the functioning of PMU, knowledge of generator operation and satellite communication lead to the invention of a technique that detect data error and loss of communication to protect the DG from nuisance tripping by preventing the corrupted data from being included in the LOM Algorithm. If it detects loss of communication it would inform the relay to deactivate the communication based LOM protection algorithm and activate the backup local LOM protection method.
2- The economic contribution is to reduce the expenses of the GPS and replace it at every DG that uses satellite communication for LOM protection by a Time Delay Estimation (TDE) Method. The work that has been done in time delay estimation is based on the concept of data stream convergence. The convergence theory is not new, and it has been used many times before in the last 50 years in the field of time delay estimation. However, the technique used in this method and integrated with LOM protection algorithm to achieve synchronization has never been proposed before. The author has invented a new method developed from data convergence and based of linearity trajectory delay estimation. This method is new and it has not been introduced before in the time delay estimation field and in data signal processing, and never been proposed in the delay estimation in general.

1.6 Thesis Outline

Chapter 1: Introduction

In this chapter, loss of mains is defined, motivation for the research work is presented, the objectives of this research are outlined, and the research contributions and originality are outlined.

Chapter 2: Review Loss of Mains Protection Methods

In this chapter, a comprehensive review of the LOM protection methods; the main LOM protection techniques and the communication based LOM method is proposed that the research development project is based on.

Chapter 3: Communication System

In this chapter, a review, evaluation and comparative analyses of the communication methods used in power system protection. The proposed utilization of satellite communication in LOM protection and the communication structure requirement that enforce a reliable and secure protection method.

Chapter 4: Communication Based Loss-of-Mains Method by Frequency Correlation (CFC)

In this chapter, the author presents the main contribution of this research, a new LOM protection method, which is communication based by frequency correlation.

Chapter 5: Linear Trajectory Delay (LTP): a Time Delay Estimation Method

This chapter, a review of the clock free methods of time delay estimation, and the presentation of the second contribution of this research, the new Linear Trajectory Delay (LTP) method for time delay estimation.

Chapter 6: Conclusions and Further work

In this chapter conclusions and further work are outlined.

Chapter 7: References

This chapter contains a list of all the references for in this thesis.

1.7 Publications

Based on the results of the research work reported in this thesis, the following papers have been published:

1- A. Makki, A. Dyśko, Martine Lee, William Huge, "Assessment of the reliability of Loss of Mains protection for Distributed Generation Utilizing Satellite Communication," presented at the DPSP 2012, Birmingham, UK, 2012.

2- A. Makki, A. Dyśko, “Communication based Loss of Mains Protection Method by Frequency Correlation (CFC),” IET transaction on Generation, Transmission, and Distribution (GTD) Journal (in preparation).

CHAPTER 2: REVIEW OF LOSS OF MAINS PROTECTION METHODS

2.1 Introduction

When a fault occurs in the power distribution system, it will be cleared instantaneously. The DG will keep supplying the local load with power regardless of the unbalance of power between the generation and load. The load is fed by the DG only because the main power supply is disconnected from the power system or the DG has lost synchronisation with the main supply after the circuit breaker reclosed. This event is called Loss of Mains (LOM) operation and it is also called islanding operation, as shown in Figure 2-1. If this continues, further destabilize the power system. This will delay the restoration of the power system to steady state and cause damages to the power system and the DG components. Hence, there should be a LOM protection relay installed to every DG that detect LOM and isolate the DG. There are many LOM protection methods that can be categorized into local and regional. The local methods are active, passive, and hybrid methods. The regional methods are remote, centralised, and communication based [12, 13, 14, 15, and 16].

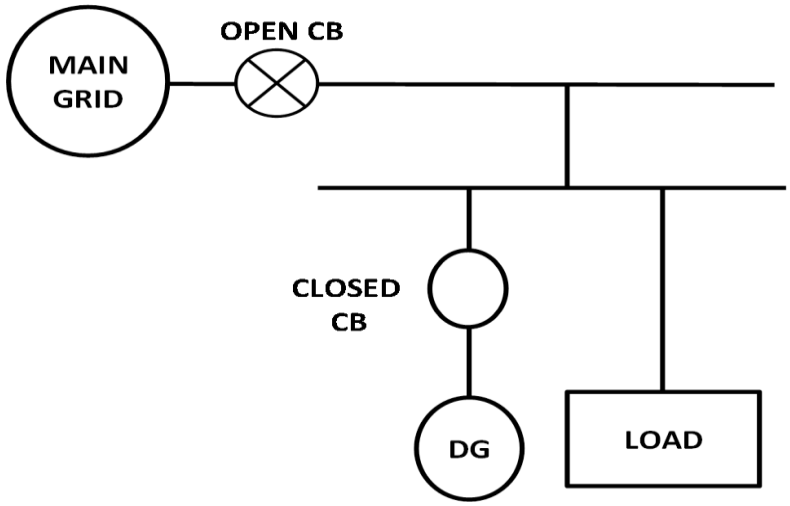

Figure 2-1: Loss of Main event

2.2 Passive Techniques

Passive methods are based on measuring local electrical parameters (at the DG side) and compare them to predefined threshold settings. The passive methods do not make changes to the power system parameters, they are very sensitive with high speed detection, and cost less to implement than the active methods. On the other hand, if a sudden change in load occurs, they may suffer nuisance tripping and no detection zones [12, 13].

2.2.1 (Under/Over) Voltage and (Under/Over) Frequency Methods

They provide an acceptable level of protection, however they may fail to operate if the change of load associated with LOM can be compensated by the DG's control system. The recommendations for settings of these types of relays are described in Table 2-1 [1, 10, and 14].

2.2.2 Rate of Change of Frequency (ROCOF) Method

This method based on making continuous calculations to the slope of frequency of the voltage waveform to calculate the rate of change of frequency (ROCOF) (that is measured in Hz/sec). The ROCOF measuring window length is 3 cycles. If the ROCOF value exceeded the threshold setting the relay will initiate a tripping signal to the circuit breaker to open, the ROCOF setting can vary 0.125-1 Hz/sec. In order to avoid false tripping at a generator start up or at short circuit faults, an intentional delay of 25 cycles of the relay operation that allows for further calculations and analysis. The ROCOF method is the most trusted and reliable LOM method, however, it showed in some cases false tripping and in other cases protection blinding (having a No Detection Zone NDZ), such as when the power imbalance between the DG power output and the local load is small or there is no imbalance at all [12, 13, 15, and 16]. The main factors that affect the relay performance are the type of load and generator inertia, because they have direct relation to the ROCOF value, as shown in equation (2-1):

$$ROCOF = \frac{\Delta f}{\Delta t} = \frac{\Delta P f_o}{2HS} \qquad (2\text{-}1)$$

Where,

(S) Rated power capacity of the DG
(H) Inertia constant of the DG

(f_o) System nominal frequency
(Δf) Change of frequency
(Δt) Time period of the frequency difference measurement window
(ΔP) Active Power unbalance

However, the ROCOF relays do not come with the same frequency estimation technique; there are relays with the Zero-Crossing technique and others with Discrete Fourier Transform (DFT) technique. When the ROCOF relays have different internal algorithms, they will perform very differently to the same event, even if they have the same ROCOF settings. The DFT based relay shows higher rates of ROCOF than the Zero-Crossing based relay for the same power system disturbance, thereby the ROCOF settings for the DFT based relay should be higher than the settings of the zero-crossing based relay [17][18]. Both of these methods suffer nuisance tripping, which require long delay times or increasing the measuring window's length, the length of the measuring window is directly related to the relay operation, and the shorter the measuring window is the higher the ROCOF will be and vice versa. The recommendation for ROCOF relay setting is shown in Table 2-1 [1]. However, since April 2014 the setting recommendation increased to a maximum of 1 Hz/sec to enforce stability, however this would make the ROCOF method less sensitive.

2.2.3 Voltage Vector Shift (VS) Method

If islanding occurs, there will be imbalance between the DG output power and the local load. Hence, the generator will accelerate or decelerate (depending on whether the load is greater than the generator output or vice versa), and the DG power angle δ will change due to the variations of cycle period duration, which will cause a proportional variation to the terminal voltage angle. When the DG loses synchronism with the main grid, the DG voltage phase angle will start to shift, and this phase angle displacement is directly related to the change in frequency of the power system [19]. The VS method operation principle is based on measuring the phase angle displacement of the voltage waveform, by measuring and comparing the cycle duration period with the previous cycle duration period. If the phase shift exceeded the pre-defined threshold setting, the relay will initiate a tripping signal. This relay is sensitive to any changes in the DG loading and it could operate in 60ms for a load change of greater than 5% of the DG capacity.

Table 2-1: Over/Under Voltage and Frequency Relays' Settings

Small Power Stations <5MW					Medium Power Stations ≥5MW	
Port Function	LV Connected		HV Connected			
	Setting	Time	Setting	Time	Setting	Time
UV Stage 1	Vϕ-n† -13%	2.5s*	Vϕ-$\phi^{\ddagger}$ -13%	2.5s*	Vϕ-ϕ -20%	2.5s*
UV Stage 2	Vϕ-n† -20%	0.5s	Vϕ-$\phi^{\ddagger}$ -20%	0.5s		
OV Stage 1	Vϕ-n† +14%	1.0s	Vϕ-$\phi^{\ddagger}$+10%	1.0s	Vϕ-ϕ+10%	1.0s
OV Stage 2	Vϕ-n† +19%	0.5s	Vϕ-$\phi^{\ddagger}$ +13%	0.5s		
UF Stage 1	47.5 Hz	20s	47.5 HZ	20s	47.5 Hz	20 s
UF Stage 2	47.0 Hz	0.5s	47.0 HZ	0.5s	47 Hz	0.5 s
OF Stage 1	51.5 Hz	90s	51.5 Hz	90 s	52Hz	0.5 s
OF Stage 2	52.0 Hz	0.5s	52.0 Hz	0.5s		
Vector Shift	$K1 \times 6$ Degrees		$K1 \times 6$ Degrees #		Inter-tripping	
ROCOF	$K2 \times 0.125$ Hz/s		$K2 \times 0.125$ Hz/s #		-	

ROCOF settings for Power Stations ≥ 5MW				
Date of Commissioning		Small Power Stations		Medium Power Stations
		Asynchronous	Synchronous	
Generating Plant Commissioned before 01/08/2014	Settings permitted until 01/08/16	Not to be less than K2 x 0.125 Hz/s$^{\#}$ and not to be greater than 1Hz/s$^{\P\# \Omega}$, time delay 0.5s	Not to be less than K2 x 0.125 Hz/s$^{\#}$ and not to be greater than 0.5Hz/s$^{\P\# \Omega}$ time delay 0.5s	Inter-tripping Expected
	Settings permitted on or after 01/08/2016	1Hz/s$^{\P\#}$ time delay 0.5s	0.5Hz/s$^{\P\# \Omega}$ time delay 0.5s	Inter-tripping Expected
Generating Plant commissioned between 01/08/2014 and 31/07/2016		1Hz/s$^{\P\#}$ time delay 0.5s	0.5Hz/s$^{\P\# \Omega}$ time delay 0.5s	Inter-tripping Expected
Generating Plant commissioned on or after 01/08/2016		*1Hz/s$^{\P\#}$ time delay 0.5s*	*1Hz/s$^{\P\# \Omega}$ time delay 0.5s*	*Inter-tripping Expected*

Notes for Table 2-1[1]:

(φ-n; φ-φ) *denote RMS phase to neutral and phase-phase values respectively of the voltage at the Connection Point*

$ *HV and LV Protection settings are to be applied according to the voltage reference at which the protection is measuring, ie:*

• If the G59 protection takes its voltage reference from LV source then LV protection settings shall be applied.

• If the G59 protection takes its voltage reference from HV source then HV protection settings shall be applied.

† A value of 230V shall be used for all DNO LV systems

‡ A value to suit the voltage of the connection point

***** *Might need to be reduced if auto-reclose dead times are <3s*

*Inter-tripping may be considered as an alternative to the use of a Loss of Mains relay*

K1 *= 1.0 (for low impedance networks) or 1.66 – 2.0 (for high impedance networks)*

K2 *= 1.0 (for low impedance networks) or 1.6 (for high impedance networks)*

§ *Rate of change of frequency,*

¶ Protection requirement is expressed in Hz/s.

The time delay *should begin when the measured rate exceeds the threshold expressed in Hz/s and be reset if it falls below that threshold. The relay must not trip unless the measured rate remains above the threshold expressed in Hz/s continuously for 500ms. Setting the number of cycles on the relay used to calculate the ROCOF is not an acceptable implementation of the time delay since the relay would trip in less than 500ms if the rate was significantly higher than the threshold.*

Ω *The minimum setting is 0.5Hz/s. For overall system security reasons, settings closer to 1.0Hz/s are desirable, subject to the capability of the generating plant to work to higher settings.*

There is no need for adding a delay for the relay operation. However, the high sensitivity of the VS relay to change of impedance could cause nuisance tripping during normal power system operation [12, 13, 14, 15, and 16]. Hence, the method offers high sensitivity on the other hand it offers low stability. The recommendation to a VS relay setting is shown in Table 2-1 [1].

2.2.4 A Combined VS and Frequency Variation Method

This method was developed to solve the problem of reliability and sensitivity of the vector shift method. This combined method consists of main criterion and auxiliary criterion calculating algorithms. The method was presented using synchronous generators as DG. By introducing frequency variation into the VS method, it was able to narrow down the NDZ, and improve the sensitivity of detection [20].

2.2.5 Rate of Change of Power Method (ROCOP)

The loss of mains causes a change in the DG loading and the DG power output. The values of the DG voltages and currents are measured at the DG terminals, and with these measurements, the relay monitors the changes in the power output by using the protection algorithm. The instantaneous DG power is calculated, as shown in equation (2-2):

$$P_g = v_a i_a + v_b i_b + v_c i_c \qquad (2\text{-}2)$$

Where,

(P_g) Instantaneous DG power
$(v_a, v_b, and\ v_c)$ Instantaneous voltages for phase a, phase b, and phase c respectively
$(ia, ib, and\ ic)$ Instantaneous currents for phase a, phase b, and phase c respectively

Tripping will occur if these changes exceeded the threshold setting of the relay, and the tripping settings for the protection algorithm is chosen so that 1% change in load due to islanding would cause tripping. In addition, this method can quickly detect out of synchronism reconnection of the DG with the main grid [12, 21].

2.2.6 Comparison of Rate of Change of Frequency (COROCOF) Method

The relay compares the rate of change of frequency of the DG with the rate of change of frequency of the rest of the system. It is assumed that the loss of mains

will cause change in DGs frequency, but not the frequency of the main grid, because the power island considered very small compared to the rest of the power system. The advantage of this method is that it differentiates between frequency changes because of loss of mains and frequency changes that are caused by wide area disturbance by applying a blocking signal [22].

2.2.7 Power Fluctuation Method

This method monitors the power output from the generator. Under normal power system, conditions the transfer function reflect both the DG and the Utility, while under islanding condition the transfer function reflects only the DG. Under extreme load fluctuations when the DG is still connected to the main grid, while operates quickly under small fluctuation when the DG is disconnected from the main grid. In addition, it detects the out of phase reconnecting of the DG with the main grid. It remains stable under a single phase faults near the DG terminal, and trip under three phase faults [12].

2.2.8 Rate of Change of Voltage (ROCOV) and Power Factor (pf)

This method is used for DG and it is based on continuously monitoring the rate of change of voltage ($\Delta V/dt$) and the change of the power factor (Δpf), and these parameters are measured at the point of common coupling (PCC). The can be derived from the instantaneous voltage and current signals measured at the PCC [23].

2.2.9 Rate of Change of Phase Angle Difference (ROCOPAD)

It starts by measuring the voltage and current at the PCC, and the ROCOPAD can be calculated (measured in Degree/second) from the phase angle information of the voltage and current signals by computing ratio of the difference between the voltage phase angle and the current phase angle over the time difference, as shown in equation (2-3):

$$ROCOPAD = \frac{\Delta(\delta v - \delta i)}{\Delta t} \qquad (2\text{-}3)$$

Where,

(δv)	Voltage angle
(δi)	Current angle
(Δt)	Time sample

If the value of ROCOPAD exceeded the threshold setting the relay trips and the threshold value is 50-100 degree/s, and the response time is 3msec. This method is capable of detecting islanding at 0% power imbalance [24].

2.2.10 Combined ROCOF and ROCOPAD method

This method operates by using the ROCOPAD relay as an interlock to the ROCOF relay in order to avoid the nuisance tripping associated when using ROCOF relay. When the ROCOF value exceeds the threshold, the ROCOPAD start to calculate the phase angles of the voltage and current, and if the ROCOPAD value exceeded the threshold, the relay will send a trip signal [25].

2.2.11 Rate of Change of Output Power (df/df)

The dp/dt at the DG side when islanding occurs will be much greater than before islanding for the same rate of the same rate of load change. This method is very effective especially when the islanding has an unbalanced load [21].

2.2.12 Rate of Change of Frequency over Power (df/df)

This method is much more sensitive than the ROCOF in case of a small mismatch between the DG and the local load. The df/dp is larger in small generation DGs than in larger generation capacity DG, due to the fact that small generators have low inertia constant, whereas large generators have high inertia constant [26].

2.2.13 Voltage Unbalance Method (VU)

The distribution networks usually include single phase loads, at islanding the load balance of the DG could change. Even if the change in the DG loads is small, the voltage unbalance will occur due to the change in network condition [12, 13, and 14].

2.2.14 Harmonic Distortion Method (THD)

This method can detect islanding by monitoring the change of the Total Harmonic Distortion (THD) of the DG terminal voltage before and after islanding. The change in the third harmonic of the DGs voltage gives a sign of when the DG is islanded [12, 13, and 14]. In [27] an algorithm was developed for wind farms induction machines protection, it starts by sampling three phase currents and calculate their THD. The THD_t and THD_{avgt}, as shown in equations (2-4) and (2-5) are measured every cycle,

when the delta lays between %0.5 and %3 for at least 3 cycles, the algorithm issues a trip signal.

$$THD_t = \left(\frac{\sqrt{\sum_{h=2}^{H} I_h^2}}{I_1} \right) \times 100 \quad (2\text{-}4)$$

Where,

(THD_i)	The THD value for one sample
(I_1)	RMS value of the first harmonic (frequency component) of the signal
(h)	Harmonic index
(I_h)	RMS value of the h^{th} harmonic of the signal
(H)	Total number of harmonics considered

$$THD_{avgt} = \frac{1}{N} \sum_{i=0}^{N-1} THD_{t-i} \quad (2\text{-}5)$$

Where,

(THD_{avgt})	Average value of THD in one cycle
(i)	Sample index
(THD_{t-i})	Value of THD for the previous sample
(N)	Number of samples taken in cycle

The algorithm eliminates relay unwanted tripping in wind farms with induction machines due to capacitor bank switching, and induction machine starting period that the relay will ride-through these events without tripping. In addition, if there is a match or nearly a match between the power production and the load, usually the THD value remains$< 3\%$, never the less; the protection algorithm detects islanding and sends a tripping signal.

2.2.15 Combined ROCOF and THD Methods

In this method, the THD algorithm is used as an interlock function which operates with ROCOF to avoid nuisance tripping of ROCOF relays during stable conditions. The THD method detect the islanding first and the ROCOF will start analysing afterwards, the idea of this method is that the THD method is more accurate than the ROCOF method; thereby, it has to detect islanding first to avoid nuisance tripping by the ROCOF relay. The disadvantage of this method is that according to the algorithm if the THD method detected islanding, while the ROCOF method did not the relay will not trip, because both of them have to detect islanding for the relay to trip. While

this method eliminates nuisance tripping, it will still fails to trip when the operation is within the ROCOF relay NDZ [28].

2.2.16 Combined VU and THD Method

This method calculates the Average Rate of Change of Voltage (AROCOV) of the three single phase voltages, $THD_{average}$ of phase (A) current, and $V_{average}$ of a line voltage, $VU_{average}$ is the average VU over the past 1s. $VU_{average}$ should be equal to or over 0.5p.u voltage. If the $VU_{average}$ does not fall below 0.5p.u, then the method checks if ΔTHD and ΔVU satisfy the following ranges:

$$[\Delta\text{THD} > +75\% \text{ or } \Delta\text{THD} < -100\%] \; [\Delta\text{VU} \geq +50\% \text{ or } \Delta\text{VU} < -100\%]$$

If ΔTHD and ΔVU are within these ranges for longer than one cycle, then islanding has occurred. The disadvantages of this method are that it does not solve the problem of the difficulty in the high quality factor (Q_f) detection, and the threshold is not easy to determine [25].

2.2.17 Logical Rule Islanding Detection Method

By monitoring four system parameters: The first is for voltage level ($V_{rms)}$ (as A), the second is for phase displacement (ΔPH) (as B), the third is for ROCOF (as C) and the fourth is for ΔTHD (as D), where A, B, C, and D, are the decision criteria terms of each parameter [29]. The determination of whether the system is in an islanding operation condition is based on logical rules as follows:

(i) IF (V_{rms} is less than 0.9 p.u.) and (ΔPH is larger than 5^o during one-cycle) and (ROCOF is larger than 0.3 Hz/s), THEN an islanding operation has occurred.

(ii) IF (V_{rms} is larger than 0.9 p.u.) and (ΔPH is less than 5^o during one-cycle) and (ROCOF is less than 0.3 Hz/s) and (ΔTHD is larger than +75 % during one-cycle), THEN an islanding operation has occurred.

(iii) IF (V_{rms} is less than 0.9 per unit) and (ΔPH is larger than 5^o during one-cycle) and (ROCOF is less than 0.3 Hz/s) and (ΔTHD is less than -100 % during one-cycle), thus an islanding operation has occurred. If the current operating condition satisfies at least one rule of them, the method finally decides that an islanding operation has occurred.

2.2.18 Pattern Recognition Based Islanding Detection

This method monitors the transient signals generated during an islanding event to detect the formation of the island. A decision-tree classifier is trained to recognize the islanding operation. The vectors required for classification are extracted from the transient current and voltage signals through discrete wavelet transform. This method is able to recognise whether it is an islanding or non-islanding operation efficiently [30, 31].

2.2.19 Accumulated Phase Angle Drift (PAD)

The Accumulated Phase Angle Drift (PAD) method was developed to reduce the NDZ range [17, 32, 33, and 34], by making a comparison between the local frequency and the estimated grid frequency (that is based on stored historical frequencies). The frequency estimated by using grid frequency that occurred in a period of 500ms-1sec before the time that the local frequency was taken, as shown in equation (2-6) and it is illustrated in Figures 2-2 and 2-3:

$$\Theta_n = \Theta_{n-12} + 2\pi\left(f_n^{est} - f_n\right)T_{12_{samples}} \quad (2\text{-}6)$$

Where,

(Θ_n)	Accumulated phase angle drift
$(T_{12_{samples}})$	Sampling time for estimating f_n^{est}
(f_n^{est})	Estimated grid frequency
(f_n)	Real time frequency
(Θ_{n-12})	Subsequent accumulated phase angle drift

This procedure of evaluation should be repeated every half a cycle, the number of sample taken every cycle is 24, which means the number of samples taken every measurement is 12 samples per half cycle. This method succeeded in minimising the NDZ to 0% power imbalance. However, the PAD method suffered some false tripping as well, because of the method used for estimating the frequency is based on linear extrapolation method, in addition to the 1s delay [32, 33, and 34].

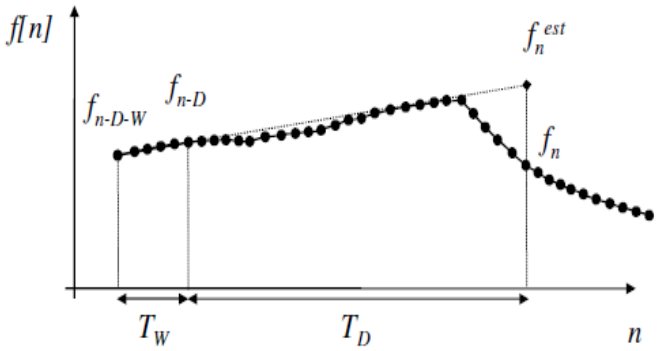

Figure 2-2: Illustration of the PAD Method [33]

(T_D) Historical time delay, (T_W) estimation window

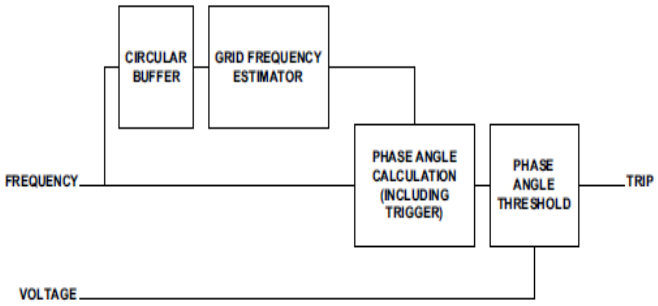

Figure 2-3: Block Diagram of the PAD Method [33]

In the ROCOF and VS methods, the time needed for the vector shift to make a measurement is 2-3 cycles for 50Hz system (the phase angle difference between the power system and the generator should be 6°-12°, imbalance of >30%Sn). The time required for the ROCOF to make a measurement is from few cycles to 32 cycles (0.64s) and this time is necessary for the ROCOF to make the right measurement and at the same time give more time for the synchronization relay and the generator governor to restore the nominal frequency and insure synchronized reclosing. The over/under voltage and over/under frequency relays, according to the UK G59/2 standard for 2010 the time setting limits have been changed. There are some proposals to increase the time delay and make the time settings in two stages to make sure that the relays trip accurately and give a time for the power system to restore its nominal values in case there is a temporary power disturbance as shown in Table 2-1[1].

2.3 Active Techniques

These techniques are based on making small changes in the state of the PCC and observing the response of the system. The response would show whether the DG unit is islanded or not, and the protection relay will try to force the DG outside the predefined threshold setting value [12]. The active techniques are very effective and do not have any no detection zone (NDZ), on the other have they have a high operation delay that could exceeds some standard limits, and they effect the stability of the power system and the quality of electricity.

2.3.1 Reactive Power Export Error Protection Method

It is also called the REED relay; it interfaces with the DG's Automatic Voltage Regulator (AVR) and forces it to generate a level of reactive power flow at the PCC. The level of reactive power flow can only be maintained when the DG is connected to the utility. The relay will trip if there is an error between the setting and the actual reactive power being exported for a time greater than the set value. There is an operation delay of 2-5s, which makes this protection method slow compared with the islanding time period limit of set by the IEEE Standard 1547™ [10, 13], that the islanding should be detected and isolated within 2s. However, this method is capable of detecting LOM even if there is no change in the generator loading due to switching operation [12, 16]. This method have the disadvantage of being slow, and that it cannot be used in a system where the DG has to generate a unity power factor, hence, it will not work with induction machine type DG.

2.3.2 System Fault Level Monitoring Method

This method uses measurements of the power source impedance close to the PCC. The system fault level is monitored by measuring the short circuit current and the reduction in supply voltage level, and this can be achieved by using a PMU on the main substation side. The source impedance is monitored while connecting a shunt inductor across (for a short period) by using point-on-wave triggered, and/or thyristor switches [16].

2.3.3 Impedance Insertion method

The concept of this method is that the closer the ratio of the overall load to the overall power output is to 1:1 the longer the islanding lasts. By inserting low value

impedance (capacitor bank or reactor) on the utility side, it is possible to suppress islanding by changing this ratio. The load consist of rotating machines and general load, it is also assumed that overall load is constant. During islanding reactors and capacitors are inserted and the islanding will be interrupted. A test was administrated for 10km long 6kV distribution line, with 100 PV system of output of 2kW each connected to the line. The test results showed that when the load to power output ratio in the range of 0.95-1.30 the islanding can lasts for more than 10s, however, the maximum permitted islanding time duration is 2s according to the IEEE 1547 standard [10]. Under similar case 0.3s is enough to detect islanding and insert the reactor, with 10kVA reactor capacity the islanding can be suppressed to a maximum islanding duration of 2.8s. If the reactor increased to 20kVA, the maximum islanding duration will be reduced to 1.2s. It shows the same pattern, when using a capacitor rather than a reactor. Hence, by increasing the capacitor or reactor value, the 2s target can be met. The load and the power output are equal, the greater the PV output is the shorter the islanding time period is, however, the PV output is not constant and changes during the day. There is also a trade-off between using a capacitor and using a reactor, this is due the reaction of the power system voltage and frequency to each choice, when inserting a reactor the voltage decreases and the frequency increases, and when inserting a capacitor the voltage increases and the frequency decreases [35]. Thereby, the impedance value should be chosen according to the minimum variation of frequency that can be detected.

2.3.4 Inter-Harmonics Injection method

This method's operation principle is to inject non-integer harmonics to the power system, and the response of the power system to the injections will change when the islanding occurs [13].

2.3.5 Voltage Magnitude Variation Method

This method works for a synchronous machine type DG; when the generator exciter output increases while holding the prime-mover power constant the rotor current increases, and when the rotor current increase the induced voltage E_o increases as well. The increase in the induced voltage (E_o) will lead to an increase in the generator reactive power output (Q), as shown in equation (2-7), and there will be a

small decrease in the power angle (δ) to keep the generator active power output (P) constant, as shown in equation (2-8).

$$P = \left(\frac{|E_O||V_r|}{X_t}\right) sin\delta \quad (2\text{-}7)$$

$$Q = \left(\frac{|V_r|}{X_t}\right)(|E_o|cos\delta - |V_t|) \quad (2\text{-}8)$$

Where,

(P)	Active Power
(Q)	Reactive power
(E_o)	Induced voltage,
(δ)	Power angle
(V_r)	Voltage at the receiving side
(V_t)	Terminal voltage
(X_t)	Terminal reactance

Due to high capacity of utility system and the parallel operation mode, any change in the magnitude of the induced voltage of the DG will cause a change in the injecting reactive power (Q) at the PCC smaller than the injecting Q at islanding event. The algorithm works: First, by measuring the voltage magnitude (V1) and the reactive power (Q1), the second step is by exporting small error of the DG's induced magnitude (ε). The third step is by measuring the voltage magnitude (V2) and the reactive power (Q2) again and compares them to the first measurement, if the difference between V2 and V1 is greater than (ε) and Q2≠Q1, then send a tripping signal and if not it will go back to the first step. This method has high sensitivity and the value of ε does not interact with the power system operation [36].

2.3.6 High Frequency Radio Signal

It is based on identifying the change in impedance that occurs at the DG site when it becomes islanded. The utility impedance is considerably smaller than the impedance of the islanded network. Thus, when the DG gets disconnected from the main grid, it will result in an increase in the DG network impedance. That is because the DG had been connected in parallel to the main grid. In addition, the change of impedance will result in a change of the system fault level. Any step change in system's impedance greater than that would occur under normal operating condition is a result of loss of mains. This method detects the islanding by sensing a step change in impedance that occurs at the DG site if the DG is disconnected from the main grid:

$$V_{out} = V_{in}\left(\frac{Z_2}{Z_1+Z_2}\right) \quad (2\text{-}9)$$

Where,

(V_{in})	Input voltage source
(V_{out})	Voltage drop on Z_2
(Z_1)	Impedance connected in series with the input voltage source
(Z_2)	Impedance connected in series with Z_1 and input voltage source

It operates by superimposing a small high frequency radio signal; via a coupling capacitor onto the mains current waveform on the DG terminal through a voltage divider, and the coupling capacitor is integrated into the divider circuit and acts as Z_1. In normal power system operation the high frequency signal's magnitude is negligible, when islanding occurs this signal's magnitude start to increase until it becomes significant (no more than 6V). A considerable change in V_{out} can be obtained for a small change in system impedance, and the V_{out} can be measured using a high-pass filter connected across the mains, as shown in equation (2-9). The high pass filter will remove the nominal frequency signal, and the magnitude value of the high frequency signal which is used as an input to the voltage divider will vary with the change of system impedance [37]. The advantage of this method is independent on the DG loading and the variation of the mains' frequency.

2.3.7 Phase Shift method

Measuring the relative phase shift can give a sign that the inverter based DG is islanded, a small perturbation is applied in a form of phase shift. When islanding occurs, the perturbation will result in significant change in frequency [12].

2.3.8 Slip Mode Frequency Shift Algorithm (SMS)

This method is for protection of islanding of PV type DG with inverter interface. It uses a positive feedback that changes the phase angle of the current of the inverter with respect to the deviation of the frequency at the PCC. SMS curve given by equation (2-10):

$$\theta = \theta_m . sin\left(\frac{\pi(f_{[k-1]} - f_n)}{2(f_m - f_n)}\right) \quad (2\text{-}10)$$

Where,

(θ_m)	Maximum phase shift that occurs at frequency f_m
(f_m)	Frequency at LOM

(f_n) Nominal frequency
$(f_{[k-1]})$ Frequency at the previous cycle
(k) Number of cycles

The SMS curve is designed in a way that its slope is greater than that of the phase of the load in the unstable region. The disadvantage of this method is that if the slope of phase of load is higher than that of the SMS line, the LOM can be undetected, as there can be stable operating point within the unstable zone [12].

2.3.9 Active Frequency Drift (AFD) Method

This method's principle is to add a short period of zero time in the current waveform of the inverter based DG, and this will cause a distortion in the current waveform. When such distortion applied and the islanding occurs the voltage frequency of the islanded system will shift up or down continuously as the inverter operating at unity power factor tends to seek the resonant frequency of the local load. This method is very effective for purely resistive load; however, it may fail for other type of loads [38, 39].

2.3.10 Sandia Voltage Shift (SVS) and Sandia Frequency Shift (SFS) Methods

The Sandia Voltage Shift (SVS) method uses positive feedback to prevent islanding based on the amplitude of voltage at the PCC [14].The Sandia Frequency Shift (SFS) method was developed to make the AFD method apply to RLC type load, by adding a positive feedback to the AFD algorithm. The SFS disadvantage is that the phase angle of the load depends on the operating frequency and this may cause a NDZ [40]. In [41] it was found that the power regulator of the inverter controller can degrade the positive feedback control, thereby, the SFS method is much more efficient for constant current controlled inverters than constant power controlled inverters. In [42] it was proven that the load's active power frequency dependence has a significant impact on islanding detection and the NDZ of the SFS method, thereby, the method could fail to detect islanding under larger active power mismatches. In [41] the SFS and SVS methods were modelled and analysed, it showed that in frequency domain the SFS loop gain did not vary with the load power, while the SVS loop gain varies with power level. If the algorithm tuned for rated DG power level it will be effective under all operating conditions, and a model was presented in this paper that will help

in the optimization of the algorithm, to ensure that the islanding will be detected efficiently [12, 14].

2.3.11 Combined SFS and SMS Method

The SFS and SMS methods were adopted for the multiple PV systems using a Photovoltaic Power Generation and Active Filter (PV-AF) system. It was shown that even though the PV systems are connected to the same distribution line, the PV-AF system could detect islanding without current distortion and phase shift [42].

2.3.12 Automatic Phase Shift (APS) Method

This method is used for single phase and three phase inverters for wind turbines and small hydro DG systems, and it is a modified SMS method; only the starting angle ($\theta_{APS_{[k]}}$) of the inverter output current is changed according to the frequency of the previous voltage cycle $f_{[k-1]}$ [1, 43], as shown in equations (2-11) and (2-12)::

$$\theta_{APS_{[k]}} = \frac{1}{\alpha} \frac{f_{[k-1]} - f_n}{f_n} 360 + \theta_{o[k]} \quad (2\text{-}11)$$

$$\theta_{o[k]} = \theta_{o[k-1]} + \Delta\theta_{sys} sign(\Delta f_{ss}) \quad (2\text{-}12)$$

$\text{sign}(\Delta f_{ss})$= {1 if $\Delta f_{ss}>0$}, {0 if $\Delta f_{ss}=0$}, {-1 if $\Delta f_{ss}<0$} and $\theta o_{[k]} = 0$

Where,

$(\theta o_{[k]})$	Additional phase angle added each time the frequency of the terminal voltage stabilizes before the tripping point
$(\theta_{APS_{[k]}})$	Starting angle of the inverter current
(f_n)	Nominal frequency
$(f_{[k-1]})$	Frequency at the previous cycle
$(\Delta\theta)$	Constant increment of angle
(Δf_{ss})	Frequency change of two adjacent steady state frequency values
(α)	Constant scaling factor

2.3.13 Constant Current Inverter Method

This method is based on analysing the I-V curve for the DG output, and it works by providing a positive feedback between the PCC voltage and the DG output current in a way that the DG maintains stable operation, however, it loses its stability in islanding condition. This method's NDZ is negligible; its detection speed meets the islanding requirements, it maintains a constant current function of the DG, and it does not need any additional block, which makes it easy to implement [44].

2.3.14 Differential Voltage Correlation (DVC) Method

It injects a perturbing periodical signal into the inverter output current and it monitors the correlation function between the periodic signal and the perturbed voltage at the PCC. If islanding occurs, the correlation would be much higher [45].

2.3.15 Cross-Correlation scheme

This method is for inverter based DG, which uses the signal cross-correlation scheme between the injected reactive current and the power frequency deviation. The existing method injects 5% reactive current to the rated current for detecting the frequency deviation, and this reduces the power quality. In this method, only 1% of reactive current is injected to the rated current, thereby, the degradation of the power quality can be neglected [46].

2.4 Communication based protection methods

The islanding detection techniques are local when the measurements and detection are based on measurements taken at the PCC on the DG side and communication based when the measurements and/or decisions are taken on the utility side. This allows the utility company to make the decisions, and it can be achieved by using two-way communication link [47].

2.4.1 Phasor Measurement Unit (PMU) based protection method

It uses a central PMU that processes data from two relays located at the main grid side and at the DG side, and monitors the rate of change of phase as a slip, and the rate of change of slip as acceleration. When combining the slip and acceleration creates the islanding detection characteristics. The communication delay is related to the coordination of the reference measurement with the multiple generator locations, which could add to 1.7s. However, the PMU based detection is faster than local methods in cases where generation matches load [48].

2.4.2 Power Line Carrier (PLC) Communications protection Method

A signal generator at the main substation continuously broadcasts a signal to the distributed feeders using the power line carriers. The DGs are equipped with signal receivers, if the receiver does not sense the signal this means that an islanding occurred. The period of time needed for islanding detection is 2 cycles (40ms) long,

however this is excluding the propagation time which is approximately 200ms (10 cycles). The DG is supplied with a PLC signal receiver, when 4 cycles are missing this means that a loss of mains has occurred, and the extra 2 cycles is for avoiding nuisance tripping [17]. There are two major disadvantages of using this method: The high expenses required implementing this system, and the method could have a small NDZ when using sub-harmonic signal [49, 50].

2.4.3 Inter-tripping Protection Method

This method works by monitoring the status of all the circuit breakers (CBs) and re-closers that could island a distribution system and control the tripping of circuit breakers so as to complete the isolation of a circuit or piece of apparatus is sympathy with the tripping of other circuit breakers. The main use of such schemes is to ensure that protection at both ends of a faulted circuit will operate to isolate the equipment concerned. Inter-tripping schemes use signalling to send a trip command to remote circuit breakers to isolate circuits. Three types of inter-tripping methods that are commonly implemented in the power protection system [51]:

2.4.3.1 Direct tripping

Tripping signals are sent directly to the master trip relay and a receipt of the command will cause a CB operation. The method of communication must be reliable and secure such that interference on the communication system does not cause spurious trips that is because any signal detected at the receiving end will cause a trip of the CB at that end. If a spurious trip occur this may result in considerable unnecessary isolation of the primary system, which is unacceptable. That is why very high security is required at all noise levels up to the maximum which might never occur [51].

2.4.3.2 Permissive Tripping

It is when a tripping command signal is always evaluated by the protection relay at the receiving end, such that the remote CB will only trip when the received command trip coincides with a tripping signal sent by the protection relay responding to a system fault. The communications channels for this method require less security than the direct tripping method that is because if an incorrect command signal has been

received, it would only trip the CB at the receiving end when the tripping command is coincided with the operation of the receiving end protection relay [51].

2.4.3.3 Trip Blocking

Blocking command signals are sent to the remote CB when a protection element detects a fault which is external to the receiving local zone. The blocking command will prevent the remote CB from tripping. This method requires less security than the direct and permissive tripping methods, because a loss of communications does not result in a failure to trip when required, however, the risk of a spurious trip is higher. Hence, high dependability is required. The disadvantage of the Inter-tripping method is that it requires extensive communication support, has design complication, and it is expensive to implement. Hence, only generators with power rate 50MW and over use Inter-tripping protection because they connected directly to the power substation (short distance within 20 metres from the substation) as shown in Table 2-1[1]. This makes it not practical and extremely expensive to be implemented for remote generators that are connected to the distribution network protection a 100km away from the nearest substation [51].

2.4.4 Centralised Islanding Protection Method

The islanding detection algorithm is installed in a central micro-controller which is connected to all the IEDs in the network. The central controller monitors the status of the circuit breakers and sends tripping commands to the DGs when islanding occurs using GOOSE messages. The communication protocol is based on IEC 61850. This method is like the inter-tripping method without predetermined logic, and it is very flexible [52].

2.5 Hybrid islanding protection methods

2.5.1 Average rate of voltage change and real power shift method

Most of the DGs operate at unity power factor, and the source of the reactive power will be capacitor banks in the islanded network when power factor is equal to 1. The amount of reactive power that the capacitor banks produce depends on the voltage and when the voltage changes at islanding, the reactive power produced will change as well. This method combines the average rate of change of voltage (AROCOV) (Passive method) and the real power shift (RPS) (Active method). The RPS

technique will not inject perturbations unless the AROCOV technique failed to detect islanding, the RPS technique only changes the real power of one DG (this is an individual action that is not associated with changes in real power for a group of DGs). This method can efficiently detect islanding even if the imbalance of power output and the local load is very small, and discriminate between islanding and other power system conditions. However, if the local load equals the DG power output the method will fail to detect islanding, any change in load or generation will cause a change in the voltage level and islanding can be detected [53].

2.5.2 Voltage Unbalance and Frequency Set Point

This method uses the power factor method (Active Method) and the voltage unbalance (VU) method (Passive method). It operates by continuously measuring the three phase voltages at the PCC. If any change of load or islanding occurs, it will result in a spike in VU and if the value of VU exceeded the threshold the relay trips. This can be determined using the equation (2-13)

$$Maximum\ VU_{spike} = 35VU_{average} \quad (2\text{-}13)$$

Where,

(VU) Voltage unbalance
$(VU_{average})$ Average voltage unbalance
(VU_{spike}) Voltage unbalance spike

However, in order to discriminate between islanding and other reasons, the frequency set point of the DG is gradually reduced from 60Hz to 59Hz (at 60Hz power system) in 1s. If the frequency falls below 59.2Hz within 1.5s it indicates that there is a disconnection between the DG and the grid, and when the frequency stays close to nominal value this indicates that the islanding has not occurred [14, 54].

2.5.3 V_q and I_d Method

This method is a combination of the rate of change of V_q ($ROCOV_q$) which is a passive method and the injection of a direct axis current (I_d) in the d_q-current controller of the interface Voltage Sourced Converter (VSC) which is an active method. When the $ROCOV_q$ exceeds the threshold setting, the I_d will be applied to the VSC. If islanding occurred, the output voltage and the frequency will exceed their threshold settings, the relay will trip [14].

2.6 Comparison of Frequency based LOM protection methods

The methods that are going to be included in the comparison are from the passive methods, the ROCOF and U/O frequency, and from the active methods, the Slip Mode Frequency (SMF), the Active Frequency Drift (AFD), and Sandia Frequency Shift (SFS). After completing an experiment to investigate the efficiency of these methods, the results showed that ROCOF method has a success rate of 77.75%, U/O frequency has 55.56%, and Sandia frequency shift has 66.67%. All these methods have difficulties in detecting islanding condition when the DG power output matches the load, because the frequency change is very small. The SFS method could have a high detection rate than the ROCOF method. However setting the sensitivity of SFS is very difficult, and finding optimum sensitivity that works with all conditions is impossible, due to the trade-off between reliability and security. The results showed that the methods failed to detect LOM when the local load is more inductive than the one on the main grid section, keeping in mind that most loads connected to DGs are for plant operation or industrial applications are likely more inductive, which results in a lead power factor. A comparative analysis between ROCOF method and VS method in [55], showed that the ROCOF relay requires smaller active power imbalance than the vector shift relay for successful islanding detection. On the other hand, the ROCOF relay is more likely to have nuisance tripping than the vector shift relay. The PAD method uses local frequency measurement and the grid's frequency (estimates the grid's frequency using an extrapolation method) to determine the accumulated phase angle shift, and this would cause instability because of the continuing drifting of phase angle difference that would results in nuisance tripping.

2.7 Voltage Phase Angle Drift (VPAD) Method

The VPAD method is based on the PAD method. However, instead of using historical (stored) main's frequency, the main's frequency measurement is sent through a wireless signal to the LOM protection equipment of the DG, and compares them with the local measurements [56], as shown in equation (2-14). This method will show some latency, but it can be tolerated as long as the delay period is not more than 300ms and the local and grid measurements will be time stamped by the GPS. At the mains the measurements will be taken by a Phasor Measurement Unit (PMU),

and at the DG the measurement will be taken by the LOM protection unit, as shown in Figure 2-4.

$$\Theta_n = \Theta_{n-1} + 2\pi.(f_l - f_r).T_{sample} \quad (2\text{-}14)$$

Where,

(Θ_n)	Accumulated phase angle
(Θ_{n-1})	Subsequent accumulated phase angle
(n)	Number of accumulations
(f_l)	Local frequency at the DG
(f_r)	Remote frequency at the substation
$(T_{samples})$	Sampling intervals

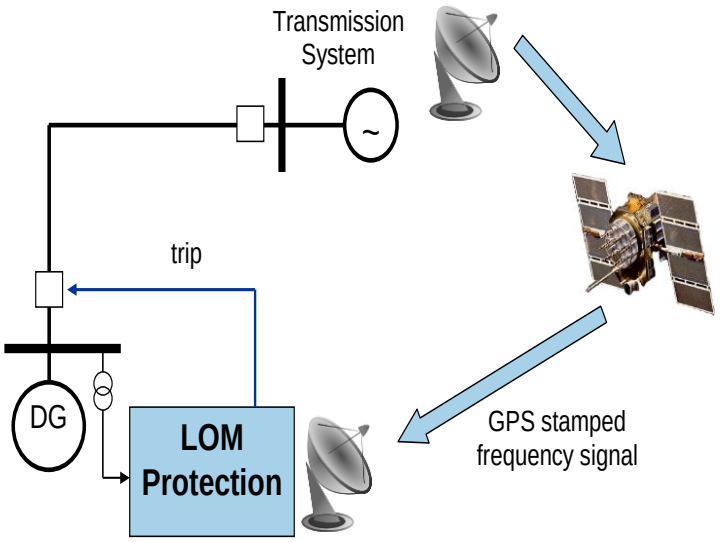

Figure 2-4: VPAD Satellite Based LOM Protection Method [56]

2.8 LOM Protection Methods' Assessment

The active LOM protection methods are limited to DG capacities lower than 50kW and/or complicated to implement and expensive. The prolonged time required for the active methods to detect LOM operation that exceeds in most cases the maximum allowed time of 2s for the LOM operation to continue [10]. Also, the perturbations that active methods make to the power system if implemented in wide area of the power network, it would cause serious instability to power system. On the other hand, the active methods have a very small NDZ or no NDZ at all. The passive methods are simple and cheaper to implement, have a fast response and can be installed for DGs with a capacity higher than 50kW. On the other hand, the passive methods have high NDZs and in many cases causes nuisance tripping that would

destabilize the power system. Hence, it is both too sensitive and unstable or unreliable, thereby; they would not satisfy both stability and sensitivity requirements. The communication based methods are expensive and complicated to implement, but by utilizing satellite communication it could be developed to be simple and less expensive to implement.

2.9 Proposed LOM protection method

The proposed LOM protection method is a communication based LOM method that is compatible with all types of communication. The new method works by implementing two accumulative of frequency difference between the local frequency at the DG side and the remote frequency at the substation side. The objective of the proposed method is to have a LOM protection method that is stable, reliable, and simple to implement. The method should be able to detect LOM and isolate the DG within 2s of the beginning of LOM operation without being affected by high communication and processing latency. This method is called communication based LOM protection method by frequency correlation (CFC) and the design and development of this method will be discussed in chapter 4.

2.10 Chapter Summary

In this chapter, the review of LOM protection methods showed that the differences between the passive methods and active methods are:

a- Passive methods are very sensitive and needs shorted time to detect LOM than active methods which need relatively prolonged time of LOM detection

b- Active methods unlike passive methods use perturbations to the power system at the PCC, that is why it is prohibited to implement active LOM methods on DGs with ratings >50kW

c- Passive relays are simpler and easier to install, while active relays have relatively complicated designs

d- Passive methods have high NDZ which makes them less reliable, while active methods are more reliable have almost neglected NDZ.

The active methods' perturbations to the power system have adverse effect on the power system, and passive methods' high NDZs put the power system equipment and the load at high risk. Thereby, to make the active protection less damaging and

reduce the perturbations times, some researchers combined them with passive method and to reduce the NDZ as well. These hybrid methods managed to reduce the NDZ and perturbations but could not eliminate them. On the other hand, the communication based methods proved to be reliable with no perturbations and with no NDZ. The VPAD Method that is based on the passive method in section (2.2.19) the Accumulated Phase Angle Drift (PAD) method, the VPAD method developed to improve the reliability and security of the PAD method by replacing the extrapolated frequency data with actual frequency data measurements, measured at the nearest power substation to ensure that the local protection make a reliable and secure operations. However, the reliability of this method heavily depends on the reliability of the communication method and accumulative phase angle difference in steady state operation would still have the problem of continuing phase angle difference drift. This problem cannot be solved by increasing the pre-set threshold, because this would only fix the stability and adversely affect the reliability of the LOM protection. Hence, the proposed method would solve the stability issue without affecting the reliability of the method. The development of the proposed CFC method will be discussed in chapter 4. In chapter three, there will be a review of the communication media methods, advantages and disadvantages of these methods and the assessment of the utilization of satellite communication to ensure the reliability of protection and reduce the time and expenses required to implement this method for up to 10000 DGs, each DG has to be with rating equal to or over 50kW and up to 50MW all over UK.

CHAPTER 3: COMMUNICATION SYSTEM

3.1 Introduction

In this chapter, the author will explore the communication structure and protocols and the communication mediums used in power system protection. Also, one of the objectives of this research is to determine the reliability of integrating satellite communication in LOM protection applications. The most important three issues that need to be determined are: communication delay effect on the LOM protection performance, the security of the communication link, and the economic advantage.

3.2 Communication Structure and Protocols

3.2.1 Communication structure layers

Communication structure is made of 4 main layers [57, 58, 59, 60, and 61]:

3.2.1.1 Data Link Layer

The link layer consists of the physical components that are capable of signalling, the electrical or optical cables that carry the signal, the definition of the data formats of the data with the signalling protocol, and the operating system components. The link layer job is to move packets from point to point over direct links. One of the link layers is the Ethernet.

3.2.1.2 Network Layer

The network layer consists of protocol elements such as header formats, signalling, and endpoint state transitions which serve the purpose of moving packets through the network, from endpoint through multiple internal nodes to endpoint. The network layer job is to move packets across the network from source to destination. Internet protocol (IP) is a network layer.

3.2.1.3 Transport Layer

The transport layer controls the movement of data between two endpoints. This is achieved by a distinct layer of protocol, which consists of header format definitions, signalling between endpoints, and endpoint state transitions. The transport layer job

is to provide a reliable service and to regulate the flow of information between endpoints, such as to maximize throughput and to minimize congestion and packet loss. The Transport Control Protocol (TCP) and the User Datagram Protocol (UDP) are transport layers.

3.2.1.4 Application Layer

The application layer consists of all and any software that makes use of the transport, network, and link layers to achieve end to end communication. The best known application layer entities are FTP (file transfer protocol), Telnet for remote log in services, and SMTP (simple mail transfer protocol).

3.2.2 Communication Structure Protocols

3.2.2.1 Internet Protocol (IP)

The network layer of TCP/IP is known as the Internet layer and its purpose is to establish a route through the Internet for the transmission of packets. IP is connectionless: that is, packets, which are called datagrams, are handled independently by routers as they pass though networks and no action is taken should a datagram be lost in transmission. A ‘best effort’ service is offered whereby there is no guarantee that any datagram will successfully arrive at the destination. Where reliable transmission is required, an appropriate protocol must be selected within the transport layer. Any lost datagrams may then be dealt with by a suitable protocol, such as the TCP, which is used to ensure reliable delivery of messages [57, 58, 59, 60, and 61]. A detailed description to the IP header format is available in Appendix A.1.

3.2.2.2 Transmission Control Protocol (TCP)

The most common of the transport layer protocols is the Transmission Control Protocol (TCP) that, along with IP, gives its name to the entire TCP/IP protocol model. TCP carries a stream of bytes from source to destination in a reliable manner using ARQ flow control techniques. The sending and receiving applications at the two end-points of a TCP connection use a port number to connect with TCP/IP [57, 58, 59, 60, and 61]. A port is the Transport Service Access Point (TSAP). The combination of a port number and an IP address uniquely defines an end-point and is

known as a socket. A detailed description to the TCP header format is available in Appendix A.2.

3.2.2.3 User Datagram Protocol (UDP)

The User Datagram Protocol (UDP) is a connectionless protocol that is unreliable because it has no flow control. UDP was originally intended for use with non-urgent data transmissions such as e-mail, but the fact that it does not use acknowledgements has led to interest in using it with protocols designed for delay-sensitive traffic such as the Real-Time Transport Protocol [57, 58, 59, 60, and 61]. A detailed description to the UDP header format is available in Appendix A.3.

3.2.2.4 Virtual Private Networks

Virtual private networks (VPNs) can be defined as the emulation of a private IP network using a shared IP infrastructure. IP tunnels are normally used to separate one VPN from another across the shared network. A point-to-point tunnel is shown in Figure 3-1 that connects the two routers and carries traffic transparently through address space Y. Both the source and destination networks are in a separate address space X. In most cases, both the service provider and the customer will use IP in their networks; thereby, the IP tunneling will use IP in IP encapsulation and the data passing through the tunnel will have two IP headers as shown in Figure 3-1. The customer datagram to be tunneled has a header X that maintains its original source and destination IP addresses. The service provider's router gives the packet a second IP header Y that contains the source and destination of the tunnel end-points. The original IP header is known as the inner IP header (X) and the carrier's IP header is called the outer IP header (Y), as shown in Table 3-1. When the datagram reaches the router at the far end of the tunnel, it is stripped of its outer header and is routed within the customer network to its destination [57, 62].

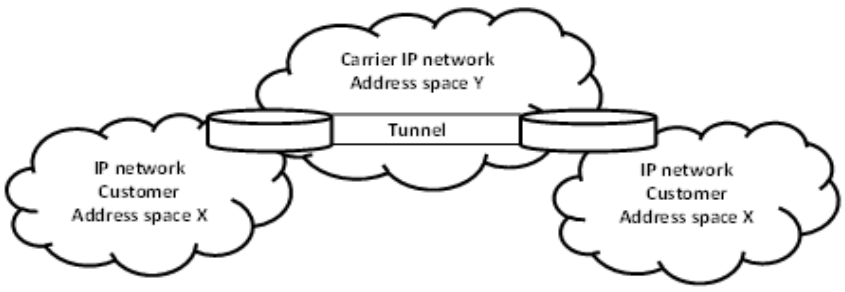

Figure 3-1**:** Point to Point IP tunnel [57]

Table 3-1: Extra IP Header for VPN

IP Header Y	IP Header X	IP Payload

3.2.2.5 IP security

The key requirements for providing secure communication within the internet are [61]:

1- Guard against unauthorized monitoring. Therefore, both eavesdropping and also monitoring traffic flow, movement and patterns.
2- Protect against the control of network traffic, for example spoofing, in which a third party creates datagrams containing bogus IP addresses.
3- Provide authentication and encryption mechanisms

Security is an important issue in IP networks especially when using VPN. A small group of protocols called IPsec, it provides security services at the IP layer by enabling a system to select required security protocols, determine the algorithm to use for the service, and put in place any encryption keys required to provide the requested services, as shown in Table 3-2. IPsec can be used to protect one or more 'paths' between a pair of hosts, between a pair of security gateways, or between a security gateway and a host.

Table 3-2: Total size of TCP/IP or UDP/IP header and payload with VPN connection

IP Header Y (20B)	IP Header X (20B)	Timestamp (4B) Encryption (4B) Options total size should be Max 40B	UDP Header (8B) OR TCP Header (12B)	Payload (32B)
The Total size of (88B-120B) and in case of TCP/IP connection (100B-132B)				

3.2.2.6 Routers

Routers work as a repeater by forwarding the message after de-capsulation and re-capsulation of the received data, for example, when sending a message from a LAN system to a WAN system the router will dispose of the received data header (suitable for LAN system) and replace it with a header suitable for a WAN system.. It also performs a variety of packet - processing functions: packet classification for handling/queuing/filtering, packet switching (also called flow control), packet transmission, and packet processing, such as compression and encryption, and support management functions such as trace route [57].

3.3 Communication Mediums used for Protection

The transmission media that provide the communication links involved in protection signalling are:

3.3.1 Pilot wires

Pilot wire is twisted pair of metallic conductors used for transmitting low voltage 50-60 Hz ac or dc signals between terminals. They're either privately-owned or dedicated leased lines, and they are installed either overhead or underground, although, public telephone circuits can be used as well. A leased line can be assigned by a service provider to connect between two points and the connection will be dedicated entirely to this customer, and nobody else will use any portion of it. The connection is secure, always available, but expensive, as service providers have to dedicate their equipment on that leased line entirely to one customer [58, 59]. The disadvantage of these wires is that their resistance restricts the distance between terminals, and it would be very expensive, time consuming and disruptive in installation when the number of connections and distances involve nationwide area.

3.3.2 Power line carrier (PLC)

The technology of using power lines for communications derives its name from the fact that the original signals were considered unmodulated RF carrier. A coupling capacitor that can also be used for potential metering couples the RF signal to one or more phases of the power line. Wave traps provide signal isolation and raise the terminal RF impedance in the presence of high bus capacitance. PLC communication can provide signal or dual frequency keyed carrier or tones. Multiple audio channel systems use a broad spectrum for voice, and tone telemetry and relaying. Typically PLC communications operate using the frequency range of 30-300 KHz. The modulation types used for this application are narrow band phase shift keying (PSK) and spread spectrum technology. The disadvantages of the PLC are that the cables are adversely affected by the electromagnetic field caused by the power cables and during power events and it share the pilot cables disadvantage when it comes to long distances and large number of connections especially in urban areas [58, 59].

3.3.3 Microwave

The microwave (Terrestrial wireless) allocated frequency bands range from 1.9 to 6GHz. Transmitter-receiver pairs must have unobstructed line of sight between them. Effective microwave path lengths are usually less than 160 km because of attenuation and earth curvature. Active repeaters receive and retransmit the signals. Passive repeaters are like giant mirrors that bounce the microwave beams. Microwave systems divide the bandwidth into 4 KHz analogue audio channels or 8 KHz digital audio channels. The effective analogue audio channels or equivalent digital audio channels have a usable voice band restricted to 300 to 3600 Hz. This allows the necessary filtering to provide good separation between adjacent audio channels. Microwave communication is adversely affected by multipath deflection because of thermal layers in the air. Severe rain and snow showers can absorb the microwave energy and disrupt communication [60].

3.3.4 Fibre Optics

Fibre optic systems operate the same way as digital microwave except they use frequencies just under the visible light spectrum. The advantage they offer over microwave communication is broader spectrums and it is far less affected by atmospheric disturbances and noise. As for its advantage over pilot wires and power line cables is its immunity against electromagnetic field disturbance such as the corona effect [59].

3.4 Phasor Measurement Units (PMU)

It is a digital recorder with synchronizing capability and time stamps, records, stores phasor measurements and sends them to the required destination and usually it is located at regional power substations at transmission or distribution networks with voltage levels of 132kV-400kV, where those substations' locations are chosen to be over 100km apart (the locations' distance could also be affected by the thermal boundaries in the UK power networks that would dictate the regions to be from 10-18 regions). The recorded measurements will be collected by the substation management, in this case, it should send the measurement to all the DGs in the selected regions through a satellite link, and the information sent should be continuo. In addition, the measurement values that exceed the user set upper and lower limits

will be flagged. The Figure 3-2 shows the PMU functionality denotes that samples from the voltage and current analogue signals to anti-alkalising filters and be converted to digital signals by A/D at the rate of 5 samples per cycle in 50Hz system frequency. The measurements are sent to the protection and measurement processor, and it receives the time stamp from the GPS and IRIG-B time code (Inter Range Instrumentation Group time code). The type B is widely used in synchronization signal for substations (specifications: un-modulated, with no carrier, shows time of year (BCD, binary coded decimal format), shows seconds of day in binary (SBS) and shows the control function (CF) but all information of the IRIG-B are presented by only 3 digits (in this case B000). The measurement processors provide the synchronized Phasor measurement and send it to the Ethernet Processor which provides communication according to (IEEE C37.118 Data) standards and send them if frame format (TCP/UDP) to the set destination. The PMU in this application is required to record and send the system frequency and the voltage phase angle for three phase, and voltage phase angle, and send 10 measurement reports per second through a satellite link to several DGs in the user predetermined region [62, 63, 64, 65, 66, 67, 68, 69, 70, and 71]:

1- The PMU operation and accuracy should be compliant with IEEE standards C37.118.1/2. It should be ~1µsec time accuracy, all the recorded data should be time stamped by GPS (UTC) and in case the GPS signal was unavailable the PMU will switch to local clock and when the GPS signal come back the PMU will resynchronize.
2- The PMU signals will be sent using floating-point format and the phase angle will be sent in polar format, $(V/2^{1/2}) \angle ø$. The phase angle will be reported in the range of ±180°and the PMU should be able to compensate for the difference.

In addition, in phase angle measurement, when calculating the phase angle the PMU needs to take into account the system frequency at that moment which is rarely equal to the nominal frequency, thereby, the time of cycle period of the signal will be shorter or longer than in nominal frequency.

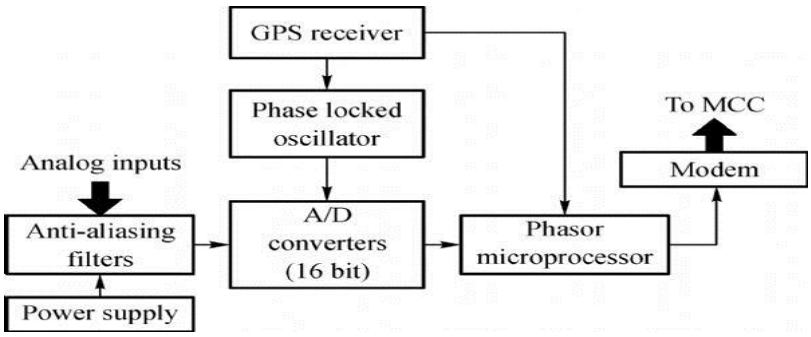

Figure 3-2: PMU function block diagram [19]

3.5 Satellite Communication

3.5.1 Satellite Link Components and Functionality

The Satellite link contains physical part and nonphysical part, the physical part is a combination of spacecraft transponder and the earth transponders. The spacecraft transponder contains the transponder components aboard the satellite, while the earth transponders are the sum of the two earth stations. The Downlink station consists of a Low Noise Blocker (LNB). The LNB receives the signal, convert it from high frequency to lower frequency, and send the signal to the receiver to get de-modulated and decoded.

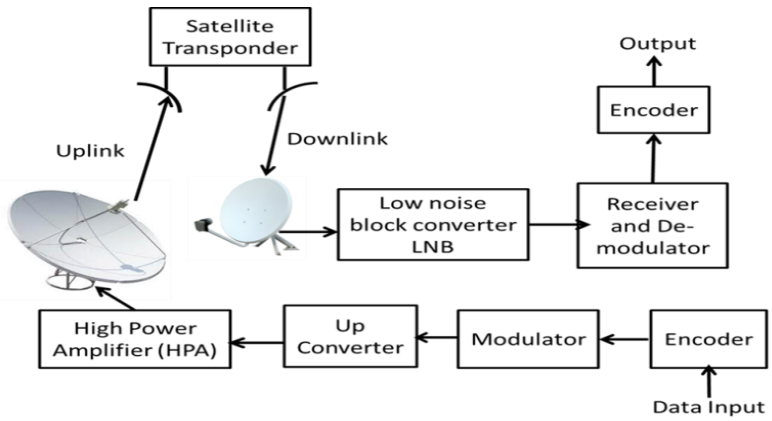

Figure 3-3: Satellite link's Physical Components

The Uplink station has a High Power Amplifies (HPA) rather than the LNB, as shown in Figure 3-3; the station will receive the signal and encoded. After encoding it would be modulated, the frequency of the signal is converted from low to high frequency in order to be transmitted. Due to the long satellite link path, the signal

needs to be amplified to compensate for the effect of high attenuation that will be suffered by the link path [72, 73, 74, and 76].

3.5.2 Satellite Link Considerations

The priority in this application is the reliability of the link, GEO (Geostationary) communication satellites have to be the choice, because they are designed for high reliability, while the commercial satellites are designed for high throughput. The type of frequency band should In addition be chosen and this choice will affect the size of the antenna, power of transmission, atmospheric losses, interference, carrier to noise ratio (C/N), carrier to noise density ratio (C/No), link availability and system reliability. Assuming that the distance between the earth station and the satellite station is fixed (42159km) for GEO stationary satellites, In addition the antennas' efficiency on both sides are fixed 65%, fixed system losses, the satellite antenna size is fixed and by that the effective satellite antenna area will In addition be fixed. The C/N and C/No ratios are desired to be high in satellite communication links in order to reduce the error and increase the efficiency of the link such as in power system protection when efficiency is very important and availability is vital. Satellite communication links, requires high frequencies, on the other hand, they require reliable links that will not be affected by rain attenuation. Especially in countries such as UK and precisely in Scotland were rain would definitely be a major issue when designing a satellite communication link. In order to reach a link availability of 99.99%, it requires a C-band (6/4GHz) system rather than Ku band and Ka- band (Ku-band 18/12, Ka-band 30/20GHz). Due to the effect of rain attenuation on the C-band link is very small and can be neglected and the free space loss will decrease.

The effect of rain attenuation on the Ku and Ka-bands is so significant and it could get to ≥ 60 times (in real value) than the effect on the C-band link. On the other hand, choosing C-band frequency will require a bigger antenna for the earth station than the case of choosing Ku-band or Ka-band, putting in mind that the cost of the antenna at the earth station is only 10% of the total cost of a VSAT link components including installation, maintenance and operation service. On the other hand, this choice will lead to a disadvantage of a decrease the C/N and C/No ratios and increase the spreading loss, and in order get over this problem, compensation is required by

increasing the transmission power of the antenna. In case of developing a device with very small antenna, it will not be possible to choose C-band, the highest frequency band available should be chosen. Hence, Ku-band or Ka-band will be the choice but with disadvantage of the low availability. In order to establish a secure and solid satellite link, it could require an increase in the transmission power, which would lead to higher costs and more system thermal losses [72, 73, 74, 75, 76, 77, and 78].

3.5.3 Latency

GEO satellites most of the channel latency is a propagation delay, assuming that the link path is linear and with fixed distance from the earth station to the satellite of choice is 42,164 km, and this was calculated according to the distance between earth and the GEO satellite, which is 35,788 km and a mean earth radius of 6371 km. According to this assumption, the round path delay should be of 120-140ms, which means that the link between a transmitter and a receiver is 240-280ms. This is the minimum propagation delay corresponding to communication between two transceivers located at sub-satellite point but the additional delay, which depends on the precise locations of the transceivers, is small. Variation in propagation delay due to the dynamics of the atmosphere can be neglected. Propagation delay for non-GEO satellites is less than that of GEO systems. For medium and low Earth orbit (MEO and LEO) satellites, the two-hop delay is of the order of 100ms and 10ms, respectively (depending on the precise orbital parameters and ground station locations). These systems could be used with low gain antennas (as is typical in satellite mobile applications) to avoid the need for antenna tracking. The disadvantage of antenna tracking is not only increased cost but decreased reliability. Failure of the tracking system would typically result in complete loss of the communication system with consequent loss of protection [72, 73, 74, 75, 76, 77, 78, 79, 80, 81, and 82].

3.5.4 Reliability

The reliability of the link, in order to achieve 99.99% availability of the link we have choose C-Band (6/4GHz) because with a C-Band link the effect of the rain attenuation can be neglected and rain is a major problem in UK and specially in Scotland. While in Ku-Band (18/12.5 GHz), K-Band (26.5/18 GHz) and K_a-Band

(40/26.5 GHz) the effect of rain attenuation will significant (10 times or more (in decibel value) than the effect in C-Band) and this will definitely cause an outage. However, the Antenna size required for a C-Band link will be very big (6-7m diameter), and the problem with availability in K_u, K and K_a –Bands can be improved by significantly increase the power to very high amounts (such as in one of the C-Band links for the uplink transmission power it was estimated to 850W). Although that this could lead to more expensive system it will require a lot smaller antenna than in C-Band link, putting in mind that the expenses of the antenna will only represent 10% of the total expenses of VSAT system (including indoor, outdoor equipment, space segment, link service, maintenance, installation and antenna. The effect of interference and noise, due to: sun, solar radiation, rain, system noise & quality, attenuation, polarization, antenna alignment, fading signal, clouds, and many more, which need to be considered when designing the satellite link. In order to, avoid link outages and burst errors, the choice of transmission power, the antenna gain, C/N, bit energy to bit noise density (E_b/N_o), and other factors that are explained in APPENDIX B. In order to have a reliable and efficient link, the error detection & correction, modulation applied the signal have to be addressed, for technical and economical reason [72, 73, 74, 75, 76, 77, 78, 79, 80, 81, 82, and 83].

3.5.5 Noise and Interference

When the signal is subjected to high attenuation which makes the noise power higher than the signals power at some periods of time and over-whelms the signal, causing error busts, there are many sources of noise and interference, five of them will be briefly discussed [72, 73, 74, 75, 83, and 84]:

1- Terrestrial Interference; happens in C-band link system due to sharing with other microwave links.
2- Cross-polarized interference: This type of interference will come from transmissions to and from the satellite on the same frequency but in opposite polarization.
3- Adjacent satellite interference: Most of Satellites have other satellites adjacent to them in the same orbit and operate at the same frequency; this interference could add ≥ 30% to the total thermal noise. Calculating the thermal noise that

this kind of interference cause would need some factors, and these factors are; the number of satellites involved the satellite's spacing (orbit separation), the side lobe characteristics, and the types of the signal used by both, the desired satellite and the interfering one. There is an equation presented by ITU [85] that estimates the gain of the side lobes at $\emptyset$ which represents the angle measured from the earth station, and is the angle between the line of sight to the desired satellite and the interfering satellite as shown in equation 3-1:

$$G(\emptyset) = 29 - 25log\emptyset \quad (3\text{-}1)$$

Where,

$(G(\emptyset))$ Side lobes gain
$(\emptyset)$ Angle measured from the earth station

If EIRP of the interfering satellite is equal to the EIRP of the desired, the maximum value of the carrier to interference ratio (C/I) will be determined by subtracting $G(\emptyset)$ (side lobes gain that is measured in dBi) from the peak gain of the antenna, and if there is a difference between EIRP for both satellites, this may increase or decrease (C/I).

4- Intermodulation noise: This noise is caused by the distortion produced by transponder and the High Power Amplifier (HPA) in the earth station and the noise caused by all components of earth station, which is called Total System Thermal Noise (T_s) and its significant compared with other sources of noise.

5- Antenna miss-alignment: This one is not directly responsible for interference and noise; it is the losses in the antenna gain caused by the earth antenna because it is not aligned with the desired satellite antenna, and this will lead to degradation in C/N.

3.5.6 Channel Encoding and Modulation

In a fixed satellite communication links with a Geo-stationary satellite were the propagation delay is very long and bit error rate is relatively high because of the significant attenuation that the signal subjected to makes noise and interference over whelming to the data signal more often. Hence, it cannot be afforded to have an Automatic Repeat Request (ARQ) which is part of the TCP protocol. In applications such as power system protection where reliability and performance is vital, and even

though high efficiency is not a priority for this application, a false measurements sent to the LOM protection devices could cause a disaster, because it will to be sent to hundreds and maybe thousands of DGs causing a false tripping or blinding. Receiving a false measurement is far more damaging than not receiving one at all, so it can be argued that efficiency is as important as the reliability for this application [57, 60, 74, and 75]. In satellite communication links that deploy geo-stationary satellite with Ku-band 15/12 GHz, the propagation delay is very long because of the significant distance between the earth station and the satellite, and the bit error rate is relatively high because the signal will suffer high attenuation. This could reduce the power of the signal to an unacceptably low level. The TCP/IP protocol provides an Automatic Repeat Request (ARQ) whenever the packet is lost or corrupted, this will require a two way channel, which in turn doubles the propagation delay, reduce the throughput of the channel, and double the required bandwidth. This cannot be afforded in this instance. Therefore, the UDP/IP protocol needs to be used instead, which has no ARQ and thus is less reliable and has higher BER level. It is known that receiving a false measurement could potentially cause unwanted tripping of large amounts of DGs causing dangerous impact on the transmission system. Thereby, it is vital to utilise additional measures to minimise these negative effects of one way communication. Some form of Forward Error Correction (FEC) with modulated analogue carrier can be used for this purpose. Many FEC methods can be applied to a digital communication signal such as turbo encoding, and Low Density Parity Check (LDPC) being the most popular in satellite communication, because they can achieve a channel capacity close to the Shannon maximum capacity, and thus reduce the required Energy per Bit to Noise Power Density ratio(E_b/N_o) . For time sensitive applications that require real time communication, the turbo method is preferred over LDPC because of the long processing delay for LDPC. In space missions, the additive Gaussian noise (AWGN) channel is a major limitation issue. That is why in deep space communication it is vital to use the most efficient coding methods. The turbo code and the LDPC code are used. For DVB-S2 channel, the type of coding considered is the LDPC code of 16.2kb or 64.8kb code words and coding rates (1/4 to 9/10). For DVB-RCS channel type the code type considered is the double binary turbo codes with 12 frame sizes from 48b to 752b couples, and 7 encoding rates of

1/3 to 6/7. By modulating the carrier after encoding the message, the carrier can be amplified to strengthen the signal to the required power level to have sufficient carrier power to noise power ratio (C/N) and the bit energy to noise density ratio (E_b/N_o) to minimize the noise effect [57, 59, 60, 62, 74, 75, 79, 82, and 84].

3.5.7 Link Budget Analysis

In order to design a satellite communication link the author needs to examine the performance for each source of gain and loss and the link budget is the most effective means since it can address and display all of the important components of the power balance equation expressed in decibels. The link budget is made of downlink budget, uplink budget and the overall link budget, the downlink involve the design and characteristics of the signal sent by the satellite antenna and received by the earth station antenna and the uplink involves the design and characteristic of the signal sent by the earth station antenna and received by the satellite antenna. Their parameters could be different, for example, the frequency of the carrier used in the uplink should be higher than the frequency of the downlink, and the transmission power needed for the uplink should be higher than the transmission power of the downlink. The decibel value of the EIRP can be estimated according to the coverage zone, the narrower the coverage zone the higher the EIRP is needed. For example, the area of the United States of America is at least 32 times the area of UK; the value of EIRP needed to cover the USA is 27dB. Thereby, the numerical value of EIRP should be increased by 32 times, which leads to EIRP equal to 42dB, and by adding 15.5dB it will be equal to 57.5dB. In order to compensate for small antennas and high frequencies, the EIRP value for the downlink was estimated at 56dBW after feeder losses. While in the uplink, the Pte was estimated to be 4 times Pts in the downlink, because the frequency used is higher, and because of the higher attenuation effects, especially rain fade. These values can be manipulated at the control centre of the transmission station according to the atmospheric conditions and the quality of the link. The EIRP value has a significant impact on the Direct to Home (DTH) receiving antennas' diameter. Whenever the numerical value of EIRP increased by four times, the EIRP value in decibels will increase by 6dB, which allows the reduction of receiving antenna diameter to 50%. Having smaller antennas is an economical advantage and time saving in installation [72, 73, 74, 75, 76, and

81]. In Appendix B.1 and B.2 all the link budget analysis steps of calculations and assumptions are presented with an example which explains the challenges in setting a satellite link and how they could affect the performance of the satellite communication link. There is also a MATLAB Simulink model representation for satellite link shown in Figure 3-3, and a detailed definition to the block functions used, shown in Appendix B.3

3.6 Performance Requirements

Overall time required for LOM to be detected and the DG to isolated has to be within 2s as mentioned in chapter 1 and 2 [10]. The communication and protection processing time is estimated to have a maximum delay of 640ms excluding the LOM protection relay operation delay and time required for LOM detection [84]:

1- Communication time:
   a- Satellite communication propagation delay of 278ms (fixed)
      Propagation delay= (round trip length)/speed of light
   b- Internet communication delay of 40ms for TCP/IP connection
   c- Sending and receiving modem processing delay of 60ms (minimum of 30ms)
2- PMU processing time delay of 60ms (55ms fixed and a variation within 5ms). This processing delay for P-class PMU with any data frequency and for M-class PMU with 50 measurements every second.
3- LOM protection relay processing, detection and operation are unknown
4- Trip signal time of 50ms
5- Circuit breaker operating time of 50ms to 150ms

The overall time must be less than the maximum time for which a fault can remain on the system before causing any power plant, generator, and protection equipment damage or causing a loss of system stability. Signals are subjected to noise and interference with all communication mediums. If noise and/or interference change the signal used to carry the command, unwanted commands may be produced. If noise occurs when command signal is being transmitted, the command may be retarded or completely missed. Performance is expressed in terms of security and

reliability. Security is assessed by the probability of an unwanted command occurring, while reliability is assessed by the probability of missing a command.

3.7 The Choice between Internet and Satellite Communications

The choice between satellite and internet communication for this application is dictated by the reliability, simplicity, as well as economical and time saving factors. The data for this application and other power system control, protection and monitoring applications is normally sent to the central control station (node). Most of the power system communicated data is designed to be transmitted to the central node in case any changes occurred in the power system behaviour or states of power system devices, which require access and processing of measurements from the wider area [62, 72]. In the case of wide area disturbance this could potentially cause congestion in the central node, while in satellite communication there is no congestion problem. Satellite communication network can be very simple. The installation of the antenna and the receiver takes about 15 minutes; in addition, the cost of installation for every generator owner will be the same [61]. While for dedicated internet access line (DIAL), the cost of installation will differ for generator owner to another, and from a city to another. It depends on the location (According to the distance of the customer end point from the nearest connection point), and due to the disruption caused by the installation, In addition, due to the low and fixed bandwidth and the data rate, the satellite communication solution will be cheaper than the DIAL [85]. The lowest data rate for the latter is 2Mbps, which means that only 9% (TCP/IP) of the line capacity will be in use, while in satellite communication a low bandwidth and high number of generators mean lower leasing costs, and all the locations can be reached regardless of their distance [86, 87].

3.8 Data and Communication Requirements Assessment

In order to obtain the data measurements, a Phasor Measurement Unit (PMU) is required; the unit available is (SEL-451), which is a protection, Automation, and control system unit with PMU functionality. This unit is compatible with the IEEE standard C37.118.1 – 2005 (revised 2011) [63], which handles the data measurement formatting and the communication of the PMU with the substation and other protective devices. As shown in Table 3-3, the data measurement formatting,

message size, and signal speed [64]. The data measurement format will be in hexadecimal, the total data size according to Table 3-3, is 32Bytes for every message, plus 58Bytes for TCP/IP headers requirement, or 46Bytes for UDP/IP headers requirement for every message, and this will add to 78 or 90Bytes. A data measurements will be sent every 20ms (50 times a second), which makes all together 4500Bytes a second. Every message will contain a GPS time stamp, frequency, rate of change of frequency, positive sequence, magnitude and phase angle of positive sequence voltage. All these measurements are presented in integer values as shown in Table 3-3. The baud values are determined by the SEL 451 manual according to the type of modulation of the signal, which either ASK or Manchester B2xx, modulation type will be deployed [60]. The ASK method will require a bandwidth with a value near the data rate value, while the Manchester method will require a bandwidth near twice the data rate. That is why the signal speed of 19200 baud was chosen for the data to pass through the PMU portal without causing any error.

Table 3-3: Phasor Measurements Format

Item	Quantity	Bytes per quantity	Data Measurement size in Bytes
Time Stamp: Sync, Frame size, IDCODE, SOC, FRAMESEC, CHK	6	2, 2, 2, 4, 4, 2	16
Phasors	1 Positive Sequence Voltage Phasor	Floating point 8	8
Frequency	1 Frequency, 1 Rate of change of frequency	Floating point 4	8
Total	9		32

The data measurements format will be according to IEEE Standard C37.118-2011, which means that the measurements will be in Hexadecimal format and with a cyclic redundancy check code (CRC-CCITT encoder)[60]. This standard is compatible with IP format, and each message will be sent in a frame (50 frames a second). As for the quality of the message, the C37.118 already has a quality standard applied by the PMU, and a GPS time stamp would be applied to the data measurement at the PMU side. The security of the link is very important; thereby the UDP/IP message should be encapsulated in VPN connection, encrypted and scrambled. Satellite communication links deploying geo-stationary satellite with Ku band 15/12 GHz, the propagation delay is very long because of the long distance between the earth station

and the satellite, and the bit error rate is relatively high because the signal will suffer high attenuation. This would reduce the power of the signal to a level that lead to the noise and interference to over whelming the channel more often. Hence, in case of using TCP/IP protocol, it cannot be afforded to wait until the original data to be retransmitted after a feedback message from the receiver to the transmitter especially for power system protection applications, because this will cause twice the original delay, reduce the throughput of the channel, and double the required bandwidth [61, 62]. In practice, filtering is implemented at the transmission and receiving sides, which introduces Inter-symbol Interference (ISI) (that occurs in the A/D or D/A process), that would degrades the BER performance. In order to have an ISI-free transmission, a larger bandwidth (BW) that occupies the carrier is required. Thereby, a raised cosine filter that gives smoother transitions in the frequency domain is needed to be utilized. Hence, a roll-off factor value (which affects the transfer function of the raised cosine pulse filter) has to be chosen. The nominal value of the roll-off factor for satellite communication is between (0-0.5) [75], for this application the roll-off factor is 0.35 [85] and it can be decreased to 0.25, it depends on the relationship between the modulation rate and encoding rate [85] as shown in equation (3-2). By employing QPSK modulation the system will require half of the energy required when employing 8PSK modulation to achieve the same BER target with twice the bandwidth.

The choice between three combinations of modulation and coding rate showed that a combination of Turbo(1/2)/QPSK requires a lowest energy among the three, while the combination of Turbo (3/4)/8PSK requires twice the energy of the first combination and third of its bandwidth. After a trade-off between the three elements lead to the combination of Turbo (3/4) and QPSK that requires 125% of the first combination energy requirement and two thirds of its bandwidth. A trade-off between the three elements also depends on what's available and how much it would cost. The trade-off is usually made by the satellite communication operator according to the expenses, power required, type of data being transmitted, and level of security. The trade-off made by the author is only considered the type of data and the performance based on the detailed performances of several encoding and modulation combinations that are shown in [88]. Modulating the signal carrier using QPSK

method would also help with improving the spectral efficiency (the ratio of transmitted bite rate to the BW that is occupied by the carrier) because this kind of modulation has two bits per element (M=4), as shown in equation (3-3). This would eventually compensate to the required redundant bits that should be added to the data in the FEC encoding and it reduces the envelope of fluctuations introduced when filtering the carrier [74, 75], which leads to a bandwidth equal to 39000Hz [64] as shown in equation (3-2):

$$BW = R_b . enc_r . mod_r' (1 + Roll_f) \quad (3\text{-}2)$$

$$Se = (\log_2 M)/(1 + Roll_f) \quad (3\text{-}3)$$

Where,

(BW)	Bandwidth occupied by the carrier
(R_b)	Bit rate
(enc_r)	Encoding rate
(mod_r)	Modulation rate
$(Roll_f)$	Roll-off factor
(Se)	Spectral efficiency
(M)	Number of modulation states

As a result the Bandwidth (BW) for the satellite link should be:

$$BW = ((32B + 46B) \times 50 \times 8) \times \frac{2}{1} \times \frac{1}{2} \times (1 + 0.25) \; = \; 39000 \; Hz$$

$$Se = (\log_2 4)/(1 + 0.35) = \; 2/1.35 = 1.48$$

This BW can be reduced to ≤ 19500 Hz by using 8PSK modulation or choosing a lower coding rate, it depends on the power level used for transmission, the Bit Error Rate (BER) required, the value of E_b/N_o , and the link margin. As shown in Figures 3-4 and 3-5 [88], and equations (3-2) and (3-3), the choice of the type of modulation and the coding rate are based on achieving the required BER with the least energy and bandwidth possible.

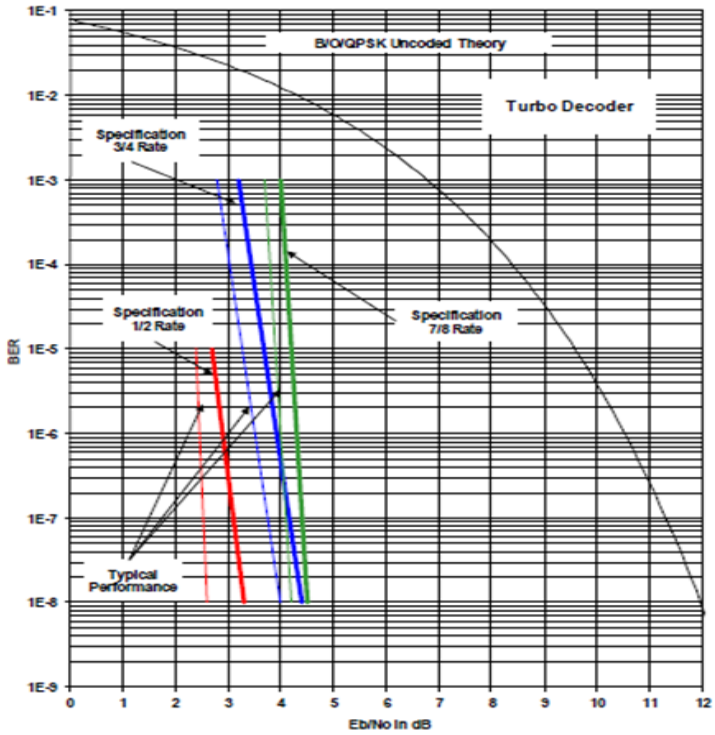

Figure 3-4: BER performance and E_b/N_o requirement for QPSK modulation with turbo coding [88]

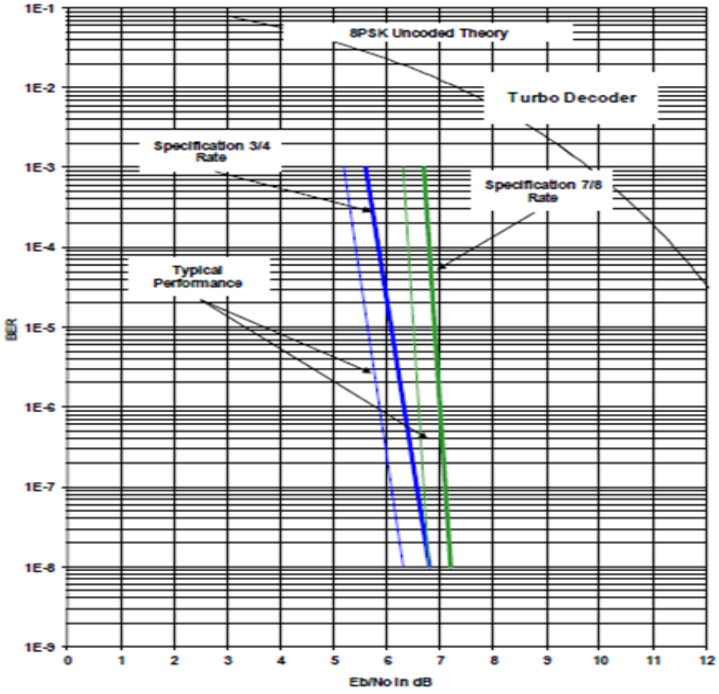

Figure 3-5: BER performance and E_b/N_o requirement for 8PSK modulation with turbo coding [88]

3.9 Chapter Summary

In this chapter, the internet and satellite communications structure of layers and components were discussed. The choice between the two was based on economic, construction, time, availability, and data requirements. The conclusion is that in order to reach all participants' DGs in all UK's geographical locations in the most economic and time saving way possible satellite communication will provide similar performance to the internet in the area of availability and reliability. Satellite communication will make a better communication method when it comes to the installation, construction, urban disruption, time saving, and the installation and annual cost on every participant. However, the latency at the satellite communication is very high (due to the long distance of free space path), considering that the LOM protection is real time application. In order to reduce this delay, rather using the reliable TCP/IP protocol connection we have to use the unreliable connectionless UDP/IP protocol. However, this can be compensated by using VPN connection, encryption, scramble, encoding, and signal modulation in signal broadcasting and the fact that unlike the internet the satellite signal will go from source to destination with only on stop at the space station. While the internet link route could pass by at least 10 routers before it reaches the destination. Also, increasing the data frequency from 10 measurement per second to 50 measurement per second will decrease the M-class PMU's processing delay by up to 240ms to bring the PMU processing delay to 60ms. Questioned raised during the literature review regarding the ability to achieve synchronisation of the remote data with the local data without using a GPS for economic reasons, and the detection of high BER and loss of communication during the operation of the LOM detection to avoid nuisance tripping that will undermine the power system security. In chapter 4, the development of the proposed communication based LOM protection by frequency correlation method will be discussed. The proposed method will be compatible with all types of communication medias.

CHAPTER 4: COMMUNICATION BASED LOSS-OF-MAINS PROTECTION METHOD BY FREQUENCY CORRELATION

4.1 Introduction

As explained in chapter one, the LOM operation is when the local load and DG get disconnected from the main grid, and the latter normally supply part of the local load. When the LOM operation starts there will be either more or less than the local DGs, the power frequency will either decrease or increase depending on mismatch between the load and the generation. Hence, in response the DG will either accelerate or reaccelerate to meet the load and control the power frequency, and when the power mismatch exceeds the capacity of the DG this will place a lot of strain on the turbine engine and the DG. Normally, the maximum turbine force increase allowed is 10% over its capacity (1.1 per unit), to prevent mechanical strain on the shaft. If the LOM operation continued long enough the DG could exceed the thermal capacity limit and damage the DG's insulation. Thereby, the LOM operation is allowed to continue for no longer than 2s [10], during that time the LOM should be detected and the DG isolated from the local load to protect both the load and the DG until the DG and load reconnect with the grid and synchronization is established.

In chapter two, many LOM protection methods were discussed and difference between them in term of their reliability, security and the period of time required for the LOM protection to detect LOM, initiate a trip signal and isolating the DG from the load. It was concluded that the communication based LOM protection methods can have a zero NDZ which makes them more reliable than other methods. However, communication methods are relatively expensive. In chapter three, many communication methods were discussed and it was concluded that the utilization of satellite communication will reduce the installation and operation expenses. In this chapter we will introduce a new LOM protection method that is based on communication, frequency accumulative difference and data convergence. Before starting with the development of the method we have to consider the type of data

used that may affect the LOM algorithm reliability, and security. We'll start with the data measurements' type with consideration to the security and delay issues that would be affected by this decision and discuss the method type with consideration to the communication delay.

4.1.1 Data Measurement Type

The data measurements provided by the PMU, as shown in Table 3-3, the format of the message includes the positive sequence voltage phasor, power frequency, and rate of change of frequency. The Phasor is a combination of two measurements which are the Phasor magnitude and angle. From these four measurements the Phasor angle and power frequency measurements were considered to be used in the LOM protection algorithm. The Phasor angle was considered first to be used as a direct accumulation of the phase angle difference between local and remote locations, rather than using the power frequency, as shown in equation (4-1):

$$\Theta_n = \Theta_{n-1} + (\Theta_l - \Theta_r) \qquad (4\text{-}1)$$

Where,

(Θ_n)	Accumulated phase angle
(Θ_{n-1})	Subsequent accumulated phase angle
(Θ_l)	Local (in this case Glasgow) phase angle measurement
(Θ_r)	Remote (in this case Manchester) phase angle measurement

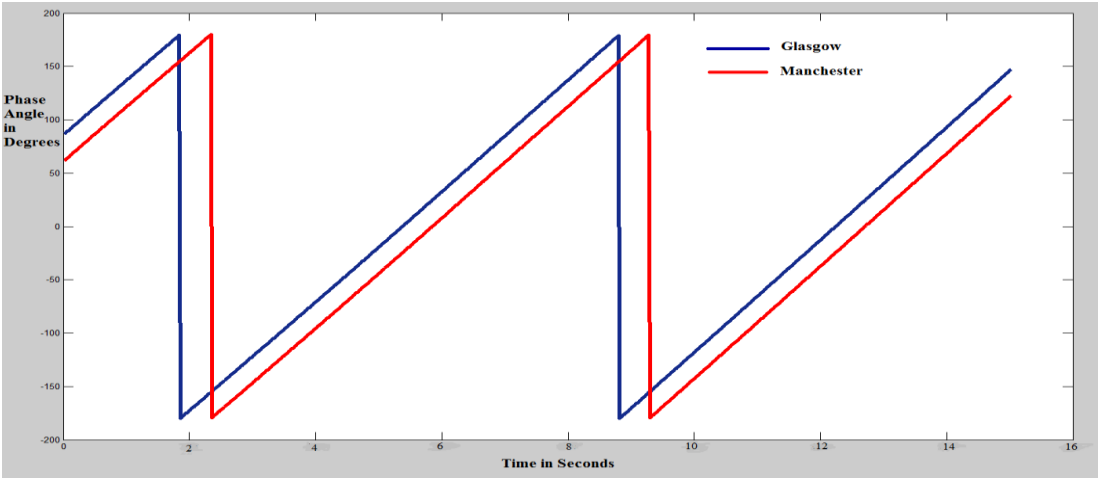

Figure 4-1: The positive sequence voltage phase angles measurements for locations at Glasgow and Manchester

However, the analysis showed that even when the two measurements are synchronized there will always be a variable difference between the two that could

reach up to 52°, as shown in Figures 4-1 and 4-2, and this difference changes with time during the day and changes throughout the week. There is also a difference is phase angle between Glasgow and London that could reach up to 60°. As shown in Figure 4-3, the change of difference between two phase angles of the same data presented in Figure 4-2 with the remote frequency delayed by 0.5s. The delay could either increase or decrease the phase angle difference. In Figure 4-3, the half a second delay caused an increase in difference from 24.9° to 51.7° as shown in Figures 4-2 and 4-3.

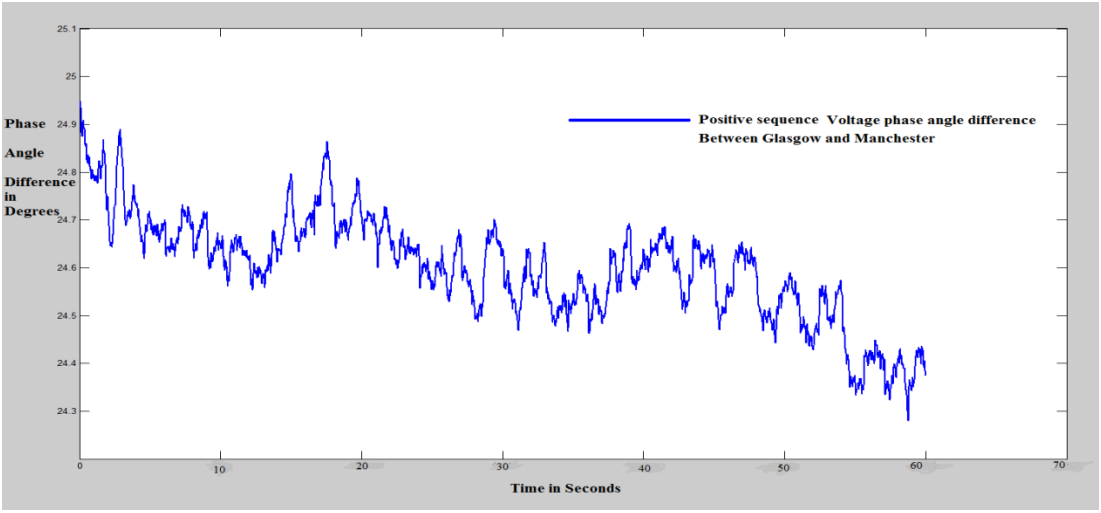

Figure 4-2: Difference in phase angle between locations of Glasgow and Manchester for the same set of positive sequence voltage shown at Figure 4-1

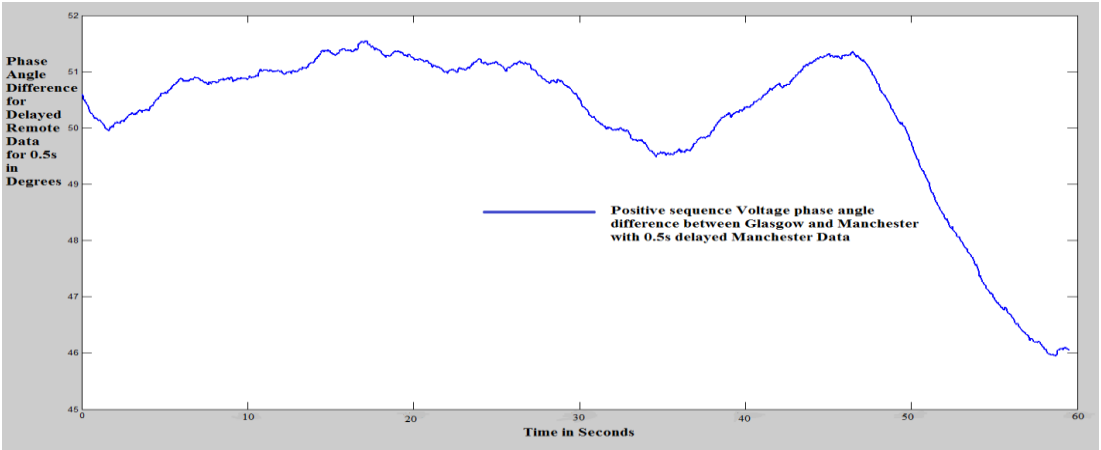

Figure 4-3: Difference in phase angle between locations of Glasgow and Manchester for the same set of positive sequence voltage phase angles shown at Figure 4-1 with a 0.5s delay for Manchester data

The phase angle difference between distant locations in UK is caused by the loads and generation that are connected along the line between these locations. The loads and generators change all the time and there are also other factors that contribute to the difference in phase angles such as power transformers, Flexible AC Transmission System (FACTS), shunt or series reactance, and shunt or series capacitor banks that are connected from time to time to control the power flow of the power system network. In order to eliminate this problem there should be a dynamic prediction model that enables us to compensate the difference of phase angle within the LOM protection algorithm. That kind of a model would be very complex and difficult to develop and it is beyond the scope of this research. Hence, the phase angle measurement cannot be used, instead the power frequency will be considered because it does not have this problem and when the frequency measurements from the locations are synchronized they show a very close match.

4.2 Frequency Correlation (CFC) LOM protection Method

The Communication based LOM protection by Frequency Correlation (CFC) method is similar to the VPAD methods defined in chapter 2, in using the power frequency accumulative sum of difference. However, the CFC algorithm is a composite of two main equations, which result in two variables. The first variable is an accumulative sum of difference (ASD), and the second variable is a frequency convergence measurement (CM). In order for the relay to trip, both of these variables should be equal or greater than the pre-set threshold values:

4.2.1 Accumulative Sum of Difference (ASD)

In steady state, when the DG is synchronised with the main grid the difference between the local and remote frequency very small and almost negligible. If LOM occurred the difference between the two frequencies will start to widen. For example, if we calculate the accumulative sum of difference (ASD) of the two frequencies at steady state (and it is measured in revolutions), at LOM operation and at load switching, as shown in equation (4-2), we will find that unlike in steady state operation, when LOM operation starts the difference between the two frequencies starts to widen up rapidly. While in case of a load switching it depends on how far

the load is from the substation and how many loads and generators connected directly to that substation.

$$ASD_{lr} = \sum_{i=1}^{i=n}(F_{l_i} - F_{r_i}) \quad (4\text{-}2)$$

Where,

(n) Number of samples obtained within one 1s, and for this method $n = 50$
(i) Sample index
(F_l) Local frequency at the DG side
(F_r) Remote frequency at the substation side

The closer the load is from the main source the more extra load the power system can supply without causing instability to the local system.

4.2.2 Convergence Measurement (CM)

The method is based on convergence and it starts with saving frequency data values of F_l and F_r for a total of 1s. The first step will be summing the difference between $'F_l$ and F_r', as shown in equation (4-3) and it is measured in samples [89]:

$$Y_{lr_{vd}} = \sum_{i=1}^{i=n}(F_{l_{ivd}} - F_{r_i}) \quad (4\text{-}3)$$

Where,

(vd) The variable delayed number of samples (vd=0, 1, 2, 3, 4 ..... n in samples)
(n) Number of samples obtained within one 1s, and for this method $n = 50$
(i) The sample index

In order to simplify this process, rather than making 2500 calculations for every second (50 calculations a second for 50 variable delays), we can determine the CM value by using only two variable delays, and predict the linear convergence equation, as follows:

By using a simple linear equation in which the result of equation (4-3) is a function of the number of samples of applied delay $Y = aX + b$

(Y) is the result of equation (4-3) with an applied delay and (X) is the sample index of the applied delay to F_l in equation (4-3) while $'a'$ and $'b'$ are constants. To solve this equation the author needs to determine the values of 'a' and 'b', and in order to do that, two values of Y and two values of X need to be chosen:

1- The value of Y at 50 samples applied delay is considered as Y_{50} and $X_{50} = 50$
2- The value of Y at 1 sample applied delay is considered as Y_1 and $X_1 = 1$

$$\left.\begin{aligned} Y_{50} &= aX_{50} + b \\ Y_1 &= aX_1 + b \end{aligned}\right\}$$

By subtracting the two equations: $Y_{50} - Y_1 = a(X_{50} - X_1)$

$$a = \frac{Y_{50}-Y_1}{X_{50}-X_1} = \frac{Y_{50}-Y_1}{49} \quad (4\text{-}4)$$

$$b = Y_1 - aX_1 = Y_1 - \frac{Y_{50}-Y_1}{49} \times 1 = \frac{49Y_1-Y_{50}+Y_1}{49}$$

$$b = \frac{50Y_1-Y_{50}}{49} \quad (4\text{-}5)$$

The CM should be equal to the value of X when Y is equal to 0s:

$$X = \frac{Y-b}{a} = \frac{0-b}{a}$$

$$CM = \frac{-\frac{49Y_1-Y_{50}+Y_1}{49}}{\frac{Y_{50}-Y_1}{49}} = \frac{Y_{50}-50Y_1}{Y_{50}-Y_1}$$

$$CM = \frac{Y_{lr_n}-nY_{lr_1}}{Y_{lr_n}-Y_{lr_1}} \quad (4\text{-}6)$$

(n) Number of samples obtained within one 1s, and for this method $n = 50$

The calculation of ASD in equation (4-2) and CM in equation (4-6), and the relationship between two are shown in Figure 4-4. The existence of two equations would prevent nuisance tripping. The ASD equation by itself is very sensitive can detect LOM, however, in order to enforce stability and prevent nuisance tripping the CM equation would be necessary to prevent false LOM detection caused by temporarily disturbance in the network like load switching. The CFC algorithm will not confirm that LOM operation has occurred and send a tripping signal to the CB unless both of ASD and CM values exceed the threshold of the pre-set setting values, as shown in Figure 4-4. In Figure 4-4 the CFC LOM algorithm for a single window position is illustrated, while the CFC LOM protection algorithm is intended for a moving measurement window. The CFC algorithm's setting parameters are determined by conducting stability and sensitivity assessment. The stability assessment will determine the CFC algorithm's security, in which the CFC algorithm should withstand load switching, faults and communication delay without causing any nuisance tripping. The sensitivity assessment is for determining the reliability of the CFC algorithm and its ability to detect LOM and isolate the DG within a maximum of 2s [10].

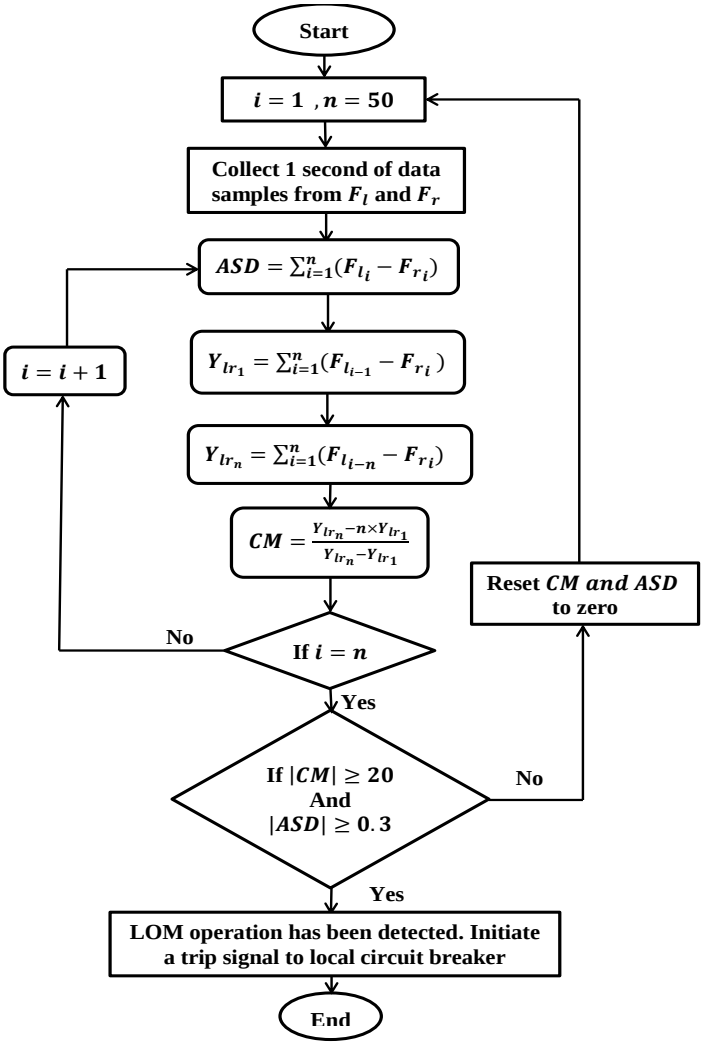

Figure 4-4: Frequency Correlation (CFC) LOM Protection Method's Algorithm of a constant measurement window's position

4.2.3 Moving window approach:

The moving window approach means that the CFC algorithms' measurement window of a period of 1s will start every 100ms. The moving window algorithm starts to operate from the start of the operation of the DG with an offset of 1s and it usually continues as long as the DG is in operation. However, for the stability and sensitivity test, the author will only present 10 window positions starting from LOM operation beginning as W0 and stop at W0.9. Hence, there are W-0.1, W-0.2, and W-0.3 ……., before window position W0.

The moving window approach works as follows:

1- W0 window will start calculating from the beginning of the LOM operation and continue calculating until the end of a period of 1s, the algorithm will reset the result value to zero and starts calculation of another 1s period of data.
2- W0.1 window starts calculation after 5 samples of frequency measurements (100ms) from the starting point of the W0 window position and continue its calculation until the period of 1s is complete then the algorithm will reset to zero and starts calculating for another 1s period.
3- W0.2 window position starts calculation after 5 samples of frequency measurements (100ms) from the starting point of the W0.1 window position and continue its calculation until the period of 1s is complete then the algorithm will reset to zero and starts calculating for another 1s period.
4- W0.3 window position will start calculation after 100ms from the start of the W0.2 window and so on, as shown in Figure 4-5.

Hence, all other windows will start 100ms after the start of the previous window as long as the generator's LOM protection is in operation, as shown in Figure 4-5.

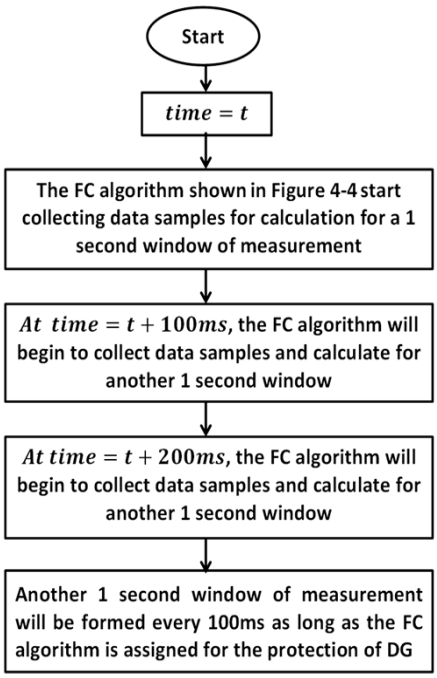

Figure 4-5: CFC Algorithm Moving Window Approach

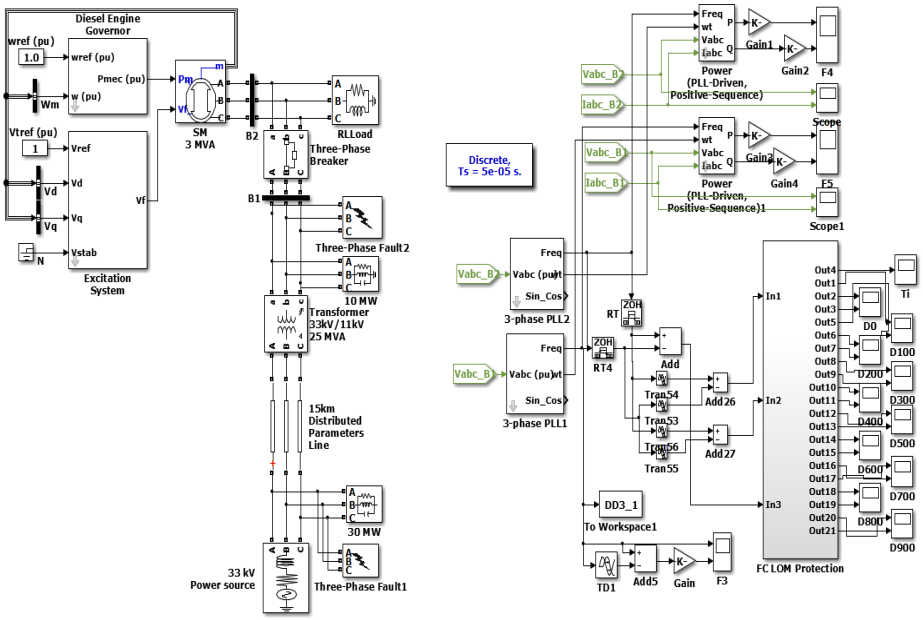

Figure 4-6: CFC-LOM protection model for a synchronous generator (SM)

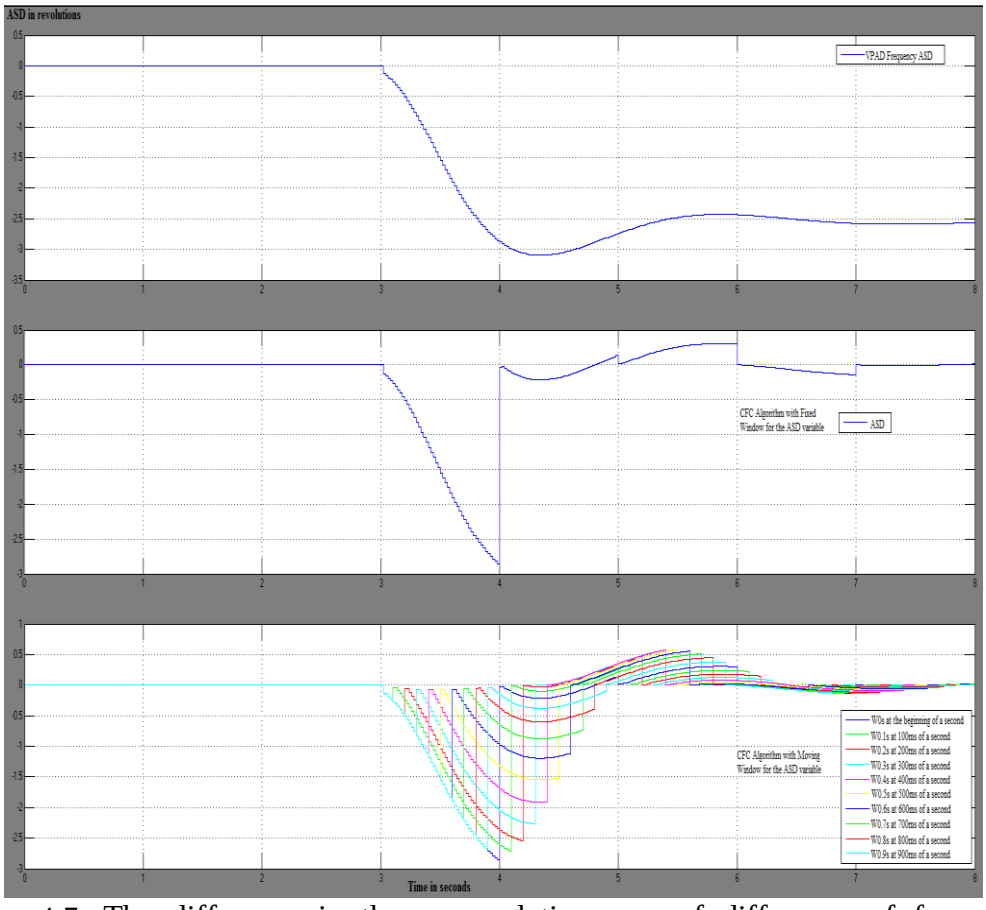

Figure 4-7: The difference in the accumulative sum of difference of frequency between VPAD, CFC with Fixed window, and CFC with Moving window

There are two approaches of assessing the results of the moving window:

1- Instantaneous approach: The algorithm in this approach will initiate a trip when the calculation results for both of ASD and CM variables have reached or exceeded the pre-setting values within the window's 1s period. This aims to make the CFC algorithm more sensitive. However, it could bring instability to the system.
2- Periodic approach: In this approach the algorithm will only respond to the results at the end of each window's 1s period right before resetting the results to zero.

Both of these approaches will be tested in the stability and sensitivity assessments to determine which one of these approaches provides the required level of stability and sensitivity for the LOM protection algorithm to be reliable and secure without causing any nuisance tripping of protection blinding. The MATLAB Simulink model of the CFC LOM protection method with a synchronous generator is shown in Figure 4-6. This MATLAB Simulink model will be used in the stability and sensitivity assessment.

4.3 Stability Assessment

As mentioned in 4.2.2, the stability assessment is very important to ensure system's security. Hence, it is required to determine the LOM algorithm's ability to withstand load switching, non LOM system faults, and communication delay of the remote power frequency without causing any nuisance tripping. In order to determine that, 3 tests need to be conducted: load switching (LS), fault testing, and the CFC algorithm tolerance to communication delays. The first step of the stability assessment will be load switching (LS), the LOM model of a synchronous generator with salient pole rotor connected to the main of 11kV through a transformer that is located 15km away from the main power source of 33kV, and both the DG and the main are connected to the local RL parallel load in which they are both supplying. In case of LS, the protection system should withstand an increase of up to 4 per unit without tripping. In another words the protection has to withstand an increase or decrease in frequency of ROCOF value of 1Hz/sec. This is because the recommended setting for ROCOF LOM protection method by the National Grid (NG) is 1Hz/sec [1]. By using the

MATLAB Simulink model in Figure 4-6, we can connect 4 per unit RL load to the existing local RL load of 1 per unit at 11kV and disconnect the extra load after 2s, as shown in Table 4-1.

Table 4-1: Load Switching Stability Assessment Parameters' Results

Parameters	4 per unit of extra RL parallel Load	Disconnecting the extra Load
ROCOF Hz/s	-2.85	1.2
CM in samples	|9.5|	|7|
ASD in revolutions	|0.0014|	|-0.001|

This assessment shows that as long as the two frequencies are synchronized and the value of ASD will be very low, while the CM value is relatively high. However, even if the CM value reaches or exceeds the threshold setting value, the CFC algorithm will not initiate a trip unless the ASD also reaches or exceeds the threshold setting. Hence, this shows the benefit of having two values in determining the occurrence of LOM operation without causing instability to the system. As shown in Table 4-1, the CFC algorithm with settings of CM and ASD of ≥ 20 samples and ≥ 0.3 revolutions respectively can withstand a load switching event of over 4 per unit of extra load that could be caused by spurious tripping of other generators on the network. The second stability test is to determine the effect of external faults on the stability of the protection method should be assessed by applying faults at 11kV and 33kV of single phase to ground, two phases to ground, and three phases to ground. The faults at the 33kV should be assessed according to the fault distance from the DG, as shown in Table 4-2, the 33kV faults were tested at 25km, 20km, 15km away from the DG [90], while the 11kV faults are not distance related as located 20m away from the DG, as shown in Table 4-3. Unlike the results of the LS assessment, the CM values at 11kV faults are very high, the CM values during the fault assessment are not consistent with the fault level, as their highest values occurred at the single phase to ground fault. Thereby, the CM setting will not be changed as it plays a vital role in the stability in the next test. As shown in Tables 4-2 and 4-3, the CFC settings at CM ≥ 20 and for ASD ≥ 0.3 were adequate to avoid nuisance tripping. The CFC algorithm runs as moving window, and if any one of the windows detects LOM operation the CFC algorithm will initiate a trip. However, there is still the matter of whether to have an instantaneous relay operation or a periodic

operation, and how this choice would effects the security and reliability of the algorithm.

Table 4-2: Faults Stability Assessment at 33kV for Periodic and Instantaneous Approaches

Synchronous Machine (SM) for 33kV system fault , clearance time of 0.2s Periodic and Instantaneous Approaches			
Fault type	Fault Distance from DG	Retained Voltage Level	Relay Response (s)
3 Phase-G	25km	50%	NT (No Trip)
3 Phase-G	20km	40%	NT
3 Phase-G	15km	30%	NT
2 Phase-G	25km	67%	NT
2 Phase-G	20km	59%	NT
2 Phase-G	15km	52%	NT
1 Phase-G	25km	85%	NT
1 Phase-G	20km	78%	NT
1 Phase-G	15km	72%	NT

Table 4-3: Faults Stability Assessment at 11kV for Periodic and Instantaneous Approaches

11kV system fault at Point of Common Connection, clearance time of 0.3s		
Fault type	Retained Voltage Level	Relay Response (s)
3 Phase-G	0%	T (Trip)
2 Phase-G	0%	NT
1 Phase-G	50%	NT

The instantaneous approach is when the relay operates any time one of its windows reaches the threshold of CM and ASD within the period of 1s. Thereby, the decision is not based on the values of CM and ASD at the end of the 1s period and it is presented in seconds (s), while with the periodic approach the algorithm will only take under consideration the values of CM and ASD at the end of every window. It is important to include both approaches in the next test and the sensitivity test in 4.4 to determine which one these approaches will fulfil the methods objectives. The difference between the VPAD, the CFC with Fixed Window, and the CFC with moving window is shown in Figure 4-7 that presents the results of the Accumulative Difference of Frequency for all three methods. In Figure 4-7, the LOM operation has started at t (time) =3s and the accumulative sum of difference for VPAD is not transformed to angle. The ASD of CFC with fixed window is more stable than the VPAD ASD because it resets the offset value of ASD at steady state for every 1s to

zero. Thereby, this would prevent the ASD at steady state from influencing the relay decision to trip. The VPAD algorithm resets the any frequency difference that is equal or less than a pre-set threshold to zero before accumulation. This is meant to prevent the algorithm result from drifting and avoid nuisance tripping.

Now, the third stability test is to determine the longest communication delay that the CFC algorithm can withstand with these setting values. In this test the power frequency data used will be measured by a real PMU and will not be measured by MATLAB Simulink simulation. This is due to the big difference in magnitude between the accumulative frequency differences of data measured by PMUs at two different locations from the accumulative frequency differences measured by software simulation. As an example, the ASD is calculated using frequency measured by PMUs for steady state operation were tested against ASD calculated using MATLAB Simulink software as shown in Figure 4-6 and the results are shown in Table 4-4.

Table 4-4: Difference between values of simulated ASD and PMU measured ASD

Time (s)	A=ASD values using frequencies measured by PMUs at two different regions	B=ASD values using frequencies measured by MATLAB Simulink software	C=A/B
1	-0.011	-4.02E-07	2.73E+04
2	0.005	-5.85E-07	-8.55E+03
3	-0.023	-4.85E-08	4.74E+05
4	0.027	2.67E-08	1.01E+06
5	-0.023	8.43E-09	-2.73E+06
6	0.027	1.85E-10	1.46E+08
7	-0.031	-4.40E-10	7.05E+07
8	0.019	1.13E-10	1.68E+08
9	-0.002	2.50E-10	-8.01E+06
10	0.027	1.84E-10	1.47E+08

According to Table 4-4, the difference between the two in magnitude is very high. Therefore, determining the maximum communication delay that can be tolerated without causing nuisance tripping require an actual frequency data measured by PMUs should be used rather than simulated power frequency, because real measured data would realistic results of what ASD values would be in a real power system steady state operation. Hence, 100 sets of frequencies were measured and collected using two PMUs, one is installed at the University of Strathclyde in Glasgow and the other is installed at the University of Manchester in Manchester. All the sets that

were collected are synchronised and measured at steady state operation at LV level. Only two sets from the 100 frequency sets were taken during two events that occurred at the 28th September 2012 and the 30th September 2012 and these sets are labelled as frequency set 78 and frequency set 77 respectively. They were not LOM events, and they were caused by a sudden disconnection of 1000MW of power generation imported from France. The disconnection caused a drop in power frequency all over UK that triggered spurious tripping of ROCOF LOM protection that further destabilised the power network. The 100 frequency sets were collected over two years. The days and hours that they were collected were chosen as follows:

1- The first set is collected on Monday 1.00 am of the first week of 2011
2- The following set is collected on the following week, following day of the week and the following hour of the day, on Tuesday 2.00 am of the second week of 2011
3- The following set is collected on the following week, following day of the week and the following hour of the day, on Wednesday 3.00 am of the third week of 2011
4- This continues until all the hours of the day, the days of the week and the weeks of the year were included in the samples. Unless, the data is not synchronised, corrupted, or not measured at steady state operation, in this case another hour would be chosen from the same day and if not available from the same week.

By testing 100 synchronized frequency sets of PMU measurements in steady state at a reset threshold of 0.005Hz (if the difference between the local frequency and the remote frequency $\leq$0.005Hz the difference between the two frequencies will be replaced with zero), 78 of the 100 frequency sets were prevented from drifting. However, 22 from 100 frequency sets have shown high ASD results, as shown in Table 4-5, the result of the ASD of three of these sets (shown in the grey cells, set number 60, 77, and 78) have exceeded the ASD pre-set threshold value of 0.3 revolutions and the CM variable has exceeded pre-set threshold value of 20 samples in the CFC algorithm, as shown in Figure 4-4. Thereby, the threshold for resetting the frequency difference to zero has to be at least 0.0271Hz, which is unacceptable because at the state of an event this could impair the sensitivity of VPAD algorithm and keeping the reset threshold on 0.005Hz will affect the stability of VPAD. The stability

problem (caused by drifting) has been avoided in the CFC method with fixed window by resetting the ASD result to zero every 1s. However, this would weaken the CFC algorithm sensitivity even more, because LOM operation could start at any time within the window of measurement, and the ASD could be reset to zero before detecting LOM. Therefore, the CFC algorithm with moving window would be more reliable and secure, as it solves the problem of stability and sensitivity at the same time.

Table 4-5: The ASD results of 22 of 100 synchronized Frequency sets

Any absolute frequency difference below or equal to 0.005 will be reset to zero	
Frequency set index	Maximum ASD value in revolutions
1	-0.055
8	+0.051
10	-0.112
11	-0.03
12	+0.005
13	+0.104
34	+0.044
35	-0.02
44	-0.03
45	+0.01
49	+0.118
50	-0.011
58	-0.069
60	-0.371
77	+0.583
78	+0.555
80	-0.052
86	-0.106
90	-0.02
95	+0.017
99	+0.177
100	+0.227

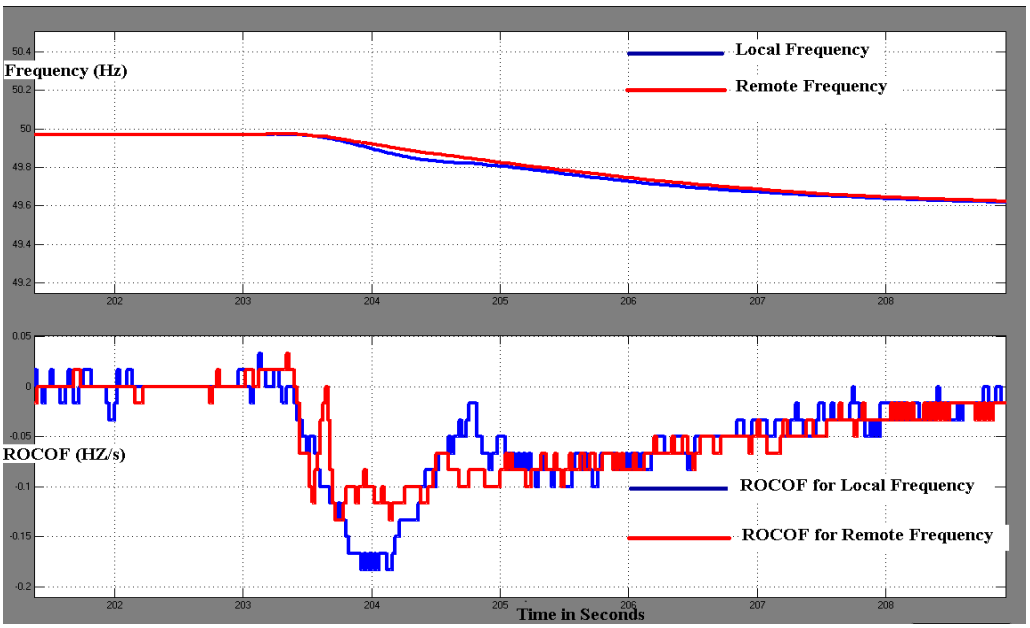

Figure 4-8: 28-09-2012 Event (Frequency Set 78) Delayed by 0.26s for Instantaneous and periodic approaches' delay tolerance

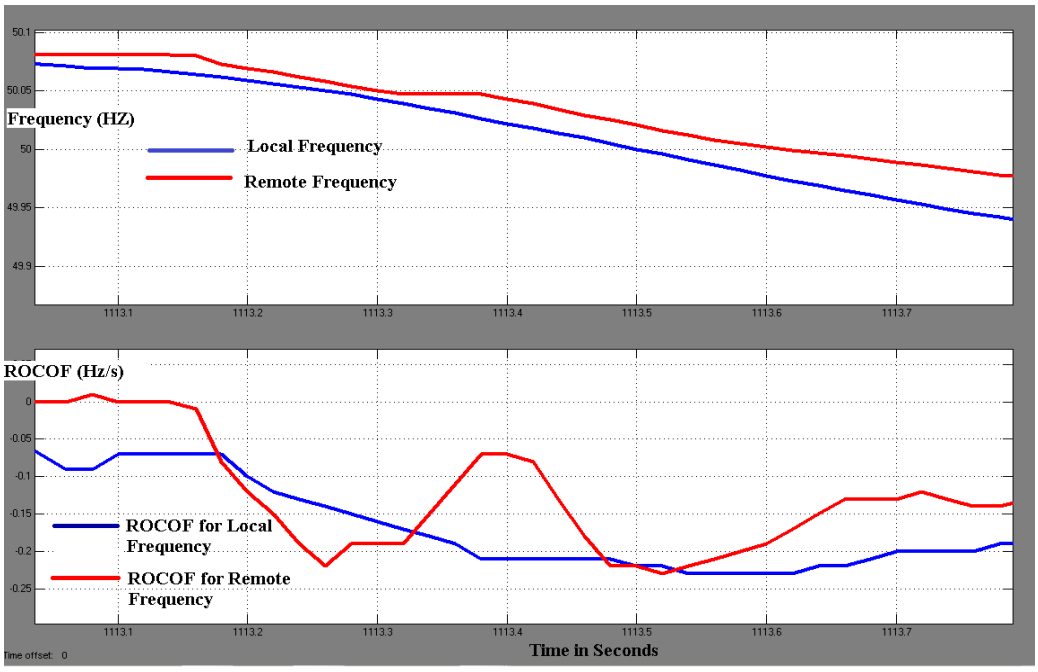

Figure 4-9: 30-09-2012 Event (Frequency Set 77) 0.22s for instantaneous approach delay tolerance and 0.24s for periodic approach delay tolerance

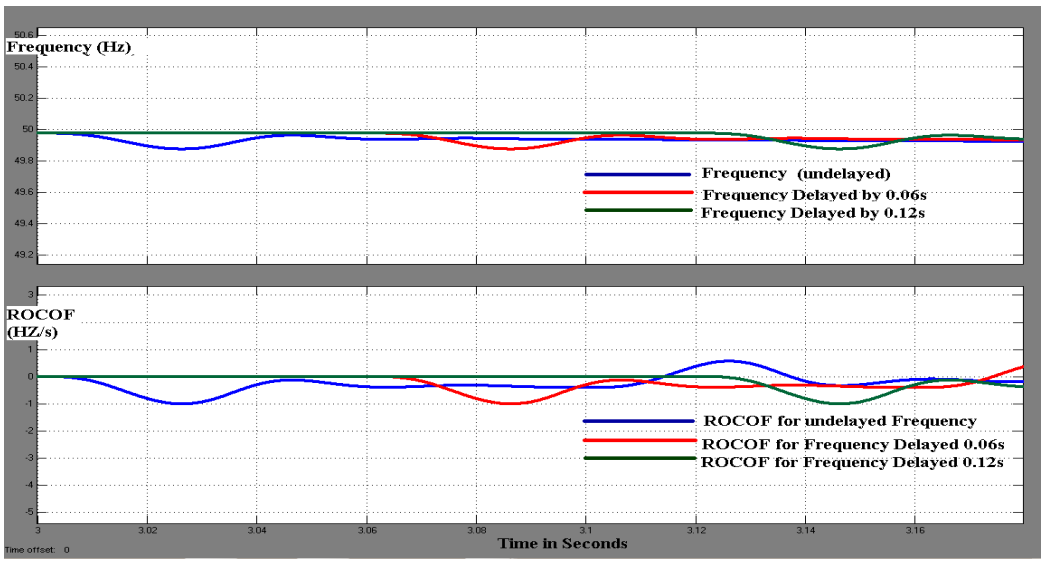

Figure 4-10: Simulated Event in which the power frequency reaches a ROCOF of 1Hz/sec, 0.06s delay is tolerated by instantaneous approach and 0.12s delay is tolerated by periodic approach

As shown in Figures 4-8 and 4-9, the maximum ROCOF value for the two sets (78 and 77) is 0.22 Hz/sec. Hence, when it comes to stability to determine the difference between the two approaches' performances, the real challenge is when the ROCOF reaches or exceeds 1Hz/s, as this ROCOF setting is recommended by the distribution code [1] to maintain stability for the ROCOF protection performance and prevent it from false tripping. Thereby, a simulated frequency that reaches a ROCOF of 1 Hz/s has been obtained to test the tolerated communication delay at ROCOF of 1 Hz/s at a load switching event. The results showed that the instantaneous approach will only tolerate 0.06s of communication delay, while the periodic approach can tolerate 0.12s, as shown in Figure 4-10. This test shows the periodic approach is more stable than the instantaneous approach. However, there is still the matter of whether the periodic approach's sensitivity level is acceptable or not.

4.4 Sensitivity Assessment

As mentioned in 4.2.3, the sensitivity test will include both approaches in order to determine the effect on the reliability of the method by applying the same CFC settings used in the stability test. The sensitivity assessment will start by setting the imbalance of active and reactive power between the DG and the local load to zero in the network shown in Figure 4-6. By starting from zero imbalance condition, we can test the CFC algorithm sensitivity to LOM operation. If the CFC algorithm detects

LOM then the algorithm is extremely sensitive. However, it is highly unlikely to detect LOM at zero power imbalances. As shown in Tables 4-6, 4-7, 4-8, and 4-9, the algorithm did not detect LOM with both instantaneous and periodic approaches at zero power imbalances. Hence, the active local load should be increased and decreased until the LOM is detected and at that point we can determine the level of sensitivity the algorithm has against active power imbalance, as shown in Tables 4-6 and 4-7. The same procedure should be applied to the reactive local load until the LOM is detected as shown in Tables 4-8 and 4-9 [90].

Table 4-6: Sensitivity test of the CFC method with Instantaneous approach for synchronous generators (SG) with Active Power (P) Imbalance

Power Factor =0.95	LOM Detection of a Moving Window										Relay Response (s)
Active Power (P) Imbalance (%)	W0 (s)	W0.1 (s)	W0.2 (s)	W0.3 (s)	W0.4 (s)	W0.5 (s)	W0.6 (s)	W0.7 (s)	W0.8 (s)	W0.9 (s)	
-1	0.4	0.48	0.54	0.64	0.76	0.4	0.4	0.4	0.4	0.4	0.4
-0.41	0.98	NT	NT	NT	NT	NT	NT	NT	NT	NT	0.98
0 (P&Q)	NT	NT	NT	NT	NT	NT	NT	NT	NT	NT	NT
+0.413	0.98	NT	NT	NT	NT	NT	NT	NT	NT	NT	0.98
+1	0.4	0.48	0.54	0.64	0.76	0.4	0.4	0.4	0.4	0.4	0.4

Table 4-7: Sensitivity test of the CFC method with periodic approach for synchronous generators (SG) with Active Power (P) Imbalance

Power Factor =0.95	LOM Detection of a Moving Window										Relay Response (s)
Active Power (P) Imbalance (%)	W0 (s)	W0.1 (s)	W0.2 (s)	W0.3 (s)	W0.4 (s)	W0.5 (s)	W0.6 (s)	W0.7 (s)	W0.8 (s)	W0.9 (s)	
-1	1	1.1	1.2	NT	NT	0.5	0.6	0.7	0.8	0.9	0.5
-0.41	1	NT	NT	NT	NT	NT	NT	NT	NT	NT	1
0 (P&Q)	NT	NT	NT	NT	NT	NT	NT	NT	NT	NT	NT
+0.413	1	NT	NT	NT	NT	NT	NT	NT	NT	NT	1
+1	1	1.1	NT	NT	NT	0.5	0.6	0.7	0.8	0.9	0.5

Table 4-8: Sensitivity test of the CFC method with Instantaneous approach for synchronous generators (SG) with Reactive Power (Q) Imbalance

Power Factor= 0.95	LOM Detection of a Moving Window										Relay Response (s)
Reactive Power (Q) Imbalance (%)	W0 (s)	W0.1 (s)	W0.2 (s)	W0.3 (s)	W0.4 (s)	W0.5 (s)	W0.6 (s)	W0.7 (s)	W0.8 (s)	W0.9 (s)	
-25	0.4	0.46	0.54	0.64	0.38	0.38	0.38	0.38	0.38	0.38	0.38
-20	0.48	0.56	0.64	0.8	NT	0.48	0.48	0.48	0.48	0.48	0.48
-12.216	0.98	NT	NT	NT	NT	NT	NT	NT	NT	NT	0.98
0 (P&Q)	NT	NT	NT	NT	NT	NT	NT	NT	NT	NT	NT
+13.867	0.98	NT	NT	NT	NT	NT	NT	NT	NT	NT	0.98
+20	0.58	0.68	0.8	NT	NT	NT	NT	0.6	0.6	0.6	0.6
+30	0.44	0.5	0.58	0.7	0.9	0.44	0.44	0.44	0.44	0.44	0.44

Table 4-9: Sensitivity test of the CFC method with periodic approach for synchronous generators (SG) with Reactive Power (Q) Imbalance

Power Factor=0.95	LOM Detection of a Moving Window										Relay Response (s)
Reactive Power (Q) Imbalance (%)	W0 (s)	W0.1 (s)	W0.2 (s)	W0.3 (s)	W0.4 (s)	W0.5 (s)	W0.6 (s)	W0.7 (s)	W0.8 (s)	W0.9 (s)	
-25	1	NT	NT	NT	0.4	0.5	0.6	0.7	0.8	0.9	0.4
-20	1	NT	NT	NT	NT	0.5	0.6	0.7	0.8	0.9	0.5
-12.216	1	NT	NT	NT	NT	NT	NT	NT	NT	NT	1
0 (P&Q)	NT	NT	NT	NT	NT	NT	NT	NT	NT	NT	NT
+13.867	1	NT	NT	NT	NT	NT	NT	NT	NT	NT	1
+20	1	NT	NT	NT	NT	NT	NT	0.7	0.8	0.9	0.7
+30	1	NT	NT	NT	NT	0.5	0.6	0.7	0.8	0.9	0.5

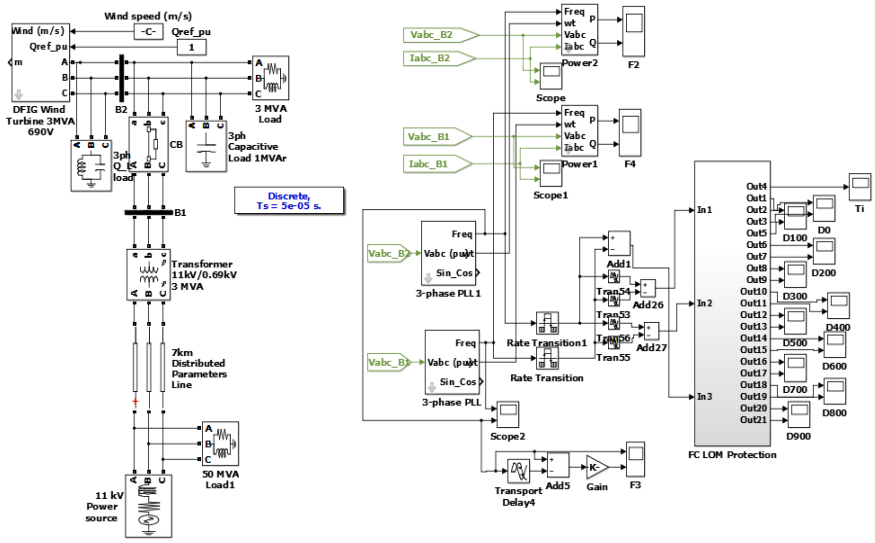

Figure 4-11: CFC-LOM Protection model of Doubly Fed Induction Generator (DFIG)

The results in Tables 4-6, 4-7, 4-8, and 4-9, show that the CFC algorithm is very sensitive to active power imbalance, while it is not very sensitive to reactive power imbalance. This is due to the fact that the power frequency is sensitive to change in the resistive load, while it is not sensitive to change in reactive load. This is also supported by the same test applied to the network with doubly fed induction generator DFIG, as shown in Figure 4-11. By applying the same procedure, as shown in Tables 4-10 and 4-11, the LOM operation was detected at zero power imbalances between the load and the DG, which is consistent with the DFIG operation that does not have frequency control and automatic voltage regulator (AVR) and it is also dependent on the wind speed in running the turbine, which makes the power frequency very sensitive and the LOM operation easy to detect.

Table 4-10: Sensitivity test of the CFC method with Instantaneous tripping for Doubly Fed Induction Generators (DFIG)

Power Factor =0.938	LOM Detection of a Moving Window										Relay Response (s)
Active and Reactive Power (P&Q) Imbalance (%)	W0 (s)	W0.1 (s)	W0.2 (s)	W0.3 (s)	W0.4 (s)	W0.5 (s)	W0.6 (s)	W0.7 (s)	W0.8 (s)	W0.9 (s)	
0	0.44	0.38	0.48	0.54	0.38	0.38	0.38	0.38	0.38	0.38	0.38

Table 4-11: Sensitivity test of the CFC method with Periodic tripping for Doubly Fed Induction Generators (DFIG)

Power Factor =0.938	LOM Detection of a Moving Window										Relay Response (s)
Active and Reactive Power (P&Q) Imbalance (%)	W0 (s)	W0.1 (s)	W0.2 (s)	W0.3 (s)	W0.4 (s)	W0.5 (s)	W0.6 (s)	W0.7 (s)	W0.8 (s)	W0.9 (s)	
0	1.1	1	1.2	1.3	1.4	0.5	0.6	0.7	0.8	0.9	0.5

As shown in Tables 4-6, 4-7, 4-8, 4-9, 4-10, and 4-11, the results show very close level of sensitivity between the periodic and instantaneous approach. However, the instantaneous approach shows slightly more sensitivity than the periodic approach by a maximum of 120ms. Hence, the periodic approach proved to have a balanced performance and can provide stability and sensitivity at the same time.

The authors in [90] have recommended the relay responses presented in Table 4-12. According to Table 4-12, the CFC algorithm performance has shown better performance in the stability assessment than the recommended relay responses where the relay is allowed to be unstable at 20% retained voltage. The CFC algorithm has also shown better performance in the sensitivity assessment with active power imbalances than the recommended relay responses.

Table 4-12: Comparison between the proposed minimum performance criteria in [90] for acceptable LOM protection and the CFC algorithm test for sensitivity and stability results

Test	Condition	Recommended Relay Response	CFC Relay Response	
			P	Q
Sensitivity	LOM with 0% imbalance (both P&Q)	NT	NT	NT
	LOM with ±2.5% imbalance (both P&Q)	NT	T	NT
	LOM with ±5% imbalance (both P&Q)	NT	T	NT
	LOM with ±10% imbalance (both P&Q)	T	T	NT
	LOM with ±15% imbalance (both P&Q)	T	T	T
Stability At 33kV	Fault with 20% retained voltage (Ph-G,2Ph-G,3Ph-G)	T,T,T	NT,NT,NT	
	Fault with 50% retained voltage (Ph-G,2Ph-G,3Ph-G)	NT,NT,T	NT,NT,NT	
	Fault with 80% retained voltage (Ph-G,2Ph-G,3Ph-G)	NT,NT,NT	NT,NT,NT	
Stability At 11kV	Fault with 20% retained voltage (Ph-G,2Ph-G,3Ph-G)	T,T,T	NT,NT,T	
	Fault with 50% retained voltage (Ph-G,2Ph-G,3Ph-G)	NT,NT,T	NT,NT,NT	
	Fault with 80% retained voltage (Ph-G,2Ph-G,3Ph-G)	NT,NT,NT	NT,NT,NT	

4.5 Chapter Summary

This chapter has presented the development of a communication type LOM protection method by frequency correlation (CFC) approach. The CFC algorithm works as a moving measurement window by 100ms difference, and for every window position it will have a period of 1s to complete the calculation of two parameters (CM, ASD). If in any of the window's position in which both of the parameters values reach or exceed the pre-set values of the threshold, then the protection algorithm will initiate a trip signal to the local circuit breaker. It can withstand a communication delay or unsynchronised frequencies up to 100ms, and the moving window will reset to zero after 1s at every window's position, and existent of two parameters would rule out the possibilities of nuisance tripping and protection blinding, and inforce the security and reliability of the protection system. According to the proposed minimum requirement for the acceptable performance of LOM relay presented in [90] and shown in Table 4-12, the CFC method has proved to be very stable with load switching, delay to up to 100ms, and both remote and local faults. As for the sensitivity test, the CFC method has exceeded the required

level of sensitivity by 9.5% for active power imbalance. However, it showed less sensitive to reactive power imbalance, as it required $\pm 2.5\%\ to\ \pm\ 3.9\%$ more reactive power imbalance to detect LOM. This due to the fact that the power frequency is sensitive to change in resistive load, while it is not sensitive to change in reactive load as mentioned in 4.4, and because the CFC algorithm is based on power frequency correlation, the lack of high sensitivity for reactive power imbalance can be tolerated in the CFC algorithm performance. As proven in 4.3 and shown in Figure 4-10, the maximum delay tolerated by the CFC algorithm is 0.12s. Hence, if there is a GPS installed at the DG, it should synchronize the local frequency with the remote frequency within a maximum error of 0.12. The GPS units available are capable to synchronize the two frequencies with a maximum synchronization error of $1\mu s$. However, in case there have been a GPS failure or the GPS has lost communication the CFC LOM protection algorithm will become vulnerable of exceeding the maximum tolerable delay, and could lead to nuisance tripping. Therefore, a time delay estimation method should developed to inform relay of the estimated delay. In chapter 5 we'll review several time delay estimation methods and discuss the stages of development of a novel time delay estimation method that is designed for power system applications, such as LOM protection, condition monitoring and other non-real time applications.

CHAPTER 5: LINEAR TRAJECTORY PATH (LTP): A TIME DELAY ESTIMATION METHOD

5.1 Introduction

Time Delay Estimation (TDE) in this thesis is introduced as the process of determining the time delay between the local (reference) measurements and the remote measurements. Normally the synchronization between two signals is achieved by considering one of the clocks at one of the two locations as a reference clock or using a third internet based clock as a reference. At this protection application the utilization of two way satellite communication connection will result in increasing the communication time delay by at least 1200ms for TCP/IP. However, by using a two way UDP/IP the time delay would be up 600ms. It all depends on the protection application implemented and whether the extra time delay can be tolerated or not.

For this application the main LOM protection algorithm decision is based on accumulated difference in phase angle between the two locations. Hence, the algorithm decision is not instantaneous (based on the value of difference between two measurements at a single point of time). However, even though the delayed remote measurements will be synchronized with the local measurements the local measurements will not be useful unless the remote measurements arrive at the local protection. Thereby, there will always be a delay of over 1s because the data measurements used are measured at a constant rate (number of times per second), this means that the protection will be blind on the real time measurements of the real time power system operation for a period of time over 1s. Keeping in mind that the maximum period of time any DG is allowed operate during a LOM operation is set as 2s, as mentioned in sections 1.2.1, 3.6 and 4.3, this means that from the time that the LOM occurs is has to be detected and the DG be isolated (de-energized) by the protection by no longer than 2s[10]. This long communication delay will limit the

ability and reliability of the protection to detect LOM and isolate the DG within 2s of LOM occurrence.

There is also the economical implication of having a two way satellite communication link, because this will double the bandwidth and add more costs to leasing expenses for each of the registered DG owners. In order to avoid having a two way connection, the synchronization can be achieved by installing a Global Positioning System (GPS) on every DG registered for this protection method. The GPS can synchronize the two signals very reliably, however, installing a GPS on every DG for up to 10000 DGs all over UK will add extra economical restrains of the project implementation, also in order for the GPS to operate reliably and have the maximum availability it need to be installed in a location that have a direct path to satellite link. Hence, the DGs have to be located outdoors or the GPS antenna should be installed outdoors, this will definitely add more restrains on the location of the DG and GPS antenna, and the installation space and facilities required for the GPS antenna. In this chapter, the author will present the second contribution of this research that aims to overcome the need to use the GPS or the internet in clock synchronization and replace them with a TDE method that uses the data measurements of power frequency of both local and remote location. For the last 50 years the TDE has been widely explored and extensively studied for medical ultrasound equipment [91,92], such as, blood flow estimation [93, 94, and 95], phase aberration correction [96, 97, and 98], motion compensation for synthetic receive aperture imaging [99], tissue elasticity estimation [100,101], radiation force imaging [102, 103, and 104]. In other fields there are many application that require TDE such as localization and tracking of a source can be determined directly from the time delay measurements, bearing and elevation angles are also evaluated from measured time delays, applications that determine the lag of time in mean sea level variations between two locations, drift velocity of ionosphere clouds, underwater acoustic sensors, and speed of propagation of an impulse along a nerve fibre [105,106]. In communication, sonar or radar detection it is possible to remove echo by using time delay estimates, and in de-convolution the time delay estimation is very important to separate and estimate the probing signal and channel response [107]. Normally, the techniques involved in time delay estimation are based on historical data

measurements, digital signal processing, cross-correlation, least mean square (LMS), regression analysis and interpolation.

5.2 Delay Estimation Methods

In digital signal processing the more the number of samples taken from a signal the more information there is and results in more accuracy of what's the actual shape of the signal wave. For example, when determining the frequency and the phase angle values of the positive sequence voltage phasor using the PMU by Discrete Fourier Transform (DFT) and usually 10000samples/sec are taking from the voltage sinusoidal wave at 50Hz system. This means 200 samples are taken from every cycle period in order to get an accurate power frequency measurement. If the number of samples taken reduces, the accuracy of the measurements will decline as well and if it increases the accuracy of the measurements will increase.

5.2.1 Signal and Noise Representation

In [108] the authors defined the telephone channel in terms of its frequency characteristics attenuation and group delay, and their definition of the function for calculations concerning linear networks that are made of components such as resistances, inductances, and capacitances, all constant with time, which lead to linear differential equations with constant coefficients, as shown in equation (5-1):

$$s(t) = A(t)\cos(wt + \varphi) \qquad (5\text{-}1)$$

Where,

(A) Signal amplitude
(φ) Angle shift
(w) The angular frequency (constant with time)

It is also proved in [109] that the distortion caused by sine wave noise is $\sqrt{3}$ times more than the distortion caused by white noise for the same magnitude. This makes the presentation of the combination of the original signal and the noise as shown in equation (5-2):

$$S_T(t) = A(t)\cos\big(w_o t + \varphi(t)\big) + A_{noise}(t)\cos(w_o t + \Delta w_n t) \qquad (5\text{-}2)$$

Where,

(φ) Angle shift
(A) Signal's amplitude

$(A_{noise}(t))$	The noise amplitude
(w)	The angular frequency (constant with time)
$(\Delta w_n t)$	Noise angle shift

However, in [18] the authors presented the original signal with sinusoidal model, as shown in equation (5-3), and only considered white noise in their experiments

$$s_i = sin4\pi(i-1)T \qquad (i=1, 2, 3; \ldots\ldots, n) \qquad (5\text{-}3)$$

Where,

(T)	Time deviation between two samples ($T = 1/f_s$)
(f_s)	Sampling frequency
(n)	Total number of samples
(i)	Sample index

In the vast majority of the time delay estimation methods the signal model used is a combination of the original signal and the noise. The representation of the reference signal and the delayed signal in most of the reviewed papers are signal measurements that were recorded by two sensors installed in two different locations while recording measurements for the same event, as shown in equation (5-4) [110]:

$$X1(t) = s(t) + n1(t) \quad \text{and} \quad X2(t) = s(t+D) + n2(t) \qquad (5\text{-}4)$$

Where,

(D)	Time delay difference between X1(t) and X2(t) in (seconds)
$(s(t))$	Reference signal
$(s(t+D))$	Delayed signal
$\big(n1(t)\big)$	Noise signal that affects the reference signal
$(n2(t))$	Noise signal that affects the delayed signal

5.2.2 TDE Algorithms

Most of the methods so far use some form of cross correlation. However, what define these methods are the types of algorithms and filtering used. In [111] the Generalized Correlation Method (GCM) is a maximum likelihood estimator to determine the time delay between two signals received at two spatially separated sensors in the present of uncorrelated noise, it uses a pre-filtering before the cross correlation take place, as shown in equations (5-5) and (5-6), to maximize the signal to noise ratio (S/N) of the signals before they enter the correlator.

The Cross Correlation Function:

$$R_{x1x2}(\tau) = E[x_1(t).x_2(t+d)] \qquad (5\text{-}5)$$

Where,

(E)	Denotes Expectation
(d)	Time delay (s)

OR

$$R_{x_1x_2}(\tau) = \frac{1}{T+d}\int_{\tau}^{T} x_1(t).x_2(t+d)dt \quad (5\text{-}6)$$

Where,

(T)	Sample time interval (s)
(t)	Time (s)
$(x_1(t))$	Original signal
$(x_2(t+d))$	Delayed signal
(d)	Time delay (s)

The result of equation (5-6) will be squared for a range of time shifts, (d), until the peak is obtained as shown in Figure 5-1:

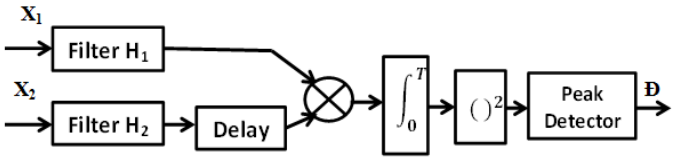

Figure 5-1: Generalized Correlation TDE Method Block Diagram

In [112] the Parameter Estimation Approach (PEA) technique, which is based on determining the peak of the generalized cross correlation between the two signals, by estimating the time delay as a Finite Impulse Response (FIR) filter, thereby, the estimation method becomes of determining the filter's coefficients. This method aims to reduce the variance and improve the resolution and stability of the estimates. It also applies the '$sinc$' function for estimation as shown in equations (5-7) and (5-8), the original signal is presented as $X1(t)$ and its delayed version is presented as:

$$X1(t) = X2(t+d)$$

$$X1(t) = \sum_{i=-\infty}^{i=\infty} x1_i(t).sinc(t-i) \quad (5\text{-}7)$$

$$X2(t) = \sum_{i=-\infty}^{i=\infty} x1_i(t).sinc(t-i+d) \quad (5\text{-}8)$$

Where,

(i)	Sample index
$(sinc(t))$	$= sin(t)/t$
(t)	Time (s)
$(x_1(t))$	Original signal
(d)	Time delay (s)

In [106] it is shown how in the generalized cross correlation approach the time delay estimation is always an integer multiple of the sampling interval, and the need in many applications for a resolution less than the sampling interval. In [113] the author investigated the small and large estimation errors in the case of the reduction of the S/N ratio in the cross correlation process, to determine whether the decrease of the S/N would cause an increase in the probability of large estimation error. The author examined the TDE variance for two modes, the first mode is when the correlation peak closest to the true time delay is used as the TDE, and the second mode is when the largest peak over a full range of the correlator delay times is used as the TDE. The author in [113] proved that in the second mode the probability of having large estimation errors is higher than in the first mode when the S/N decreases. In [114] a method that uses the average magnitude difference function (AMDF) combined with logic decision to estimate the pitched period of speech sounds to be isolated from the noise sounds for quality processing. The AMDF method performed by applying various delays and summing the absolute of the difference between the original signal and the delayed one and calculates the average difference for a chosen number of samples for every delay, as shown below in equation (5-9):

$$Average\ Difference\ (AMDF) = \frac{1}{N}\sum_{k=0}^{N-1} |S_k - S_{k-n}\ | \qquad (5\text{-}9)$$

Combined with the average square difference function (ASDF) of the two signals, as shown in equation (5-10), developed for voice pitch extraction that lead the formation of the formula shown in equation (5-11):

$$\left(Average\ Square\ Difference\ (ASDF)\right) D_n = \frac{1}{N}\sum_{k=0}^{N-1}(S_k - S_{k-d}\ )^2 \qquad (5\text{-}10)$$

$$\frac{1}{N}\sum_{k=0}^{N-1} |S_k - S_{k-d}\ | \cong \beta_n(\frac{1}{N}\sum_{k=0}^{N-1}(S_k - S_{k-d}\ )^2\ )^{1\prime 2} \qquad (5\text{-}11)$$

$$D_n \cong \beta_n(\frac{1}{N}\sum_{k=0}^{N-1} S_k^2 + \frac{1}{N}\sum_{k=0}^{N-1} S_{k-d}^2\ - \frac{2}{N}\sum_{k=0}^{N-1} S_k\, S_{k-d}\ )^{1\prime 2} \qquad (5\text{-}12)$$

Leading to

$$(\frac{2}{N}\sum_{k=0}^{N-1} S_k^2\ - \frac{2}{N}\sum_{k=0}^{N-1} S_k\, S_{k-d}\ )^{1\prime 2} \qquad (5\text{-}13)$$

Where,

(β_n)	Scaling factor and it varies between 0.6-1.0
(S_k)	Original signal
$(S_{k-n}\ )$	Delayed signal
(d)	Number of delayed samples

The first part as in equation (5-9) represents AMDF for time delay estimation; while the second part was developed from the ASDF TDE method, as shown in equation (5-10), and transformed to equations (5-11)(5-12) and (5-13) that makes it suitable for determining (by a logical decision) the end of the voice pitch period in order for it to be extracted.

In [115] the author investigated three cross correlation TDE methods. These methods differ in whether applying a sign or not as follows:

1- Direct correlation (DC) algorithm is shown in equation (5-14):

$$R_{DC}(\tau) = \frac{1}{N}\sum_{i=1}^{N} x1_i(t).x2_i(t+d) \qquad (5\text{-}14)$$

2- Hybrid-Sign correlation (HS) algorithm is shown in equation (5-15):

$$R_{HS}(\tau) = \frac{1}{N}\sum_{i=1}^{N} x1_i(t).sign\big(x2_i(t+d)\big) \qquad (5\text{-}15)$$

3- Polarity-Coincidence correlation (PC) algorithm is shown in equation (5-16):

$$R_{PC}(\tau) = \frac{1}{N}\sum_{i=1}^{N} sign\big(x1_i(t)\big).sign\big(x2_i(t+d)\big) \qquad (5\text{-}16)$$

Where,

(N)	Total number of samples
(t)	Time (s)
$(x_1(t))$	Original signal
$(x_2(t+d))$	Delayed signal
(d)	Time delay (s)

In the DC method both signals magnitude are taken as an absolute values before multiplication as shown in equation (5-14). In the HS method, as shown in equation (5-15) the delayed signal keeps its sign, while in the PC method, as shown in equation (5-16) both signals keep their own signs. The author of [115] concluded that when increasing the number of samples used with all three methods by a factor of 2-3 times the original number of samples, the PC method can be as accurate as the other two methods. In [26] the authors made another comparison between five TDE correlation methods among them the three methods (that where compared in [115]) and the AMDF method. The authors of [116] have obtained the variances of those methods by computer simulation from 300 independent simulations with a range of SNR of 0-40dB and a range of sample numbers of 100-1000 samples, while the analogue to digital conversion was quantized to a resolution of 8bits. The simulations for a constant SNR of 10dB and a variable number of samples show that the number

of samples needed to achieve the same accuracy of TDE variance of the DC method, is for the AMDF method 1.3 times the number of the samples needed for the DC method, 3.2 times for the HS method and 10 times for the PC method. However, these results are for a variance of 0.003, which is very low. However, to achieve a variance of 0.02, the PC method needs 2.22 times the number of samples of the DC method. After performing the same number of independent simulations for a variable SNR and a fixed number of 500 samples, the authors of [116] concluded that the AMDF method accuracy was the closest to the DC method accuracy for both sets of simulations. Furthermore; in [117] the authors investigated the DC, AMDF, and ASDF TDE methods by using a fixed 100 samples, and interval period of 1s and a range of SNR of -10 to 40dB, the variances of all three methods were obtained by performing 2000 independent simulations for three incremental delays of 0, 0.25, and 0.5s. The results show that the AMDF and ASDF methods outperformed the DC method as the SNR value gets bigger than 10dB.

Interpolation is used in many TDE methods to estimate the delay by determining the best match between the two signals. In [109] a spline based algorithm for continuous TDE presented, the method is based on taking discrete data samples from the two analogue signals using FFT and perform a parabolic curve fitting to match the two discrete signals. If the TDE achieved without interpolating one or both of the input signals before matching it would be straight forward and simpler to calculate. However, by doing so the level of accuracy will be highly dependent on the sample interval; thereby, the impact of sample interval can be reduced by using signal interpolation before pattern matching computation for both signals. That is why the processing of that method is extremely complicated and expensive, which makes undesirable to integrate with LOM protection relay. Interpolation is also applied in both [118] and [119] to improve the adaptive TDE method to provide fractional TDE by using the '$sinc$' function that is because the latter method developed by [110] provide only integer estimations. The [Etter and Stearns][110] method iteratively estimate the time delay between two highly correlated sampled signals. The adaptive TDE algorithm uses a gradient technique to determine the value of the adaptive estimation that has the minimum correlation mean square error. This algorithm is similar to the adaptive filter coefficient algorithm developed by 'Widrow' in [120].

The technique used in the adaptive estimator is a steepest gradient technique, thus it requires that the signals have a unimodal or periodically unimodal cross-correlation function. The adaptive delay estimation algorithm uses a gradient technique to find the value of adaptive delay that minimises the squared error function, as shown in equations (5-17) and (5-18):

$$e_i = s_{i-D} - s_{i-d} \quad (5\text{-}17)$$

$$e_i^2 = (s_{i-D} - s_{i-d})^2 \quad (5\text{-}18)$$

Where,

(D)	Actual delay of the remote signal
(d)	Variable delay applied to the reference signal
(s_{i-D})	Delayed signal
(s_{i-d})	Variably delayed signal

The block diagram representation for the adaptive method testing is shown in Figure (5-2), while n_1, n_2, and n_3 are representing the white noise applied to the signals. The noise power is equal to the signal's power. The noise is applied to the original signal before applying the delay (n_1) at one test, applied to both signals (n_2 and n_3) at another test, or no noise applied ($n_1 = n_2 = n_3 = 0$) in another test.

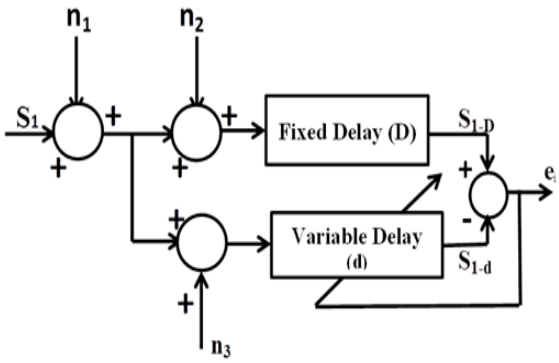

Figure 5-2: Adaptive Estimation of Time Delay Block Diagram

5.3 Linear Trajectory Path (LTP) Estimation Method

5.3.1 Data Measurement Frequency

The PMU SEL-451 gives a choice of 10, 25, 50 measurements per second. The choice of fs effect the link bandwidth (BW), the bit rate, and the processing delay of the PMU as explained in chapter 3, which would only be a significant difference in case of using M class PMU's, however, the utilization of P-class PMU's will not be affecting the measurement processing delay as much due to the range of processing

delay of only 50-70ms. While the M-class type which is more likely to be used due to its high accuracy as it has a wider measurement estimation window (MEW) around 0.5s and has two more stages of harmonics filtering than the P-class type that has a very narrow MEW of up to 0.1s and lacks of harmonics filtering. The M-class PMUs processing delay reduces when the fs increases, thereby, the choice of measurement rating should be the highest and in this case its 50Hz. However, during the development of the TDE algorithm we'll only use fs value of 10Hz in computer simulations when testing the 100 sets of frequencies available. The reason for that is time limitation, because using 50Hz data rating will require over 15300 independent simulations in MATLAB Simulink, while 10Hz data rating will require fewer than 3500 independent simulations.

5.3.2 Data Signal Representation

In all the TDE methods earlier discussed in 5.2 the data was presented by some form of a sinusoidal function and that is because of the nature of the data that been used for estimation the time shift, as discussed in 5.2.1 for the presentation of the data in a telephone channel in terms of attenuation and group delay in [108] and the presentation of data in [110], also in [109] where the data is presented by a discrete data samples taken from two analogue signals using FFT. In this application the data used have been measured by applying DFT method on sinusoidal voltage signal to determine the power frequency at two locations. However, the power frequency data cannot be presented by an analogue or sinusoidal signal because this will change its characteristics. Thereby, the data will be presented as discrete data samples.

5.3.3 Convergence Estimation (CE) Technique

The convergence technique explained in 4.2.2 is designed to determine the linear convergence shift between the local frequency and the remote substation frequency as a secondary LOM measurement. In this chapter the objective is to design a TDE algorithm based on the convergence technique to estimate the time delay of the remote frequency "F_r" compared to the reference frequency "F_l". The required TDE method performance in which it achieves a maximum estimation error of 5 cycles (0.1s). The TDE should be determined with an estimation window of 3 minutes by obtaining the average of three one minute TDE using 3000 samples a minutes. The

algorithm starts with saving frequency data values of (F_l) and (F_r) for a total of 1 minute. The first step of processing the data is by summing the difference between (F_l) and (F_r) for 3000 samples (1 minute) at zero applied delay (vd=0) to the local frequency (F_l) as shown in equation (5-19):

$$Y_{lrvd} = \sum_{i=1}^{i=n} (F_{l_{ivd}} - F_{r_{icd}}) \quad (5\text{-}19)$$

Where,

(F_l)	Frequency at the local location (DG side)
(F_r)	Frequency at the remote location (Substation side)
(vd)	Variable delayed number of samples (vd=0, 1, 2, 3, 4 ....50 samples)
(cd)	Actual remote signal delay and it is assumed to be constant
(n)	Total number of samples for every CEM ($n = 3000$ samples)
(i)	Sample index

This process will be repeated 50 times, with a variable applied delay (vd) of a range from 1 to 50. The 51 resulting values will form almost a straight line as illustrated in Figure 5-3 and 5-4. The TDE is equal to the variable applied delay where the result of equation (5-19) is zero. However, the TDE based on equation (5-19) will not be 100% accurate because the frequencies on both sides are not identical due to the load switching and DG connections along the line, that could be 100km distance between the remote and local location of measurements.

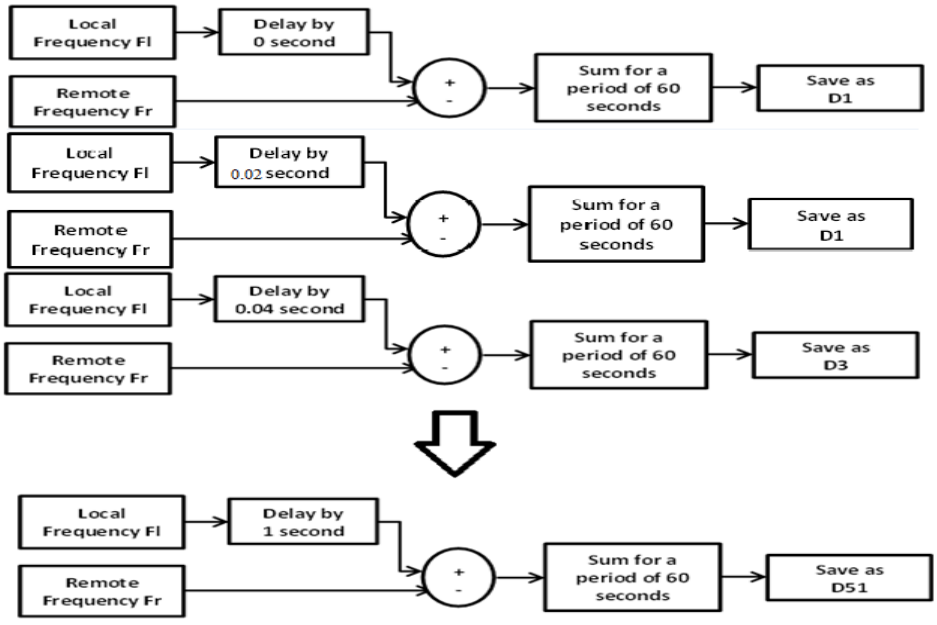

Figure 5-3: Data Convergence Block Diagram

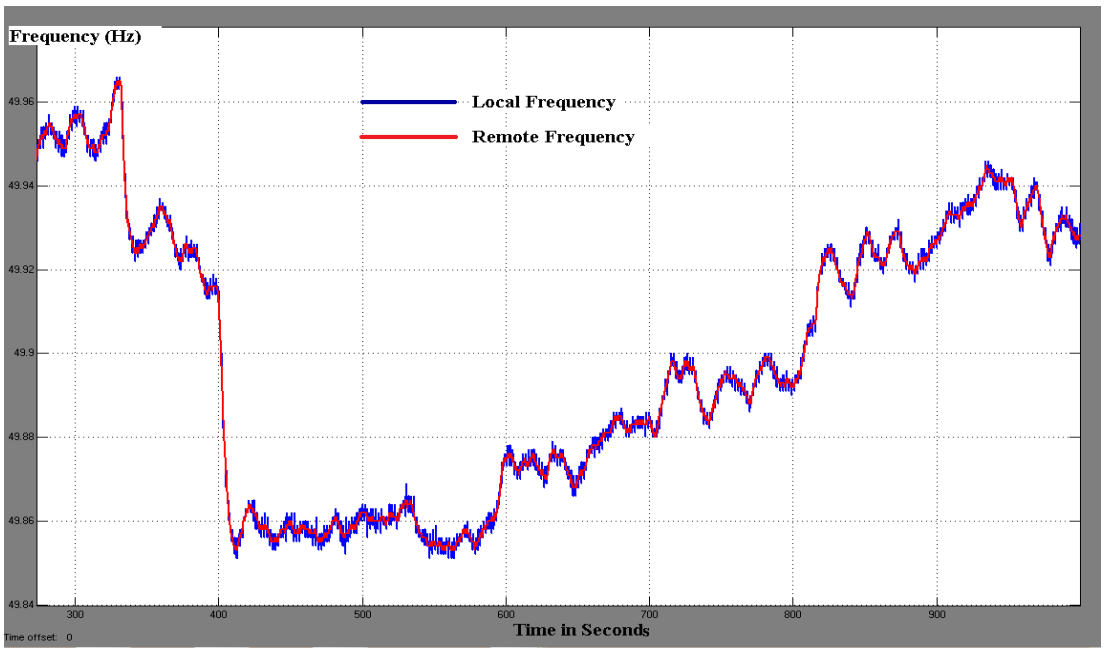

Figure 5-4: A power frequency set measured by two PMUs at two different locations

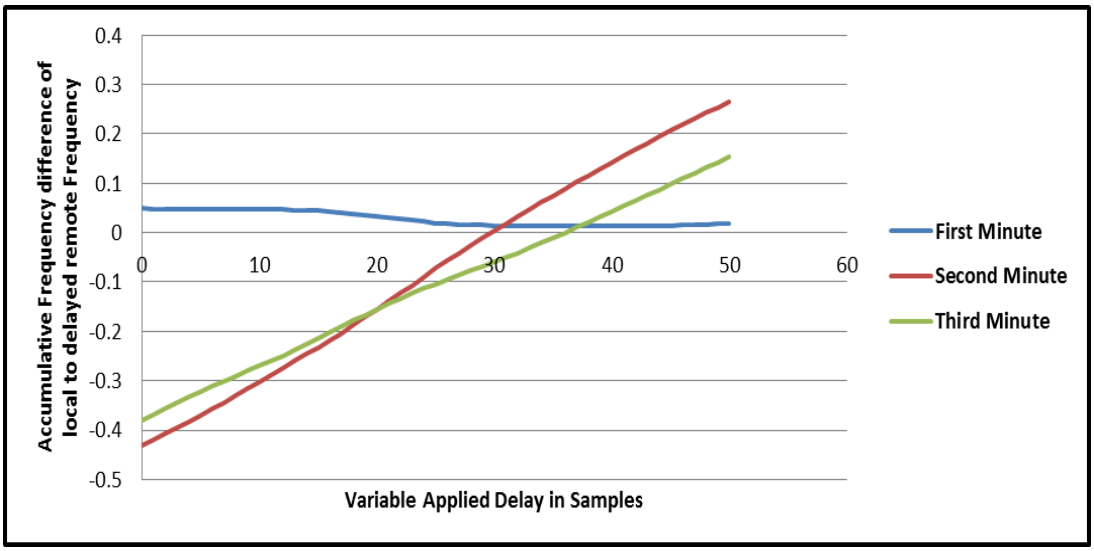

Figure 5-5: Equation (5-19) results for three minutes period (by measuring the delay of remote frequency at a constant applied delay of 0.6s and compare the delayed data to the not delayed local frequency) for the frequency set in Figure 5-4

This is shown in Figure 5-5, the result for the first minute is a disarrayed line that converge at many points along the line makes it impossible to determine which convergence represents the TDE. The result for the second minute gives a correct estimation; however, the estimation of the third minute has an error of 6 samples. In order to determine whether to include or correct the result of the first and third minute or not, and it is possible to achieve more accurate results by determining from using convergence calculation of $(F_l - F_r)$ for 60s accumulative summation and

compare the result to its counterpart result of equations (5-20) and (5-21). Equation (5-20) compares the local frequency with its delayed value, while equation (5-21) compares the remote frequency with its delay value as shown in equations (5-20) and (5-21) and Figures 5-6 and 5-7:

$$Y_{lvd} = \sum_{i=1}^{i=3000}(F_{l_{ivd}} - F_{l_{icd}}) \quad (5\text{-}20)$$

$$Y_{rvd} = \sum_{i=1}^{i=3000}(F_{r_{ivd}} - F_{r_{icd}}) \quad (5\text{-}21)$$

Where,

(F_l)	Frequency at the local location (DG side)
(F_r)	Frequency at the remote location (Substation side)
(vd)	Variable delayed number of samples (vd=0, 1, 2, 3, 4....50 samples)
(cd)	Actual remote signal delay and it is assumed to be constant
(n)	Total number of samples for every CEM ($n = 3000$ samples)
(i)	Sample index

Apart from the result of the first minute, the results obtained by using equations (5-21) and (5-22) gives an accurate TDE for the second and third minutes for the same applied delay (0.6s) as the one in Figure 5-5, as shown in Table 5-2 and Figures 5-6 and 5-7. The results show that the lines resultant from applying equations (5-21) and (5-22) apart from the results of the first minute, are linearly proportional to the variable applied delays.

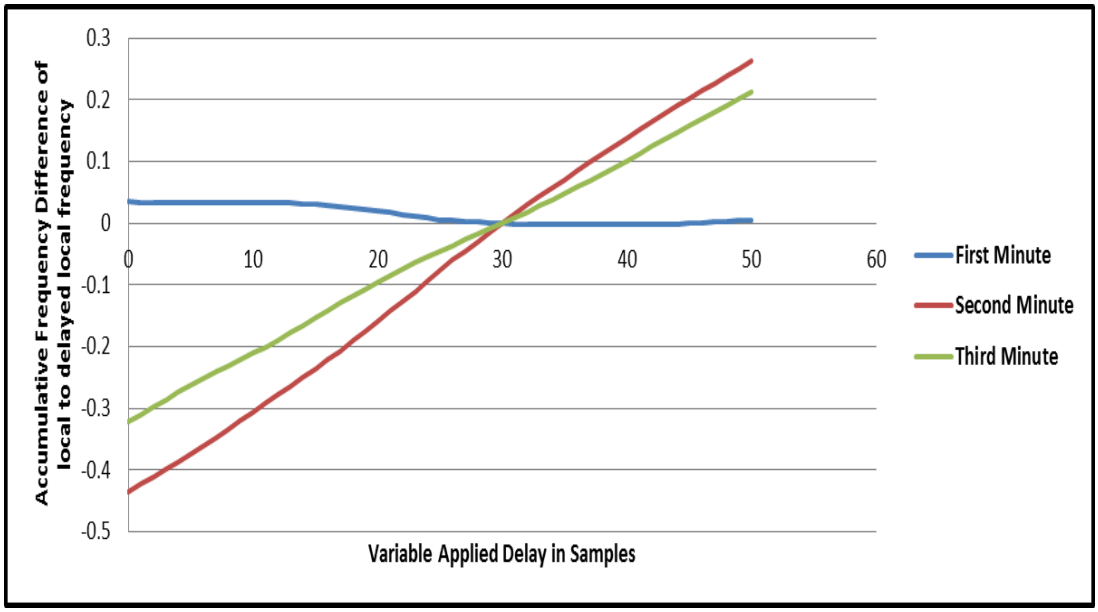

Figure 5-6: Equation (5-20) results for 3 minutes period (by measuring the delay of local frequency at a constant applied delay of 0.6s and compare the delayed data to the not delayed local frequency) for the local frequency shown in Figure 5-4

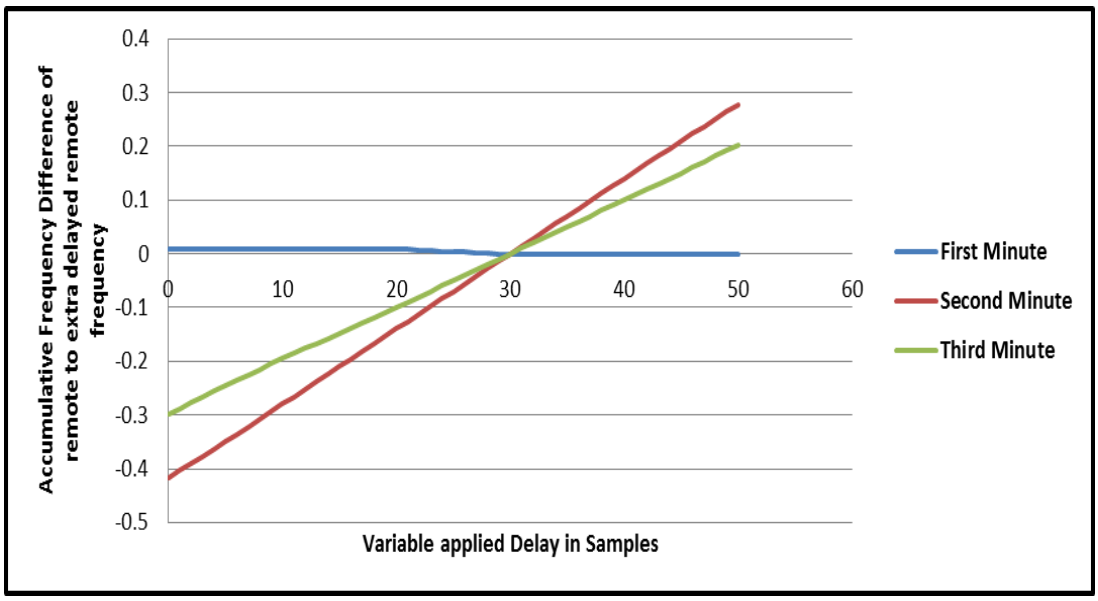

Figure 5-7: Equation (5-21) results for 3 minutes period (by measuring the delay of remote frequency at a constant applied delay of 0.6s and compare the delayed data to the not delayed remote frequency) for remote frequency in Figure 5-4

This means that the result for the summing of the difference between non-delayed F_l and 0.2s ($10_{samples}$) delayed F_l is nearly equal to ten times the result for F_l and 1 sample delayed (F_{l_1}), as shown in equation (5-22):

$$Number\ of\ variable\ delayed\ samples\ (i) \geq \frac{F_{l_i}}{F_{l_1}} \qquad (5\text{-}22)$$

Where,

(i) Number of variable delayed samples
(F_l) Frequency at the DG side

This will give us the opportunity to use the values of equations (5-20) and (5-21) as a reference when compared to the same values for equation (5-19).

Table 5-1: Equations (5-19, 5-20, 5-21) results' matrix

Variable Delay (vd) in samples	0	1	2	3	4	.....	50
60s Sum of Difference (di)	$d1$	$d2$	$d3$	$d4$	$d5$	.....	$d51$

Table 5-2: The difference between a variably delayed frequency and a constantly delayed frequency, of the Frequency set in Figure 5-4 for an MEW of three minutes

Variable Delay(s)		0.1	0.2	0.3	0.4	0.5	0.6	0.7	0.8	0.9	1
Data for Figure 5-4	1st Minute	0.048	0.047	0.044	0.034	0.019	0.014	0.013	0.013	0.014	0.019
	2nd Minute	-0.37	-0.30	-0.23	-0.15	-0.07	0.004	0.075	0.142	0.206	0.266
	3rd Minute	-0.32	-0.27	-0.21	-0.15	-0.10	-0.06	-0.01	0.043	0.098	0.153
Data for Figure 5-5	1st Minute	0.034	0.033	0.03	0.02	0.005	0	-0.00	-0.00	-6E-13	0.005
	2nd Minute	-0.37	-0.30	-0.23	-0.16	-0.07	0	0.071	0.138	0.202	0.262
	3rd Minute	-0.26	-0.21	-0.15	-0.09	-0.04	0	0.049	0.102	0.157	0.212
Data for Figure 5-6	1st Minute	0.008	0.008	0.008	0.008	0.004	0	-4E-13	-4E-13	-6E-13	-0.00
	2nd Minute	-0.35	-0.28	-0.21	-0.14	-0.07	0	0.07	0.14	0.21	0.278
	3rd Minute	-0.25	-0.19	-0.15	-0.1	-0.05	0	0.05	0.1	0.15	0.20

In order to simplify this process, rather than making 2500 calculations for every second (50 calculations a second for 50 variable delays), we can determine the CM value by using only two variable delays, one for 1 sample applied delay and the other for 50 samples applied delay and predicting the linear convergence equation, as follows:

$$Y = aX + b \quad \text{(Linear equation)}$$

Y is the result of equation (5-19) with the delay applied and X is the delay applied index on F_l in equation (5-19) while 'a' and 'b' are constants. To solve this equation the author needs to determine the values of a and b, and in order to do that, two values of Y and two values of X need to be chosen:

- The value of Y at 50 samples applied delay is considered as Y_{50} and $X_{50} = 50$
- The value of Y at 1 sample applied delay is considered as Y_1 and X_1 =1

$Y_{50} = aX_{50} + b$ By subtracting the two equations:

$Y_1 = aX_1 + b$

$$Y_{50} - Y_1 = a(X_{50} - X_1)$$

$$a = (Y_{50} - Y_1)/(X_{50} - X_1) = \frac{Y_{50}-Y_1}{49} \quad (5\text{-}23)$$

$$b = Y_1 - aX_1 = Y_1 - \frac{Y_{50}-Y_1}{49} \times 1 = \frac{49Y_1-Y_{50}+Y_1}{49}$$

$$b = \frac{50Y_1-Y_{50}}{49} \quad (5\text{-}24)$$

The delay estimation should be equal to the value of X when Y is equal to 0s:

$$X = (Y - b)/a = \frac{0-b}{a}$$

$$CE = \frac{-\frac{49Y_1-Y_{50}+Y_1}{49}}{\frac{Y_{50}-Y_1}{49}} = \frac{Y_{50}-50Y_1}{Y_{50}-Y_1}$$

$$Convergence\ Estimation\ (CE) = \frac{Y_n-nY_1}{Y_n-Y_1} \quad (5\text{-}25)$$

(n) Maximum number of variable delay samples and it is equal to 50

Where 'n' is the highest number of applied delay samples, in this thesis the highest applied variable delay to F_l is 1s, which is equal to 50 samples. Therefore, by using equation (5-25) we will reduce the memory needed down to 4%, avoid multi-convergence (multi-model), non-convergence, provide a fraction of sample estimations, and simplify the process of estimation to a point that allows more development. However, ignoring the multi-convergence and non-convergence could provide wrong estimations and have a negative effect on the power frequency delay pattern characteristics. In order to prevent that from happening, an evaluation method is required to cancel out the unwanted individual estimations before calculating the individual estimations' average.

5.3.4 Convergence Linearity Evaluation Method (CLE)

The CE estimation obtained by equation (5-25) provides reasonable 60s individual results. However, because of the non-linearity of the processed data, some of the data evaluated by CE do not converge until it is out of variable delay range (range of 0-1s variable delay) or take a horizontal shape or extremely non-linear that would cause multi-convergence within a maximum variable delay of 1s , as shown in Figures 5-4,5-5, and 5-6. Hence, in order to exclude incorrect CE estimations, we have to evaluate the linearity of the results of equation (5-25) by using the linear scalar estimation (LSE), as shown in equation (5-26) at 0s variable delay for equations (5-

19),(5-20) and (5-21). The result of LSE will be compared with the CE to determine whether to include the measurement in averaging or not:

$$Linear\ Scalar\ Estimation\ (LSE) = \frac{2Y_{lr1}}{(Y_{l1}+Y_{r1})} \quad (5\text{-}26)$$

Where,

(Y_{lr1}) Equation (5-19)
(Y_{l1}) Equation (5-20)
(Y_{r1}) Equation (5-21)

The difference between one power frequency and another delayed power frequency from another UK region will not have the same linearity as the difference between a power frequency and the delayed value of the same frequency, and in some cases the results of equation (5-19) will be highly deviated from linearity and does not represent the proper increase or decrease of the scale values resulted from the variable applied delay to F_l data. As shown in Figures 5-6 and 5-7, the lines for 1st minute are disarrayed (nonlinear), which in turn caused the line for 1st minute in Figure 5-5 to be disarrayed as well. That is why the 1st minute's estimation should not be considered in the delay estimation process. In order to evaluate the CE estimation obtained from equation (5-25), the difference between CE and LSE (equation (5-26)) and compare the result with the chosen threshold setting, as shown in equation (5-27):

$$Delay\ Estimation\ Difference\ = |CE - LSE\ | \quad (5\text{-}27)$$

Where,

(CE) Convergence estimation
(LSE) Linear scalar estimation

If the result of equation (5-27) is less than or equal to the threshold setting then the CE estimation will be included and the result will be corrected to the average of the two estimations CE and LSE as shown in equation (5-28):

$$Convergence\ Evaluation\ Measurement\ (CEM) = \frac{CE+LSE}{2} \quad (5\text{-}28)$$

The threshold of the difference between them can be decided by the author from 1 to 5 cycles; it depends on the period of time that the estimations were determined by. The shorter the time period is the higher the threshold would be. For example, if we decided to estimation the time delay using the average of 3 (60s) measurements during 3 minutes period, the threshold should be 1 to 2 cycles difference between the

two measurements (CE and LSE) with an average of 3 CEM measurements. In other case where the measurement estimation window (MEW) is a period of 30s to obtain the average of at least 3 consecutive measurements, the threshold should be 2-3 cycles. In case of using a 10s period for each measurement, the threshold should be raised to 5-6 cycles. These threshold settings were based on the assumption that the longer the time periods taken the more accurate the result will be, and determined by testing three different sets of frequencies of F_l and F_r for a constant delay range of delay 0.1-1s and a threshold of 1-9 cycles, for MEWs of 3 minutes, 2 minutes and 1 minute and provisional measurement periods of 60s, 30s and 10s as shown in Appendix C.1. This has also been demonstrated in a small scale in Tables 5-3, 5-4, and 5-5, for a single constant delay of 0.6s and a threshold of 1-6 cycles for only the first set that demonstrate the legitimacy of these chosen thresholds.

Table 5-3: CE, LSE and CEM methods' calculations and decisions for a MEW of 3 minutes and a constant delay of 0.6s, for the frequency set in Figure 5-4

Time (s)	CE	LSE	Diff.	Thresh 1cycle	CEM	Thresh 2cycles	CEM	Thresh 3cycles	CEM
60	30.00	28.79	1.21	NA	NA	1.00	29.40	1.00	29.40
120	81.67	0.15	81.52	NA	NA	NA	NA	NA	NA
180	30.92	1.40	29.52	NA	NA	NA	NA	NA	NA
Estimation	47.53	10.11	NA	NA	NA	1.00	29.40	1.00	29.40

Table 5-4: Demonstration of CE, LSE and CEM methods' calculations and decisions for MEW of 2 minutes and a constant delay of 0.6s for Frequency set in Figure 5-4

Time (s)	CE	LSE	Diff.	Thresh 2cycle	CEM	Thresh 3cycles	CEM	Thresh 4cycles	CEM
30	30.00	29.00	1.00	1.00	29.50	1.00	29.50	1.00	29.50
60	30.00	29.00	1.00	1.00	29.50	1.00	29.50	1.00	29.50
90	24.66	28.00	3.34	NA	NA	NA	NA	1.00	26.33
120	81.67	96.00	14.33	NA	NA	NA	NA	NA	NA
Estimation	41.58	45.50	NA	2.00	29.50	2.00	29.50	3.00	28.44

Table 5-5: Demonstration of CE, LSE and CEM methods' calculations and decisions for a MEW of 1 minute and a constant delay of 0.6s for Frequency set in Figure 5-4

Time (s)	CE	LSE	Diff.	Thresh 4cycles	CEM	Thresh 5cycles	CEM	Thresh 6cycles	CEM
10	30.0	29.0	1.0	1.00	29.5	1.00	29.5	1.00	29.5
20	31.4	34.0	2.6	1.00	32.7	1.00	32.7	1.00	32.7
30	33.7	31.7	2.0	1.00	32.7	1.00	32.7	1.00	32.7
40	45.6	36.2	9.4	NA	NA	NA	NA	NA	NA
50	29.3	24.2	5.1	NA	NA	NA	NA	1.00	26.75
60	37.78	40.75	2.97	1.00	39.27	1.00	39.27	1.00	39.27
Estimation	34.66	32.64	NA	4.00	33.55	4.00	33.55	5.00	32.19

In the case of 10s measurements, the higher the threshold the more accurate the estimation will be when it leads to including more provisional CEM values as shown in Table 5-5.

In Appendix C2, a full test to determine the value of CEM for variable delay range of 0-50 samples (0-1s) for a window of measurement of 3 minutes and a threshold of 1.5 cycles, using 100 sets of real PMU data of power frequency measured in two separate locations in UK one in Glasgow and the other in Manchester. The results showed that for a TDE error tolerance of 5 cycles (0.1s) the probability of accurate estimations is 93.3%. However, in addition to the delay estimation, there should be a correction method available to reduce the delay estimation error and improve the probability of success to 100%.

5.3.5 Linear Trajectory Path (LTP)

The first stage of this method is based on creating a trajectory path of extra range of delays from 0-1s to the delayed remote power frequency data which would give an indication of the level of the linearity of the CEM measurements. This can be achieved by using the LTP algorithm shown in Figure 5-8, for data set 2 with a constant applied delay of 0.6s and a threshold of 2 cycles as shown in Table 5-6. The second stage can be achieved by using two different techniques, the first technique is calculating the average of CEM estimation of 3 minutes period with the closest value from the estimations generated by the linear trajectory path model (LTP); this approach is called the linear trajectory path with magnitude (LTPM). The second techniques is by calculating the average deviation of the LTP results from the actual linear applied delay and compensate the difference to the CEM estimation and it is called Linear Trajectory Path with Average linear error compensation (LTPA). The two approaches' performances will be demonstrated in Table 5-6. Now, because each of the two techniques is biased because for the LTPM method, the closest LTP estimation to the CEM estimation does not necessarily belongs to same actual delay, and for the LTPA method the average deviation does not necessarily apply for an individual actual delay. Hence, they have to be averaged to determine the time delay estimation for a period of 3 minutes. The actual delay of the remote data will not affect the results of the trajectory of added delay, because the trajectory delay of 0s is

been used as a reference and the accumulated difference between the local and the remote data for 60s window at zero trajectory delay was subtracted from itself. Hence, the trajectory delay estimation at 0s delay will always be zero and it will not take part in the LTP calculation of linearity error as shown in Table 5-6. The final LTP estimation will be determined by calculating the average of LTPM and LTPA as shown in Figure 5-8 and equation (5-29):

$$LTP_i = \frac{LTPM_i + LTPA_i}{2} \quad (5\text{-}29)$$

$(LTPM)$ Linear trajectory path with Magnitude
$(LTPA)$ Linear Trajectory Path with Average linear error compensation
(LTP) Linear Trajectory Path
(i) LTP Estimations' index

Table 5-6: Linear Trajectory Path (LTP) Estimations for 0.6s Delay

LTP Added Delay in samples	5	10	15	20	25	30	35	40	45	50
Trajectory Estimation Delay	3.03	7.99	13.06	18.35	22.22	27.2	32.2	37.16	42.1	47.1
Deviation from Linearity	-1.97	-2.0	-1.94	-1.65	-2.8	-2.8	-2.8	-2.84	-2.8	-2.8
CEM Estimation	28.71									
LTPM Estimation	27.96									
LTPA Estimation	31.15									
$LTP_{M\&A}$ Estimation	29.55									

5.3.6 Variance Elimination Assessment (VEA)

In order to determine the level of accuracy of this method, the estimations should be evaluated by using calculating the variance of a number of estimations. The variance is calculated using equation (5-30) [89]:

$$Estimation\ Variance\ (\sigma_y^2) = \frac{1}{n}\sum_{i=1}^{n}(y_i - \bar{y})^2 \quad (5\text{-}30)$$

Where,

(y) Time delay estimation in samples
$(\bar{y})$ The average of estimations in samples
(i) Estimation variance index
(n) Total number of estimations involved in the variance calculation

The variance can be calculated based on the population number or based on the elements number. In this case the variance is calculated based on the population number.

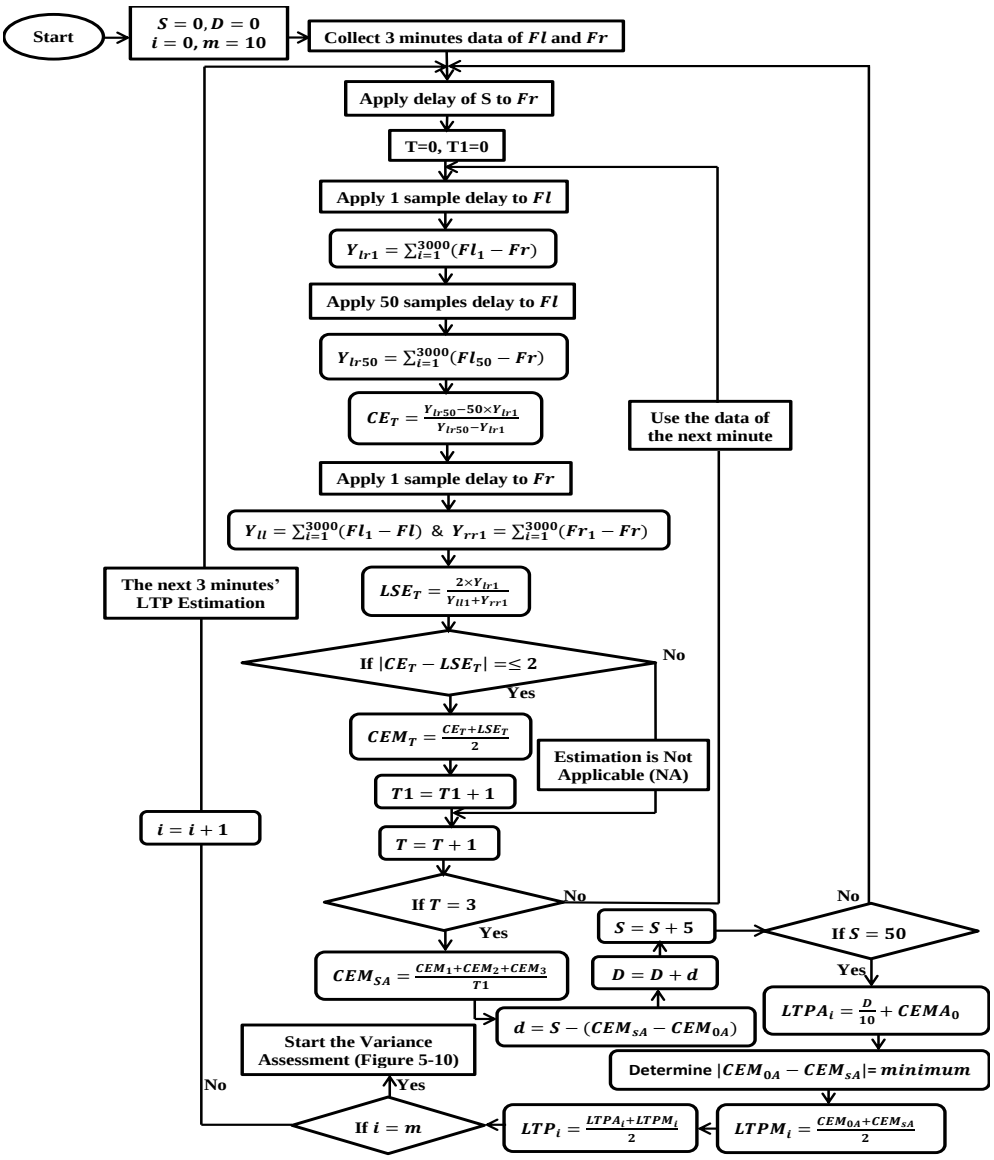

Figure 5-8: Linear Trajectory Path (LTP) Algorithm for Time Delay Estimation

That is why the sum of the square difference between each estimation and the average of the three estimations is divided by the number of estimations included in the calculation, which is "n" according to equation (5-30), while if the variance calculation is based on the number of elements, the sum of square difference will be divided by "$n-1$". The variance should be calculated between all the estimations involved, for example: If we have 3 estimations there will be 6 variance calculations $v(1,2), v(1,3), v(2,1), v(2,3), v(3,1),$ and $v(3,2)$. However, the repeated variances of $v(2,1), v(3,1),$ and $v(3,2)$ will be cancelled. Hence, we will have only 3 variances. In Figure 5-9, the required variances' calculations are shown for 10 estimations and in Figure 5-10 the variance assessment's algorithm is shown for any

number of LTP estimations. In order to determine whether the estimations are acceptable or not, the deviation should be less than 3 samples. The variance of two estimations that differ by 6 samples is 9. Hence, the author has chosen 9 as the threshold for this assessment.

(i)	Estimations	Variance (Var)								
1	$Est_{1\,(180s)}$									
2	$Est_{2\,(360)}$	$Var_{(1,2)}$								
3	$Est_{3\,(540s)}$	$Var_{(1,3)}$	$Var_{(2,3)}$							
4	$Est_{4\,(720s)}$	$Var_{(1,4)}$	$Var_{(2,4)}$	$Var_{(3,4)}$						
5	$Est_{5\,(900s)}$	$Var_{(1,5)}$	$Var_{(2,5)}$	$Var_{(3,5)}$	$Var_{(4,5)}$					
6	$Est_{6\,(1080s)}$	$Var_{(1,6)}$	$Var_{(2,6)}$	$Var_{(3,6)}$	$Var_{(4,6)}$	$Var_{(5,6)}$				
7	$Est_{7\,(1260s)}$	$Var_{(1,7)}$	$Var_{(2,7)}$	$Var_{(3,7)}$	$Var_{(4,7)}$	$Var_{(5,7)}$	$Var_{(6,7)}$			
8	$Est_{8\,(1440s)}$	$Var_{(1,8)}$	$Var_{(2,8)}$	$Var_{(3,8)}$	$Var_{(4,8)}$	$Var_{(5,8)}$	$Var_{(6,8)}$	$Var_{(7,8)}$		
9	$Est_{9\,(1620s)}$	$Var_{(1,9)}$	$Var_{(2,9)}$	$Var_{(3,9)}$	$Var_{(4,9)}$	$Var_{(5,9)}$	$Var_{(6,9)}$	$Var_{(7,9)}$	$Var_{(8,9)}$	
10	$Est_{10\,(1800s)}$	$Var_{(1,10)}$	$Var_{(2,10)}$	$Var_{(3,10)}$	$Var_{(4,10)}$	$Var_{(5,10)}$	$Var_{(6,10)}$	$Var_{(7,10)}$	$Var_{(8,10)}$	$Var_{(9,10)}$

Figure 5-9: Variance Elimination Assessment (VEA) Map

5.4 Assessment of the LTP estimation method

In 4.3 it was determined that the communication based LOM protection method by Frequency Correlation (CFC) can withstand an estimation error of 5 cycles (0.1s) without causing any nuisance tripping. However, the variance assessment threshold is determined based on a threshold of 3 cycles (samples). The variance assessment threshold is estimated by using equation (5-30) for two estimations with 3 cycles (samples) of error which resulted in the value of 9. Any estimation that has a variance sum that exceeds the value of 9, a decision will be made to exclude the estimation, as shown in Figure 5-10. Now, CEM and LTP estimations were obtained from the frequency set number 6, the estimations are for 3 minutes each and a total of 30 minutes. The estimations average and total variance has been determined, as shown in Tables 5-7 and 5-8. The number of CEM estimations that exceeded the error of 3 cycles (samples) are 32 and the number of CEM estimations exceeded the error of ± 5 cycles are 27. On the other hand, the LTP estimations that exceeded the error of ± 3 cycles are 15 estimations and the LTP estimations that exceeded the error of ± 5 cycles are 32 estimations.

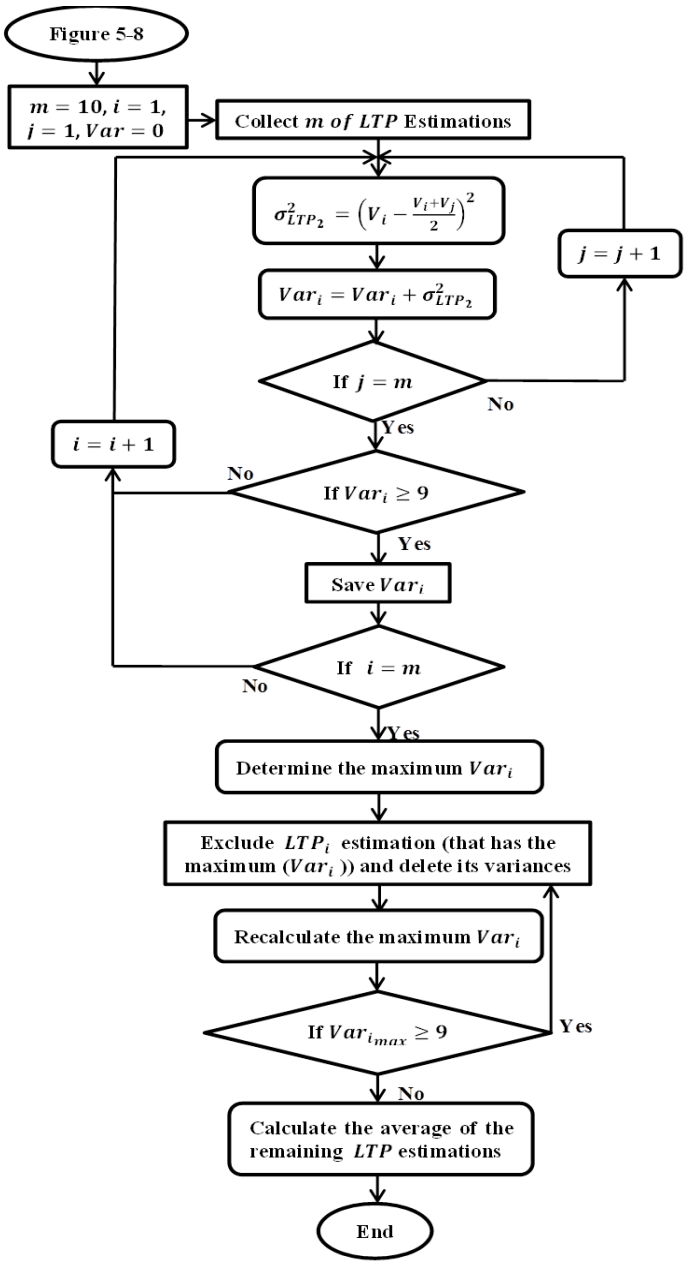

Figure 5-10: Variance Elimination Assessment (VEA) Algorithm

However, the results show that 3 from 10 CEM delay estimations' average of 30 minutes in Table 5-7 have exceeded the error threshold of ± 3 cycles (samples), while only one has exceeded the error of ± 5 cycles, and in Table 5-8, 4 from 10 of the LTP average estimations have exceeded the error threshold of ± 3 cycles, while only one has exceeded the error of ± 5 cycles. Even though the estimations that exceeded the error of ± 5 cycles have also exceeded the error of ± 3 cycles, the will not be included in the group of estimations that exceeded ± 3 cycles.

Notes: For Tables 5-7, 5-8, 5-9, and 5-10
Frequency set number 6 is chosen from the 100 frequency sets because it showed high errors in the CEM and LTP estimations
The symbol **(*)** underneath an estimation value means that this estimation has an error that exceeded the absolute of ± 3 samples (cycles)
The symbol **(**)** underneath an estimation value means that this estimation has an error that exceeded the absolute of ± 5 samples (cycles)
(NA) stands for Not Applicable: this means that the average estimation of 3 minutes estimation window has failed the Convergence Linearity Evaluation (CLE) test for all three estimations, and this failure is determined when the result of equation (5-27) exceeds the pre-set threshold value.
Grey cells in Tables 5-7, 5-8, 5-9, and 5-10 are the estimations that showed increase of error from over ± 3 cycles in CEM estimation to over ± 5 cycles in the LTP estimation. They are selected to show how the variance elimination assessment (VEA) is efficient in eliminating estimations with high error
Empty cells in Tables 5-9 and 5-10 are the estimations that were eliminated by the variance elimination assessment and they will no longer be considered

Table 5-7: CEM estimations for frequency set number 6

Estimations Time Window	Constant Delays in samples									
	5	10	15	20	25	30	35	40	45	50
0-180s	5.41	10.43	15.40	20.24	25.27	20.12 **	35.26	30.61 **	45.06	50.13
180-360s	11.37 **	12.53	13.9	18.08	20.44 *	25.01 *	41.46 **	33.04 **	37.72 **	57.46 **
360-540s	4.18	4.24 **	6.99 **	12.13 **	17.29 **	22.42 **	31.93 *	36.99 *	38.15 **	43.26 **
540-720s	1.92 *	NA	NA	NA	NA	NA	31.97 *	36.0 *	40.02 *	44.04 **
720-900s	7.35	8.76	43.98 **	18.46	23.47	28.53	39.47 *	44.65 *	45.42	55.03 **
900-1080s	2.45	7.42	11.50 *	16.44 *	21.50 *	26.32 *	31.12 *	35.98 *	40.87 *	46.72 *
1080-1260s	5.68	10.54	15.44	20.40	25.37	30.13	35.25	40.38	49.74 *	50.70
1260-1440s	0.96 *	5.85 *	8.59 **	11.97 **	15.35 **	18.84 **	31.02 *	36.8 *	42.36	NA
1440-1620s	4.36	4.82 **	9.97 **	10.09 **	14.99 **	21.96 **	NA	NA	NA	40.69 **
1620-1800s	2.08	6.82 *	11.80 *	16.71 *	21.74 *	26.68 *	31.61 *	36.35 *	41.44 *	46.52 *
Average Estimations	4.58	7.93	15.29	16.06 *	20.60 *	24.45 **	34.34	36.76 *	42.31	48.28
Variance	8.69	7.11	110.4	12.73	13.88	13.14	13.22	14.27	13.21	27.27

Table 5-8: LTP estimations for frequency set number 6

Estimations Time Window	Constant Delays in samples									
	5	10	15	20	25	30	35	40	45	50
0-180s	6.55	11.67	16.50	22.34	26.33	16.68 **	35.70	25.98 **	44.96	50.18
180-360s	15.24 **	12.55	15.31	18.86	20.73 *	28.73	51.46 **	34.62 **	43.98	83.46 **
360-540s	7.27	4.98 **	7.91 **	13.06 **	18.49 **	23.21 **	39.67 *	49.79 **	52.12 **	47.75
540-720s	2.89	NA	NA	NA	NA	NA	41.93 **	49.97 **	58.02 **	66.06 **
720-900s	8.50 *	8.53	69.23 **	19.92	24.53	29.55	40.49 **	44.98 *	45.86	58.81 **
900-1080s	3.57	8.37	11.94 *	16.91 *	22.15	26.52 *	30.83 *	35.93 *	40.96 *	48.10
1080-1260s	5.78	10.52	15.27	20.03	24.78	29.50	34.88	39.88	51.48 **	50.30
1260-1440s	1.44 *	5.98 *	9.42 **	14.51 **	15.51 **	19.28 **	34.63	46.20 **	57.31 **	NA
1440-1620s	4.99	4.99 **	10.98 *	10.98 **	19.00 **	23.58 **	NA	NA	NA	41.86 **
1620-1800s	2.82	7.39	12.38	17.29	22.51	27.57	32.39	36.81 *	41.87 *	47.79
Average Estimations	5.91	8.33	18.77 *	17.10	21.56 *	24.96 **	38.00	40.46	48.51 *	54.92 *
Variance	14.11	6.95	325.5	11.96	10.71	18.99	34.98	56.53	36.77	146.3

5.4.1 Variance Elimination Assessment's Findings

By applying the variance elimination assessment (VEA) on the results shown in Tables 5-7 and 5-8 by using the VEA algorithm illustrated in Figure 5-10, the number of estimations in Tables 5-7 and 5-8 will be reduced to the estimations shown in Tables 5-9 and 5-10. The VEA has shown higher performance with the LTP estimations than with the CEM estimations. The VEA has reduced the number of estimations that exceeded the error of 3 cycles for CEM estimations by 18.18%, and for LTP estimations by 60%. The VEA has also reduced the estimations that exceeded the error of ± 5 cycles for the CEM estimations by 77.78%, and for LTP estimations by 96.8% as shown in Table 5-11. After eliminating the unwanted estimations, the remaining CEM estimations' average estimations as shown in (of the

delay range of 5 to 50 cycles) that exceeded the error of ± 3 cycles has increased from 3 to 6 estimations, and it reduced their counterpart of LTP estimations' average from 4 to 1 estimations. On the other hand, the single average estimation that exceeded the error of ± 5 cycles for LTP estimation has been eliminated because of the VEA assessment, however, it persisted for the CEM VEA assessment.

Table 5-9: VEA Assessment's results for CEM estimations in Table 5-7

Estimations Time Window	Constant Delays in samples									
	5	10	15	20	25	30	35	40	45	50
0-180s	5.41			20.24						
180-360s			13.91	18.08	20.44 *	25.01 *				
360-540s	4.18					22.42 **	31.93 *	36.99 *		43.26 **
540-720s	1.92 *						31.98 *	36.00 *	40.02 *	44.04 **
720-900s		8.76		18.46	23.48					
900-1080s	2.45	7.42	11.50 *	16.44 *	21.50 *	26.32 *	31.12 *	35.98 *	40.87 *	46.72 *
1080-1260s	5.68									
1260-1440s		5.85 *					31.02 *	36.80 *	42.36	
1440-1620s	4.36	4.82 **	9.97 **							
1620-1800s	2.08	6.82 *	11.80 *	16.71 *	21.74 *	21.96 **	31.61 *	36.35 *	41.44 *	46.53 *
Average Estimations	3.40	6.73 *	11.79 *	17.98	21.79 *	23.93 **	31.53 *	36.42 *	41.17 *	45.14 *
Variance	1.73	1.80	1.96	1.87	1.19	3.26	0.16	0.17	0.73	2.29

Table 5-10: VEA Assessment's results for LTP estimations in Table 5-8

Estimations Time Window	Constant Delays in samples									
	5	10	15	20	25	30	35	40	45	50
0-180s			16.50				35.70		44.96	50.18
180-360s			15.31	18.86		28.73		34.62 **	43.98	
360-540s										47.75
540-720s	2.89									
720-900s		8.53		19.92	24.53	29.55			45.86	
900-1080s	3.57	8.37		16.91 *	22.15	26.52 *		35.93 *		48.10
1080-1260s	5.78		15.27	20.03	24.78	29.50	34.88			50.30
1260-1440s		5.98 *					34.63			
1440-1620s	4.99									
1620-1800s	2.82	7.39	12.38	17.29	22.51	27.57		36.81 *	41.87 *	47.79
Average Estimations	4.01	7.57	14.87	18.60	23.49	28.37	35.07	35.79 *	44.17	48.82
Variance	1.39	1.03	2.30	1.69	1.38	1.37	0.21	0.81	2.20	1.35

Table 5-11: VEA Assessment's Findings and Analysis

Constant Delays in samples	CEM number of errors before variance assessment Table 5-7		CEM number of errors after variance assessment Table 5-9		LTP number of errors before variance assessment Table 5-8		LTP number of errors after variance assessment Table 5-10	
	> ± 3 cycles	> ± 5 cycles	> ± 3 cycles	> ± 5 cycles	> ± 3 cycles	> ± 5 cycles	> ± 3 cycles	> ± 5 cycles
5	2	1	1	0	2	1	0	0
10	2	2	2	1	1	2	1	0
15	2	4	2	1	2	3	0	0
20	2	3	2	0	1	3	1	0
25	3	3	3	0	1	3	0	0
30	3	4	2	2	1	4	1	0
35	6	1	5	0	2	3	0	0
40	6	2	5	0	3	5	2	1
45	6	2	4	0	2	4	1	0
50	2	5	2	2	0	4	0	0
Total errors	32	27	28	6	15	32	6	1
Average Estimations' Errors	3	1	6	1	4	1	1	0

5.4.2 Analysis of LTP Method

Before applying the VEA assessment, the LTP method reduced the estimations that exceed the error of ± 3 cycles by 17 estimations (53.12%); on the other hand it

increased the estimations that exceed the error of ±5 cycles by 5 estimations (18.51%) as shown in Table 5-11, and the sum of all exceeded limits estimations (for ±3 cycles and ±5 cycles) has decreased by 12 estimations. The increase in number of estimations that exceed the error of ±5 cycles may seem at first as weakness in the LTP method's performance. The LTP technique corrected 12 estimations that exceeded the error of ±3 cycles to less than ±3 cycles. It also corrected 2 estimations that exceeded the error of ±5 cycles to less than ±3 cycles. However, it increased the estimation error of 7 estimations from over ±3 cycles to over ±5 cycles, and that explains the increase in estimations' error that exceeds ±5 cycles. According to Tables 5-7, 5-8, 5-9, 5-10 and 5-11 five of the seven estimations that changed from exceeding the error of ±3 cycles to exceeding the error of ±5 cycles (presented in cells highlighted by the colour of grey) were not eliminated by applying the VEA assessment to the CEM estimations, however, they were eliminated by the VEA assessment when applied to the LTP estimations. By increasing the error of these five estimations made it possible for the VEA assessment to detect these estimations and eliminate them, because their variances have exceeded 9. Hence, the LTP method reduced the total incorrect estimations by 14 (23.72%) and increased some of the incorrect estimations to increase their probability of elimination by the VEA. As shown in Table 5-11 and explained in 5.4.1, the VEA assessment reduced the total incorrect LTP estimations by 85.106%, while it reduced the incorrect CEM estimations by only 42.37%. This shows how the combination of LTP method and VEA assessment, the incorrect estimations can be reduced to zero.

5.5 Decision, Error interpretation and Synchronization

As mentioned earlier, this TDE method is designed for an accumulate LOM method more specifically for VPAD method that was presented in chapter 2. Therefor the acceptable delay estimation error can be tolerated up to ±6 cycles (120ms) as mentioned in chapter 4. The difference between internet and GPS synchronisation and the LTP is that the latter basically depends on data convergence, and even if the delay estimation is wrong it will not cause any sudden increase or decrease in the result of the VPAD accumulate phase angle difference that would compromise the security of relay operation and lead to spurious tripping. Therefore, the method would have a major improvement on the security level of the VPAD and lead to the

illumination of nuisance tripping without compromising the reliability of LOM method in correctly detecting LOM and isolating the DG within the allowed period of time 2s [10] (In fact some corporations like the Scottish and Southern Energy (SSE) show more flexibility in the maximum period of LOM operation allowed to up to 3s but only as trade-off to having the most reliable and secure LOM protection method). However, this effect is questionable in the case of MEWs longer than 10s. When the delay estimation gets accepted a notification signal will be issued to delay the local data by the delay time estimation in order to synchronise the two frequency data. In the event of a change in the accepted delay estimation another notification will be sent to update synchronisation. If the delay estimation of LTP was rejected or there was not even any CEM estimation the existing delay to the local frequency will stay unchanged. This could cause some inconsistency in the LOM protection decision, considering that it would require 3-3.5 minutes to determine the time delay estimation. However, according the PMU processing delay and communication latency sum to a minimum of 380ms and a maximum of 440ms, as explained in 3.3; therefore the variation of delay is within 50-60ms ($\pm$3 cycles), hence the desired estimation tolerated error would be $\pm$3 cycles. Although it is unnecessary, it is desired that in the case of detection the LOM after the estimation rejection to not to operate the protection instantaneously, and apply some delay to the operation. Unless the LOM operation has already passed 2s, then the priority is to isolate the DG [10].

5.6 Communication Link Loss Detection Method (CLD)

When the satellite communication performance degrades to a level that exceeds threshold for period of time, the link should be considered unavailable. This limit can also be reached when the increase of noise and the increase of bit error rate (BER) are no longer acceptable. Recommendations (ITU-R and ITU-T) [85], state that a communication link will be considered unavailable in case the following conditions occurs at the receiving ends for more than 10s: BER>10^{-3}, loss of frame alignment or timing, and the received signal's C/N is 10dB lower than expected. According to the ITU-T and ITU-R recommendations, and the European standard ETS [85], which is relevant to the DVB-S2 system for a Ku band, the objective is a quasi-error free (QEF) operation, which means only one uncorrected error per hour, and the BER for this could be between 10^{-7} and 10^{-11} depending on the data rate. For this application

BER=10^{-7} is sufficient because the message information data rate is low (32 Bytes fifty times per second = 12800 b/s), and with BER=10^{-8} after FEC, the result will be 0.4608s, which is less than one bit of uncorrected error for every hour.

Hence, the BER could be 10^{-5} before correction by the FEC and 10^{-8} after correction. Furthermore, when using the CLD method it is vital that we should be able to differentiate between loss of link and high data error from LOM event by examining the received data values. For example if the received data read numbers like 0, negative number, integer, number in value of hundreds or thousands or the number is over 70 or less than 30 then it cannot be a LOM event. If there is a communication loss or high level of BER there will be numbers like the ones that was earlier mentioned in this paragraph, as shown in Figure 5-11.

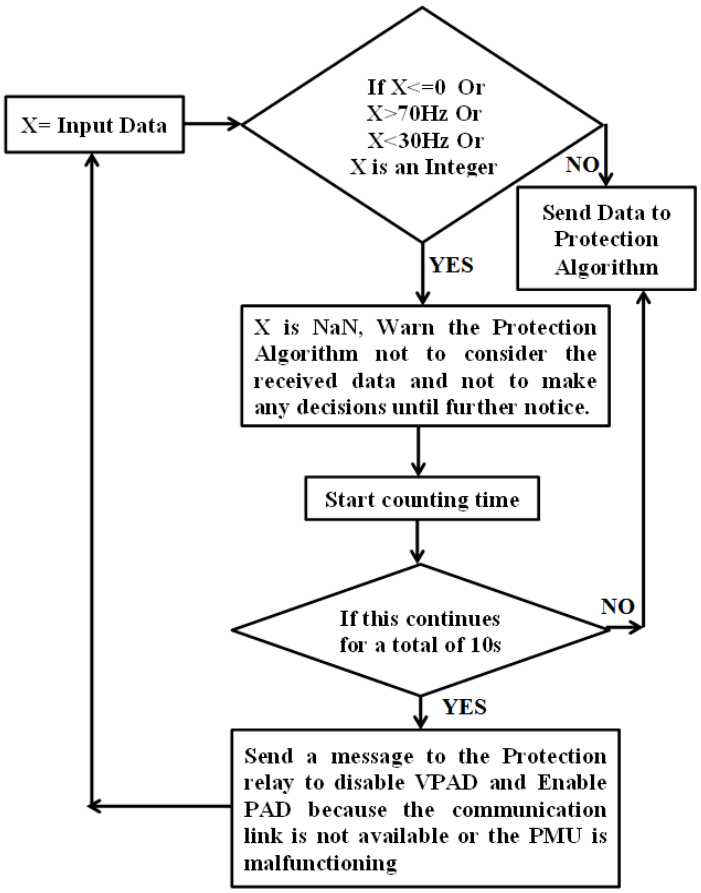

Figure 5-11: Loss of Link Detection (CLD) Algorithm

Also, the generators' reaction to changes could be different from a generator to another and from their turbine engines' fuel and technology. If this continuous for 10s (Ten 1s CEM estimations) then it indicates that the satellite link is unavailable or

there is a PMU malfunction. This makes a big improvement to the TDE estimation and the LOM detection algorithm because it will support the operation of LOM detection in detecting loss of link and data error, at the same time it will give highly important information to the LTP method in determining the reason behind the no estimation result and put an end to the continuing attempt to make an estimation for an extra 30s and inform the LOM algorithm of this for it to act by comparing its ongoing calculation to the accumulated phase angle difference and either resetting the calculation until further notice or by deactivating the VPAD algorithm and activate the local PAD algorithm. This method can also be used with internet communication methods and for satellite communication methods for other applications as well, because it can be used separately for each of the satellite communication and power system applications. If the PMU at the substation suffered from loss of synchronisation caused by an error at the GPS, this will cause time quality issues that leads to a series of automatic reset, that could take few seconds for every attempt. This would seem as if the communication is lost, or a LOM event has occurred. If the LOM protection was not notified it would cause a series of nuisance tripping all around that substations region. Hence, implementing this method with LOM protection unit is very necessary and in some circumstances it is more important than the TDE method and synchronisation.

5.7 Chapter Summary

In this chapter we discussed the reason behind developing a data method for TDE, and we explored many methodologies. The findings were that these methods always have a sinusoidal function for the data signal and the number data samples used in these methods were far higher than the number of samples available for this application. However, because of the data measurements were obtained using DFT a signal processing method by sampling the sinusoidal function of the voltage by 10000 samples, the sinusoidal function will not be necessary. Also, the number of samples required is far less than other application that may cause high error levels.

The LTP method succeeded in correcting some of the CEM estimations, but it was not successful in eliminating all the error. However, by applying the variance elimination assessment (VEA) on the LTP estimations and succeeded in eliminating

the unwanted estimations. By making these changes only the estimations that have an error of lower than 5 cycles will be accepted and only the estimations that exceeded the error threshold will be rejected. The method will notify the LOM protection algorithm of the delay estimation within a maximum period of 30 minutes. If the TDE algorithm failed to obtain an estimation or the estimation was rejected the VPAD and CFC will be notified by the LTP to hold the previous delay estimation. If the estimation was accepted a notification will sent to the VPAD and CFC to make the changes accordingly.

There is also the invention of the Communication Link Loss and Low Quality (corrupted data) Detection (CLD) algorithm that will successfully detect a loss of communication link in 10s, and instantaneously detect and block error bursts or inconsistent measurements that do not apply for power frequency measurements in power system applications.

CHAPTER 6: CONCLUSIONS AND FURTHER WORK

6.1 Conclusions

The main objective of this research is to develop a communication based LOM protection method that is both secure and reliable to replace the ROCOF method that suffers from nuisance tripping. The developed method should be compatible with all communication mediums and techniques and be more reliable and stable than the ROCOF LOM protection method.

The development and testing of the CFC LOM protection method has shown that the method is very sensitive and stable, and enforces security and reliability to the system. The CFC can withstand un-synchronization of local data with remote data to up to 100ms, and it is immune against nuisance tripping in case of load switching and faults. The CFC method is compatible with both internet and satellite communication. The CFC algorithm with the periodic approach proved to have more stability that the CFC with the instantaneous approach, without compromising the reliability of the method. The sensitivity tests showed that the maximum relay response to LOM operation is 1s. However, the actual isolation of the DG will take longer than that when including the communication time required for the remote data to reach the DG, the relay processing time delay, the remote PMU processing delay, the time required for the initiated trip signal to reach the CB, and the CB operation time. Hence, the total trip time is equal to 1.640s for satellite communication and 1.310s for internet communication. Thereby, it is less than the maximum tolerated LOM operation.

The development stages of the new TDE method called Linear Trajectory Path (LTP) that is designed for power system applications. The author concluded in chapter 4 that 5 cycles (100ms) of estimation error can be tolerated without undermining the reliability and security of the protection system and this conclusion was based the LOM algorithm function and data communication requirements. The combination of the LTP method and variance elimination assessment (VEA) method proved to be able to provide time delay estimations with a maximum estimation error of 100ms (5

cycles). The issues regarding communication loss or high data error occur and the necessity of detection those events and inform the LOM detection algorithm to avoid undermining the integrity of the algorithm operation and decision. These issues were discussed and a new method was developed in order to detect these events, block those values and inform the LOM protection algorithm. The knowledge of the data requirements of the LOM protection, data measurements, the functioning of PMU, knowledge of generator operation and satellite communication lead to the invention of the CLD technique that detect data error and loss of communication to protect the DG from nuisance tripping by preventing the corrupted data from being included in the LOM Algorithm. If it detects loss of communication or corrupted data, it would automatically block received data and inform the relay to deactivate the communication based LOM protection algorithm (only in the case of loss of communication) and activate the backup local LOM protection method

6.2 Further Work

Further development to both of the two methods:

1- Further development to the CFC LOM protection method is necessary to simplify the CFC algorithm, by finding correlation between the two parameters (ASD, CM).

2- The LTP method would require further development to eliminate the probability of error by using more than two data streams in the process of delay estimation, and develop more control to obtain 100% reliable and accurate estimations.

3- In order to reduce the total TDE period of 30 minutes, an assessment should be conducted in applying the moving window approach described in chapter 4 (for the CFC algorithm) on the LTP method combined with a VEA assessment to reduce the total time needed and to a have more accurate results.

4- A research should be conducted to transform the frequency data obtained by the PMU to a power network that will react normally to the changes applied to it. This transformation should include existing research development of dynamical prediction of the system inertia from the obtained frequency measurements. This would be invaluable in the development of power system applications and in this case in the LOM protection development where realistic events can be simulated.

CHAPTER 7: REFERENCES

[1] The Distribution Code Panel, " The Distribution Code and the Guide to the Distribution Code of Licensed Distribution Network Operators of Great Britain", Issue 25, 01 November 2014.

[2] O. Raipala, S. Repo, K. Mäki, and P. Järventausta, "Studying the Effects of Distributed Generation on Auto-reclosing with a Real Time Digital Simulator and Real Protection Relays," 2004.

[3] Dai, F.T., "Impacts of distributed generation on protection and auto reclosing of distribution networks," Developments in Power System Protection (DPSP 2010), Managing the Change, 10th IET International Conference on, pp.1-5, March 29 2010-April 1 2010.

[4] Kumpulainen, L.K.; Kauhaniemi, K.T., "Analysis of the impact of distributed generation on automatic reclosing," Power Systems Conference and Exposition, 2004. IEEE PES, pp.603-608, vol.1, 10-13th October 2004

[5] Venmathi, M.; Vargese, J.; Ramesh, L.; Percis, E.S., "Impact of grid connected distributed generation on voltage sag," Sustainable Energy and Intelligent Systems (SEISCON 2011), International Conference on, pp.91-96, 20-22th July 2011

[6] S. H. Horowitz and A. G. Phadke, "Power System Relaying", 2nd edition, 2008.

[7] C. R. Bayliss and B. J. Hardy, "Transmission and Distribution Electrical Engineering," 3rd edition, 2007.

[8] J. M. Gers and E. J. Holmes, "Protection of Electricity Distribution Networks", 2nd edition, IEE, 2004.

[9] Brundlinger, R.; Bletterie, B., "Unintentional islanding in distribution grids with a high penetration of inverter-based DG: Probability for islanding and protection methods," Power Tech, 2005 IEEE Russia, pp.1-7, 27-30th June 2005

[10] IEEE Application Guide for IEEE Std. 1547(TM), IEEE Standard for Interconnecting Distributed Resources with Electric Power Systems," IEEE Std. 1547.2-2008, pp.1-217, April 15th 2009.

[11] Dyśko, A.; Burt, G.M.; Moore, P.J.; Glover, I.A.; McDonald, J.R., "Satellite Communication Based Loss-of-Mains Protection," Developments in Power System Protection, 2008. DPSP2008. IET 9th International Conference on, pp.687-692, 17-20th March 2008

[12] Mahat, P.; Zhe Chen; Bak-Jensen, B., "Review of islanding detection methods for distributed generation," Electric Utility Deregulation and Restructuring and Power Technologies, 2008. DRPT2008. Third International Conference on, pp.2743-2748, 6-9th April 2008.

[13] Funabashi, T.; Koyanagi, K.; Yokoyama, R., "A review of islanding detection methods for distributed resources," Power Tech Conference Proceedings, 2003 IEEE Bologna, vol.2, pp.1-6, vol.2, 23-26th June 2003.

[14] Wei Yee Teoh, Chee Wei Tan, "An Overview of Islanding Detection Methods in Photovoltaic Systems," World Academy of Science, Engineering and Technology, 2011.

[15] De Mango, F.; Liserre, M.; Aquila, A.D.; Pigazo, A., "Overview of Anti-Islanding Algorithms for PV Systems. Part I: Passive Methods," Power Electronics and Motion Control Conference, 2006, EPE-PEMC2006, 12th International, pp. 1878-1883, August 30th 2006-September 1st 2006.

[16] Chowdhury, S.P.; Chowdhury, S.; Chui Fen Ten; Crossley, P.A., "Islanding protection of distribution systems with distributed generators — A comprehensive survey report," Power and Energy Society General Meeting - Conversion and Delivery of Electrical Energy in the 21st Century, 2008 IEEE, pp.1-8, 20-24th July 2008.

[17] Ten, C.F.; Crossley, P.A., "Evaluation of ROCOF Relay Performances on Networks with Distributed Generation," Developments in Power System Protection, 2008. DPSP2008. IET 9th International Conference on, pp.523-528, 17-20th March 2008.

[18] Affonso, C.M.; Freitas, W.; Xu, W.; da Silva, L.C.P., "Performance of ROCOF relays for embedded generation applications," Generation, Transmission and Distribution, IEE Proceedings, vol.152, no.1, pp.109-114, 10th January 2005.

[19] H. Meiyi, G. Houlei, L. Bingxu, Z. Guibin, "Vector Shift Method for Islanding Detection Based on Simulation Test," 2008.

[20] Hou, Meiyi; Houlei Gao; Yijun Lu; Yongwu Zhang; Huaming Cao; Yong Lin, "A Composite Method for Islanding Detection Based on Vector Shift and Frequency Variation," Power and Energy Engineering Conference (APPEEC), 2010 Asia-Pacific, pp.1-4, 28-31th March 2010.

[21] Redfern, M.A.; Usta, O.; Fielding, G., "Protection against loss of utility grid supply for a dispersed storage and generation unit," Power Delivery, IEEE Transactions on, vol.8, no.3, pp.948-954, July 1993

[22] Bright, C.G., "COROCOF: comparison of rate of change of frequency protection. A solution to the detection of loss of mains," Developments in Power System Protection, 2001, 7th International Conference on (IEE), pp.70-73, 2001

[23] Salman, S.K.; King, D.J.; Weller, G., "New loss of mains detection algorithm for embedded generation using rate of change of voltage and changes in power factors," Developments in Power System Protection, 2001, 7th International Conference on (IEE), pp.82-85, 2001.

[24] Samui, A.; Samantaray, S.R., "Assessment of ROCPAD Relay for Islanding Detection in Distributed Generation," Smart Grid, IEEE Transactions on, vol.2, no.2, pp.391-398, June 2011.

[25] Sung-Il Jang; Kwang-Ho Kim, "An islanding detection method for distributed generations using voltage unbalance and total harmonic distortion of current," Power Delivery, IEEE Transactions on, vol.19, no.2, pp.745-752, April 2004.

[26] Fu-Sheng Pai; Shyh-Jier Huang, "A detection algorithm for islanding-prevention of dispersed consumer-owned storage and generating units," Energy Conversion, IEEE Transactions on, vol.16, no.4, pp.346-351, December 2001.

[27] Karegar, H.K.; Shataee, A., "Islanding detection of wind farms by THD," Electric Utility Deregulation and Restructuring and Power Technologies, 2008, DRPT2008, 3rd International Conference on, pp.2793-2797, 6-9 April 2008

[28] Jahdi, S.; Loi Lei Lai, "DG islanding operation detection methods in combination of harmonics protection schemes," Innovative Smart Grid Technologies (ISGT Europe), 2011, 2nd IEEE PES International Conference and Exhibition on, pp.1-8, 5-7th December 2011.

[29] Sung-Il Jang; Kwang-Ho Kim, "Development of a logical rule-based islanding detection method for distributed resources," Power Engineering Society Winter Meeting, 2002, IEEE, vol.2, no., pp.800-806, vol.2, 2002.

[30] Lidula, N.W.A.; Rajapakse, A.D., "A Pattern Recognition Approach for Detecting Power Islands Using Transient Signals—Part I: Design and Implementation," Power Delivery, IEEE Transactions on, vol.25, no.4, pp.3070-3077, October 2010.

[31] Lidula, N.W.A.; Rajapakse, A.D., "A Pattern Recognition Approach for Detecting Power Islands Using Transient Signals—Part II: Performance Evaluation," Power Delivery, IEEE Transactions on, vol.27, no.3, pp.1071-1080, July 2012.

[32] Yip, H.T.; Millar, G.; Lloyd, G.J.; Dyśko, A.; Burt, G.M.; Tumilty, R., "Islanding detection using an accumulated phase angle drift measurement," Developments in Power System Protection (DPSP 2010), Managing the Change, 10th IET International Conference on, pp. 1-5, March 29th 2010-April 1st 2010.

[33] An, C.; Millar, G.; Lloyd, G.J.; Dyśko, A.; Burt, Graeme M.; Malone, F., "Experience with accumulated phase angle drift measurement for islanding detection," 2012 47th

International Universities Power Engineering Conference (UPEC), pp. 1-6, 4-7th September 2012

[34] Lloyd, G.; Hosseini, S.; Chang An; Chamberlain, M.; Dyśko, A.; Malone, F., "Experience with accumulated phase angle drift measurement for islanding detection," Electricity Distribution (CIRED 2013), 22nd International Conference and Exhibition on, pp.1-4, 10-13th June 213

[35] Hopewell, P.D.; Jenkins, N.; Cross, A.D., "Loss-of-mains detection for small generators," Electric Power Applications, IEE Proceedings, vol.143, no.3, pp.225-230, May 1996.

[36] Kim, J.E.; Hwang, J.S., "Islanding detection method of distributed generation units connected to power distribution system," Power System Technology, 2000, Proceedings. PowerCon2000. International Conference on, vol.2, pp.643-647 vol.2, 2000

[37] O'Kane, P.; Fox, B., "Loss of mains detection for embedded generation by system impedance monitoring," Developments in Power System Protection, Sixth International Conference on (Conf. Publ. No. 434), pp.95-98, 25-27th Mar 1997.

[38] Ropp, M.E.; Begovic, M.; Rohatgi, A., "Analysis and performance assessment of the active frequency drift method of islanding prevention," Energy Conversion, IEEE Transactions on, vol.14, no.3, pp.810-816, September 1999.

[39] Wang Zhen-yue; Zhao Bao-chang; Shi Xin-chun; Zhu Yan-wei, "A new method of detecting PV Grid-connected Inverter Islanding based on the frequency variation," Materials for Renewable Energy & Environment (ICMREE), 2011 International Conference on, vol.1, pp.44-48, 20-22th May 2011.

[40] A. Etxegarai, P. Eguía, I. Zamora, "Analysis of Remote Islanding Detection Methods for Distributed Resources," in the International Conference on Renewable Energies and Power Quality, Spain, 2011.

[41] Xiaoyu Wang; Freitas, W.; Wilsun Xu; Dinavahi, V., "Impact of DG Interface Controls on the Sandia Frequency Shift Antiislanding Method," Energy Conversion, IEEE Transactions on, vol.22, no.3, pp.792-794, September 2007.

[42] Gyeong-Hun Kim; Hyo-Rong Seo; Seong-Jae Jang; Sang-Soo Park; Sang-Yong Kim; Nam-Won Kim; Minwon Park; In-Keun Yu, "Performance analysis of the anti-islanding function of a PV-AF system under multiple PV system connections," Electrical Machines and Systems, 2009. ICEMS2009. International Conference on, pp. 1-5, 15-18th November 2009.

[43] Guo-Kiang Hung; Chih-Chang Chang; Chen, Chern-Lin, "Automatic phase-shift method for islanding detection of grid-connected photovoltaic inverters," Energy Conversion, IEEE Transactions on, vol.18, no.1, pp. 169-173, Mar 2003.

[44] Ghaderi, A.; Esmaeilian, A.; Kalantar, M., "A novel islanding detection method for constant current inverter based distributed generations," Environment and Electrical Engineering (EEEIC), 2011 10th International Conference on, pp.1-4, 8-11th May 2011

[45] Yang, H.-T.; Peng, P.C.; Chang, J.C.; Wang, C.Y., "A new method for islanding detection of utility-connected wind power generation systems," Power Tech, 2005 IEEE Russia, pp. 1-6, 27-30th June 2005

[46] Hye Yeon Lee; Byung Moon Han; Han Ju Cha, "Novel islanding detection method for distributed generation," Energy Conversion Congress and Exposition, 2009, ECCE2009. IEEE, pp.3378-3384, 20-24th September 2009.

[47] Rintamaki, Olli; Kauhaniemi, Kimmo, "Applying modern communication technology to loss-of-mains protection," Electricity Distribution - Part 1, 2009. CIRED2009, 20th International Conference and Exhibition on, pp. 1-4, 8-11 June 2009.

[48] Laverty, D.M.; Morrow, D.John; Best, R.; Crossley, P.A., "Internet based phasor measurement system for phase control of synchronous islands," Power and Energy Society General Meeting - Conversion and Delivery of Electrical Energy in the 21st Century, 2008 IEEE, pp.1-6, 20-24 July 2008.

[49] Ropp, M.E.; Aaker, K.; Haigh, J.; Sabbah, N., "Using power line carrier communications to prevent islanding [of PV power systems]," Photovoltaic Specialists Conference, 2000. Conference Record of the 28th IEEE, pp.1675-1678, 2000.

[50] Wilsun Xu; Guibin Zhang; Chun Li; Wencong Wang; Guangzhu Wang; Kliber, J., "A Power Line Signaling Based Technique for Anti-Islanding Protection of Distributed Generators—Part I: Scheme and Analysis," Power Delivery, IEEE Transactions on , vol.22, no.3, pp.1758-1766, July 2007

[51] ALSTOM GRID, "Network Protection and Automation Guide," chapter 8, May 2011

[52] Coffele, F.; Moore, P.; Booth, C.; Dysko, A.; Burt, G.; Spearing, T.; Dolan, P., "Centralised Loss of Mains protection using IEC-61850," Developments in Power System Protection (DPSP 2010). Managing the Change, 10th IET International Conference on, pp.1-5, March 29th 2010-April 1st 2010

[53] Mahat, P.; Zhe Chen; Bak-Jensen, B., "A Hybrid Islanding Detection Technique Using Average Rate of Voltage Change and Real Power Shift," Power Delivery, IEEE Transactions on, vol.24, no.2, pp.764-771, April 2009.

[54] Menon, V.; Nehrir, M.H., "A Hybrid Islanding Detection Technique Using Voltage Unbalance and Frequency Set Point," Power Systems, IEEE Transactions on, vol.22, no.1, pp.442-448, February 2007.

[55] Hutiri, N.; Chowdhury, S.; Chowdhury, S. P., "Performance Comparison of Frequency Based Loss of Grid Protection Schemes," Universities' Power Engineering Conference (UPEC), Proceedings of 2011 46th International, pp.1-6, 5-8 September 2011.

[56] Li, X.; Dyśko, A.; Abdulhadi, I.; King, R., "Hardware prototype and real-time validation of the satellite communication based Loss-of-Mains protection," Developments in Power System Protection (DPSP 2014), 12th IET International Conference on, pp.1-6, March 31th 2014-April 3rd 2014.

[57] W. Stallings, "Data and Computer Communications," 9th edition, 2011.

[58] A. Simmond, "Data Communications, and Transmission Principles: An Introduction," 1st edition 1997.

[59] M. Duck and R. Read, "Data Communications and Computer Networks for Computer Scientists and Engineers," 2nd edition, 2003.

[60] B. A. Forouzan, "Data Communications and Networking," 4th edition, 2007.

[61] K. INIEWSKI, C. MCCROSKY, D. MINOLI, "Network Infrastructure and Architecture/Designing High-Availability Networks," 1st edition, 2008.

[62] SEL, "SEL-451 Relay: Protection, Automation, and Control System (Instruction Manual)," 2008.

[63] IEEE Standard for Synchrophasor Measurements for Power Systems," IEEE Std C37.118.1-2011 (Revision of IEEE Std C37.118-2005), pp.1-61, December 28th 2011

[64] IEEE Standard for Synchrophasor Data Transfer for Power Systems," IEEE Std C37.118.2-2011 (Revision of IEEE Std C37.118-2005), pp.1-53, December 28th 2011

[65] Martin, K.E.; Hamai, D.; Adamiak, M.G.; Anderson, S.; Begovic, M.; Benmouyal, G.; Brunello, G.; Burger, J.; Cai, J.Y.; Dickerson, B.; Gharpure, V.; Kennedy, B.; Karlsson, D.; Phadke, A.G.; Salj, J.; Skendzic, V.; Sperr, J.; Song, Y.; Huntley, C.; Kasztenny, B.; Price, E., "Exploring the IEEE Standard C37.118–2005 Synchrophasors for Power Systems," Power Delivery, IEEE Transactions on, vol.23, no.4, pp.1805,1811, October 2008.

[66] Sykes, J.; Koellner, K.; Premerlani, W.; Kasztenny, B.; Adamiak, M., "Synchrophasors: A primer and practical applications," Power Systems Conference: Advanced Metering, Protection, Control, Communication, and Distributed Resources, 2007, PSC2007, pp. 213-240, 13-16th March 2007.

[67] Ahmed A. Makki and A. Dyśko, "Application of satellite communication to Loss-Of-Mains protection," Technical Report, EEE, Strathclyde, 2012.

[68] Kang, H.; Cvorovic, B.; Mycock, C.; Tholomier, D.; Mai, R., "PMU simulation and application for power system stability monitoring," Power Systems Conference and Exposition, 2009, PSCE'09, IEEE/PES, pp.1-7, 15-18th March 2009.

[69] Apostolov, A.P., "Synchrophasors — Can we use them for protection?," Developments in Power Systems Protection, 2012. DPSP2012. 11th International Conference on, pp.1-6, 23-26th April 2012.

[70] Naduvathuparambil, B.; Valenti, M.C.; Feliachi, A., "Communication delays in wide area measurement systems," System Theory, 2002, Proceedings of the 34th South-eastern Symposium on, pp.118-122, 2002.

[71] Lixia, M.; Muscas, C.; Sulis, S., "On the accuracy specifications of Phasor Measurement Units," Instrumentation and Measurement Technology Conference (I2MTC), 2010 IEEE, pp.1435-1440, 3-6th May 2010.

[72] J. Louis J. Ippolito,"Satellite Communications System Engineering (Atmospheric effects, Satellite link design, and System performance," 1st edition, 2008.

[73] B. R. Elberti, "The Satellite Communication Applications Handbook", 2nd edition, 2004.

[74] D. Roddy, "Satellite Communications," 4th edition, 2006.

[75] G. Maral, M. Bousquet, "Satellite Communications System: Systems, Techniques, and Technologies," 5th edition, 2009.

[76] B. R. Elbert, "Introduction Satellite Communication," 3rd edition, 2009.

[77] Madani, V.; Vaccaro, A.; Villacci, D.; King, R.L., "Satellite based communication network for large scale power system applications," Bulk Power System Dynamics and Control – VII, Revitalizing Operational Reliability, 2007 iREP Symposium, pp.1-7, 19-24th Aug. 2007.

[78] J. E. Kadish and T. W. R. East, "Satellite Communications Fundamentals," 1999.

[79] M. Richharia, "Satellite Communications Systems," 2nd edition, 1999.

[80] M. Richharia and L. D. Westbrook, "Satellite Systems for Personal Applications Concepts and Technology," 1st edition, 2010.

[81] J.E.Allnutt, "Satellite-to-Ground Radiowave Propagation," 2nd edition, 2011.

[82] Nandra, A.; Govil, J.; Govil, J., "Causes of degradation of C/N and its mitigation in Satcom," Information, Communications & Signal Processing, 2007 6th International Conference on, pp.1-6, 10-13th December 2007.

[83] Vanelli-Coralli, A.; Corazza, G.E.; Karagiannidis, G.K.; Mathiopoulos, P.T.; Michalopoulos, D.S.; Mosquera, C.; Papaharalabos, S.; Scalise, S., "Satellite

Communications: Research Trends and Open Issues," Satellite and Space Communications, 2007, IWSSC'07, International Workshop on, pp.71-75, 13-14th September 2007.

[84] Makki, Ahmed A.; Dyśko, Adam; Lee, M.; Hung, W., "Assessment of the reliability of loss of mains protection incorporating satellite communications," Developments in Power Systems Protection, 2012. DPSP2012. 11th International Conference on, pp.1-6, 23-26th April 2012.

[85] International Telecommunications Union, "Handbook on Satellite Communications," 3rd edition, 2002.

[86] Onestopclick, "The Falling Costs of Wide Area Networks," White paper, October 2008.

[87] Xingquan Xiao; Zhong Fu; Ge Liu; Chuang Deng, "A backup data network for power system automations based on satellite communication," Power System Technology (POWERCON), 2010 International Conference on, pp.1-5, 24-28th October 2010.

[88] Comtech, " Universal Satellite Modem (DMD50) Installation and Operating Manual," 2009.

[89] Douglas C. Montgomery, Elizabeth A. Peck, G. Geoffrey Vining, "Introduction to Linear Regression Analysis", 4th Edition, John Wiley & Sons, 9th April 2012.

[90] Dyśko, A.; Booth, C.; Burt, A.G.; Yip, H.T., "Testing methodology for LOM protection performance assessment," Developments in Power System Protection (DPSP 2010), 10th IET International Conference on, pp.1-5, March 29th 2010-April 1st 2010.

[91] G. C. Carter, Coherence and Time Delay Estimation: An Applied Tutorial for Research, Development, Test, and Evaluation Engineers. Piscataway, NJ: IEEE, 1993.

[92] IEEE Trans. Ultrasonic., Ferro-elect., Freq. Contr. (Special Issue on Correlation Techniques and Applications to Ultrasonic), vol.41, pp. 577-663, 1994.

[93] L. N. Bohs, B. H. Friemel, B. A. McDermott, and G. E. Trahey,"A real-time system for quantifying and displaying two dimensional velocities using ultrasound," Ultrasound Med. Biol.,vol.19, no.9, pp.751-761, 1993.

[94] O. Bonnefous and P. Pesque, "Time domain formulation of pulse-Doppler ultrasound and blood velocity estimation by cross correlation," Ultrasonic. Image, vol.8, pp.73-85, 1986.

[95] Embree, P.M.; O'Brien, W.D., "Volumetric blood flow via time-domain correlation: experimental verification," Ultrasonic, Ferroelectrics, and Frequency Control, IEEE Transactions on, vol.37, no.3, pp.176-189, May 1990.

[96] Flax, S.W.; O'Donnell, M., "Phase-aberration correction using signals from point reflectors and diffuse scatterers: basic principles," Ultrasonic, Ferroelectrics, and Frequency Control, IEEE Transactions on, vol.35, no.6, pp.758-767, Nov. 1988.

[97] Ng, G.C.; Worrell, S.S.; Freiburger, P.D.; Trahey, G.E., "A comparative evaluation of several algorithms for phase aberration correction," Ultrasonic, Ferroelectrics, and Frequency Control, IEEE Transactions on, vol.41, no.5, pp.631-643, September 1994.

[98] Y. Sumino and R. C. Waag, "Measurements of ultrasonic pulse arrival time differences produced by abdominal wall specimens," The Journal of the Acoustical Society of America, vol. 90, no. 6, pp.2924-2930, 1991.

[99] Trahey, G.E.; Nock, L.P., "Synthetic receive aperture imaging with phase correction for motion and for tissue in homogeneities. II. Effects of and correction for motion," Ultrasonic, Ferroelectrics, and Frequency Control, IEEE Transactions on, vol.39, no.4, pp.496-501, July 1992.

[100] O'Donnell, M.; Skovoroda, A.R.; Shapo, B.M.; Emelianov, S.Y., "Internal displacement and strain imaging using ultrasonic speckle tracking," Ultrasonics, Ferroelectrics, and Frequency Control, IEEE Transactions on, vol.41, no.3, pp.314-325, May 1994.

[101] J. Ophir, I. C´espedes, H. Ponnekanti, Y. Yazdi, and X. Li, "Elastography: A quantitative method for imaging the elasticity of biological tissues," Ultrasonic. Imag., vol. 13, pp. 111-134, 1991.

[102] W. F. Walker, F. J. Fernandez, and L. A. Negron, "A method of imaging viscoelastic parameters with acoustic radiation force," Phys. Med. Biol., vol. 45, pp. 1437-1447, 2000.

[103] Viola, F.; Walker, W.F., "Radiation force imaging of viscoelastic properties with reduced artifacts," Ultrasonic, Ferroelectrics, and Frequency Control, IEEE Transactions on, vol.50, no.6, pp.736-742, June 2003.

[104] K. R. Nightingale, M. S. Soo, R. Nightingale, and G. E. Trahey, "Acoustic radiation force impulse imaging: In vivo demonstration of clinical feasibility," Ultrasound Med. Biol., vol. 28, no. 2, pp. 227–235, 2002.

[105] Hamon, B.V. and E.J. Hannan, "Spectral Estimation of Time Delay for Dispersive and Non-dispersive Systems", Applied Statistics, pp. 134-142, 23, No. 2, 1974.

[106] Chan, Y.T.; Hattin, R.; Plant, J.B., "The least squares estimation of time delay and its use in signal detection," Acoustics, Speech and Signal Processing, IEEE Transactions on, vol.26, no.3, pp.217-222, June 1978.

[107] Hassab, Joseph C.; Boucher, R., "Optimum estimation of time delay by a generalized correlator," Acoustics, Speech and Signal Processing, IEEE Transactions on, vol.27, no.4, pp.373-380, August 1979.

[108] Maniere, M.; Benoit-Gonin, R., "Telegraph Distortion on High-Speed Frequency Shift Data Transmission Systems," Communications Systems, IRE Transactions on, vol.9, no.3, pp.259-270, September 1961.

[109] Viola, F.; Walker, W.F., "A spline-based algorithm for continuous time-delay estimation using sampled data," Ultrasonic, Ferroelectrics, and Frequency Control, IEEE Transactions on, vol.52, no.1, pp.80-93, January 2005.

[110] Etter, D.M.; Stearns, Samuel D., "Adaptive estimation of time delays in sampled data systems," Acoustics, Speech and Signal Processing, IEEE Transactions on, vol.29, no.3, pp.582-587, June 1981.

[111] Knapp, C.; Carter, G. Clifford, "The generalized correlation method for estimation of time delay," Acoustics, Speech and Signal Processing, IEEE Transactions on, vol.24, no.4, pp.320-327, August 1976.

[112] Chan, Y.T.; Riley, J.; Plant, J.B., "Modeling of time delay and its application to estimation of non-stationary delays," Acoustics, Speech and Signal Processing, IEEE Transactions on, vol.29, no.3, pp.577-581, June 1981.

[113] Ianniello, J.P., "Time delay estimation via cross-correlation in the presence of large estimation errors," Acoustics, Speech and Signal Processing, IEEE Transactions on, vol.30, no.6, pp.998-1003, December 1982.

[114] Ross, M.; Shaffer, H.; Cohen, A.; Freudberg, R.; Manley, H., "Average magnitude difference function pitch extractor," Acoustics, Speech and Signal Processing, IEEE Transactions on, vol.22, no.5, pp.353-362, October 1974.

[115] Gabriel, K.J., "Comparison of three correlation coefficient estimators for Gaussian stationary processes," Acoustics, Speech and Signal Processing, IEEE Transactions on, vol.31, no.4, pp.1023-1025, August 1983.

[116] Fertner, A.; Sjolund, A., "Comparison of various time delay estimation methods by computer simulation," Acoustics, Speech and Signal Processing, IEEE Transactions on, vol.34, no.5, pp.1329-1330, October 1986.

[117] Jacovitti, G.; Scarano, G., "Discrete time techniques for time delay estimation," Signal Processing, IEEE Transactions on, vol.41, no.2, pp.525-533, February 1993.

[118] So, H.C.; Ching, P.C.; Chan, Y.T., "A new algorithm for explicit adaptation of time delay," Signal Processing, IEEE Transactions on , vol.42, no.7, pp.1816-1820, July 1994.

[119] Raman, J.; Weyten, L., "Adaptive fractional delay estimation without lock-up," Electronics, Circuits and Systems, 1999, proceedings of ICECS '99. The 6th IEEE International Conference on, vol.2, pp.737-740 vol.2, 5-8th September 1999.

[120] Widrow, B.; McCool, J.M.; Larimore, M.; Johnson, C.R., "Stationary and non-stationary learning characteristics of the LMS adaptive filter," Proceedings of the IEEE, vol.64, no.8, pp.1151-1162, August 1976.

[121] A. A. Atayero, M. K. Luka, and A. A. Alatishe, "Satellite Link Design: A Tutorial," International Journal of Electrical & Computer Sciences IJECS-IJENS, August 2011.

[122] A. Nandra and J. Govil, "Causes of degradation of C/N and its mitigation in Satcom," in Information, Communications & Signal Processing, 6th International Conference, 2007.

[123] A. Vanelli-Coralli, G. E. Corazza, G. K. Karagiannidis, P. T. Mathiopoulos, D. S. Michalopoulos, C. Mosquera, S. Papaharalabos, and S. Scalise, "Satellite Communications: Research Trends and Open Issues," in Satellite and Space Communications, IWSSC '07, 2007.

[124] S. C. Ekpo and D. George, "Impact of Noise Figure on a Satellite Link Performance," Communications Letters, IEEE, 2011

APPENDIX A: INTERNET PROTOCOLS

A.1 Internet Protocol (IP) header

The header contains a minimum of 20 bytes, but can accommodate further option fields, each of 4 bytes.

The IP header fields are as follows:

1- Version: IP version number, which will be either 4 or 6.
2- IHL: Internet header length is the number of 32-bit words in the header.
3- Type of service: Priority value that specifies whether the sender prefers the datagram to travel over a route with minimum delay or a route with maximum throughput.
4- Total length: Total number of bytes in the datagram, including the header.
5- Identifier: Sequence number that is intended to uniquely identify a datagram even if it has been fragmented.
6- Flags: Indicate whether a datagram has been fragmented or is a complete datagram.
7- Fragment offset: Tells a receiver how to order fragments within a particular datagram. It specifies where in the original datagram the fragment belongs.
8- Time to live: used to prevent a datagram from travelling indefinitely around internet. Each router that handles the datagram decrements the time to live by 1, if the counter reaches zero, the datagram is discarded and a warning is sent back to the source. The maximum time of live is 127.
9- Protocol: Determine the transport layer used, such as TCP or UDP.
10- Header checksum: Error checks the header only.
11- Source address: IP address of the originator of the datagram.
12- Destination address: IP address of the destination.
13- Options and padding: The options field is intended to be used to indicate various options:
    a. Security: Provides hosts with a way to use security

b. Loose Source Routing: Provides a list of addresses that must be included in the route
c. Strict Source Routing: Provides the complete route from source to destination
d. Record Route: Records the route of a datagram as it traverses the network
e. Stream Identifier: Provides a way for a stream identifier to be carried
f. Time Stamp: Provides the time and date when a router handles a datagram

Table A1: IP header format a total size of 20Bytes excluding options and padding

0	1	2	3	4	5	6	7	8	9	10	11	12	13	14	15	16	17	18	19	20	21	22	23	24	25	26	27	28	29	30	31
Version				IHL				Type of service								Total Length															
Identifier																Flags			Fragment offset											
Time of live								Protocol								Header Checksum															
Source IP address																															
Destination IP address																															
Optional and Padding																															

A.2 Transmission Control Protocol (TCP)

The TCP header fields are as follows [57-61]:

1- The source and destination ports identify the local end-points of the connection.
2- A segment sequence number identifies the first byte carried in the TCP segment.
3- The acknowledgement number field contains the sequence number of the next byte expected to be received.
4- The header length is the number of 32-bit words contained in the header.
5- The next field contains six single-bit flags.
   a- URG is set if a segment contains a block of data that is urgent.
   b- ACK indicates a valid acknowledgement number in the corresponding field.
   c- PSH (push) indicates data to be handed to an application immediately on arrival, but is now outdated.
   d- RST flag is used to reset a connection that has become confused.
   e- SYN is used in the handshaking used to establish connections and to set initial sequence numbers.
   f- FIN flag is used to indicate that a sender has finished sending data.

6- The window size is the number of bytes that a receiver is able to receive at a time.

7- The checksum is the 1's complement of the sum of all the 16-bit words in the segment. The checksum is carried out on the complete segment including the header plus a pseudo-header that is only used at the time of the calculation of the checksum.

8- The urgent pointer field is used in conjunction with the URG flag and gives an offset to the sequence number field needed to find the last byte of a block of urgent data.

9- Options: This field contains from 0 to 40 bytes of TCP option information. Unlike the IP options field, this field has at least one significant role: carrying the maximum segment size from receivers to senders, to avoid buffer overrun in TCP receivers.

Table A2: TCP header format a total size of 20Bytes excluding options

<table>
<tr><th>0</th><th>1</th><th>2</th><th>3</th><th>4</th><th>5</th><th>6</th><th>7</th><th>8</th><th>9</th><th>10</th><th>11</th><th>12</th><th>13</th><th>14</th><th>15</th><th>16</th><th>17</th><th>18</th><th>19</th><th>20</th><th>21</th><th>22</th><th>23</th><th>24</th><th>25</th><th>26</th><th>27</th><th>28</th><th>29</th><th>30</th><th>31</th></tr>
<tr><td colspan="16">Source port</td><td colspan="16">Destination port</td></tr>
<tr><td colspan="32">Sequence number</td></tr>
<tr><td colspan="32">Acknowledgment number</td></tr>
<tr><td colspan="4">Header Length</td><td colspan="6">Reserve</td><td>URG</td><td>ACK</td><td>PSH</td><td>RST</td><td>SYN</td><td>FIN</td><td colspan="16">Window size</td></tr>
<tr><td colspan="16">Checksum</td><td colspan="16">Urgent Pointer</td></tr>
<tr><td colspan="32">Options</td></tr>
<tr><td colspan="32">Data</td></tr>
</table>

A.3 User Data Protocol (UDP)

The UDP length field gives the length of the UDP segment. The other fields have the same functions as in TCP. The UDP header is slimmer than the TCP header by 12B, because the UDP header does not have acknowledgment, sequence numbers, flow control and no options [57-61].

Table A3: UDP header format a total size of 8Bytes

<table>
<tr><th>0</th><th>1</th><th>2</th><th>3</th><th>4</th><th>5</th><th>6</th><th>7</th><th>8</th><th>9</th><th>10</th><th>11</th><th>12</th><th>13</th><th>14</th><th>15</th><th>16</th><th>17</th><th>18</th><th>19</th><th>20</th><th>21</th><th>22</th><th>23</th><th>24</th><th>25</th><th>26</th><th>27</th><th>28</th><th>29</th><th>30</th><th>31</th></tr>
<tr><td colspan="16">Source port number</td><td colspan="16">Destination port number</td></tr>
<tr><td colspan="16">Total Length</td><td colspan="16">Checksum</td></tr>
<tr><td colspan="32">Data</td></tr>
</table>

APPENDIX B: SATELLITE COMMUNICATION LINK BUDGET ANALYSIS AND MODULLING

In order to design a satellite communication link the authors need to examine the performance for each source of gain and loss and the link budget is the most effective means since it can address and display all of the important components of the power balance equation expressed in decibels. The link budget is made of downlink budget, uplink budget and the overall link budget, the downlink involve the design and characteristics of the signal sent by the satellite antenna and received by the earth station antenna and the uplink involves the design and characteristic of the signal sent by the earth station antenna and received by the satellite antenna. There parameters could be different, like the frequency of the carrier used in the uplink should be higher than the frequency of the downlink and the transmission power needed for the uplink should be higher than the transmission power of the downlink.

The decibel value of the EIRP can be estimated according to the coverage zone, the narrower the coverage zone the higher the EIRP is needed. For example, the area of the United States of America is at least 32 times the area of UK; the value of EIRP needed to cover the USA is 27dB. Thereby, the numerical value of EIRP should be increased by 32 times, which leads to EIRP equal to 42dB, and by adding 15.5dB it will be equal to 57.5dB. In order to compensate for small antennas and high frequencies, the EIRP value for the downlink was estimated at 56dBW after feeder losses. While in the uplink, the Pt_e was estimated to be 4 times Pt_s in the downlink, because the frequency used is higher, and because of the higher attenuation effects, especially rain fade. These values can be manipulated at the control centre of the transmission station according to the atmospheric conditions and the quality of the link. The EIRP value has a significant impact on the Direct to Home (DTH) receiving antennas' diameter. Whenever the numerical value of EIRP increased by four times, the EIRP value in decibels will increase by 6dB, which allows the reduction of receiving antenna diameter to 50%. Having smaller antennas is an economical advantage, and time saving in installation [73].

B.1 Link Budget Analysis, Assumptions, Equations Used, and Definitions:

B.1.1 Assumptions

1) The transmitting antenna Diameter =2.4m, and the receiving diameter= 0.6m
2) Both antennas are with efficiency of 60%
3) The parameters for the uplink and downlink are:

   K_u Band 15/12GHz,

   Downlink = R_d= 39006Km, E_d=25.7°, P_d= -5.7°, A_d =173.6°

   Uplink = R_u= 38510Km, E_u=31°, P_{od}= -5.6°, A_d=174.7°

1) The beam width of downlink= 1.75° and satellite separation of 3°
2) The beam width of uplink= 0.625° and satellite and /or earth station separation of 2°
3) The satellite transponder is a regenerative and not transparent.
4) The modulation of QPSK and turbo encoding of (1, 2) rate
5) The polarization is circular; polarization tilt angle is equal to 45°
6) The cross-polarization and atmospheric affects are for exceeding 0.01% of the time

   σ=10° for exceeding 0.01% of the time
7) The Roll off factor = 0.25
8) R_b= 6240 b/s, which comprised of information = 32Bytes plus UDP=46Bytes transmitter 10 times per second
9) The channel frequency isolation factor is 1.08

B.1.2 Parameters

K_u Band 14/12GHz, B_n=8000Hz, Downlink parameters (R_d =39006km, E_d =25.7°, P_{od} =-5.7°, A_d =173.6°, D_r=1m) and Uplink parameters (R_u =38510km, E_u=31°, P_{ou} =-5.6°, A_u =174.7°, D_u=2.4m), the satellite antenna diameter= 1m

B.1.3 Definitions

E (Elevation angle), P_o (Polarization angle), A (Azimuth angle), R (Path Length), G (Antenna gain), I (Channel Interference), C (Carrier Power), N_o (Noise Power Density); Subscript: (r) receiving, (t) transmission, P (Power), G/T (Figure of Merit),

Pf_d (Power Flux Density), Lf_s (Free space loss), L_{At01} (Atmospheric losses), L_f (Feeder losses), BO_i (Input Back off), BO_o (Output Back off), D (Antenna Diameter), L_{am} (Antenna miss-alignment), L_{pl} (Polarization miss-match) XPD (Cross Polarization Discrimination), Subscript: (r) receiving, (t) transmission, (u) uplink and (d) downlink.

B.1.4 Equations used in calculating the link budget

[73, 74, 78, 79, 85, and 121]

$$\left(\frac{E_b}{N_o}\right) = \left(\frac{C}{N+I}\right)\frac{B_n}{R_b} \quad \text{(B-1)}$$

$$B_n = \left(\frac{1}{\text{mod rate}}\right)\left(\frac{1}{\text{coding rate}}\right)(1 + R_{off})R_b \quad \text{(B-2)}$$

1- Free space loss:

$$[Lf_s] = 20\log\left(\frac{4\pi r}{\lambda}\right) \quad \text{(B-3)}$$

$$[Lf_s]_d = 20\log\left(\frac{4\pi \times 39006000m}{\frac{c}{f_d}}\right) = 205.85dB,$$

$$[Lf_s]_u = 20\log\left(\frac{4\pi \times 38510000m}{\frac{c}{f_u}}\right) = 207.675dB$$

2- Total path losses:

$$[Losses] = [Lf_s] + [Lf_r] + [Laa_{01}] + [L_{am}] + [Lp_l] \quad \text{(B-4)}$$

Downlink:

$$[Losses]_d = 205.85dB + 0.5dB + 7.488dB + 0.3dB + 3dB = 217.138dB$$

Uplink:

$$[Losses]_u = 207.675dB + 0.5dB + 9.278dB + 0.3dB + 3dB = 220.753dB$$

3- Antenna Gain:

$$[G] = 10\log(effa \times 109.66 \times f^2D^2) \quad \text{(B-5)}$$

Downlink receiving and transmitting antenna gain:

$$[G_r]_d = [G_t]_d = 10\log(0.7 \times 109.66 \times 12^2 \times 1^2) = 40.435dBi$$

Uplink transmitting gain:

$$[G_t]_u = 10\log(0.7 \times 109.66 \times 15^2 \times 2.4^2) = 49.93dBi$$

Uplink receiving gain:

$[G_r]_u = 10\log(0.7 \times 109.66 \times 15^2 \times 1^2) = 42.37dBi$

4- Effective Isotropic Radiated Power (EIRP):

$$[EIRP] = [P_t] + [G_t] - [Lf_t] \quad \text{(B-6)}$$

$$[EIRP]_u = [P_t]_u + [G_t]_u - [Lf_t]_u = 23dB + 49.93dBi - 1.5dB$$
$$= 71.43 \sim 71.5dBW$$

5- Transmission power P_t:

$$[P_t]_d = [EIRP]_d - [G_t]_d + [Lf_t]_d = 57.5dBW - 40.435dBi + 1.5dB = 17dBW$$

6- Receiving power P_r:

$$[P_r] = [EIRP_t] + [G_r] - [Losses] \quad \text{(B-7)}$$

$$[P_r]_d = [EIRP]_d + [G_r]_d - [Losses]_d = 56dBW + 40.435dBi - 217.138dB$$
$$= -120.703dBW$$

$$[P_r]_u = [EIRP]_u + [G_r]_u - [Losses]_u = 71.5dBW + 42.37dBi - 220.753dB$$
$$= -106.883dBW$$

7- Noise Power N:

$$[N] = [K] + [B_n] + [T_s] \quad \text{(B-8)}$$

$$Boltzmann\ factor\ (k) = 1.38 * 10^{-23} = -228.6dB$$

$$B_n = 10log8400 = 39.24dBHz,\ T = 10log240 = 23.8dBK$$

$$[N]_d = [K] + [B_n] + [T_s]_d = -228.6dB + 39.24dBHz + 10log240$$
$$= -165.555dBW$$

$$[N]_u = [K] + [B_n] + [T_s]_u = -228.6dB + 39.24dBHz + 10\log(240 * 4)$$
$$= -159.537dBW$$

8- Figure of Merit G/T:

$$\left[\frac{G}{T}\right]_r = [G_r] - [L_{am}] - [Lf_r] - \left[L_{pl}\right] - T \quad \text{(B-9)}$$

$$\left[\frac{G}{T}\right]_d = [G_r]_d - [L_{am}] - [Lf_r] - \left[L_{pl}\right] - T_d$$
$$= 40.435\text{dBi} - 0.3\text{dB} - 0.5\text{dB} - 3\text{dB} - 10\log240 = 12.83\text{dBK}^{-1}$$

$$\left[\frac{G}{T}\right]_u = [G_r]_u + [L_{am}] - [lf_r] - [Lpi] - T_u$$
$$= 42.37dBi - 0.3dB - 0.5dB - 3dB - 10\ log(240 * 4) = 8.747dBK^{-1}$$

9- Carrier to noise ratio C/N:

$$\left[\frac{C}{N}\right] = [EIRP_t] - [Losses] + \left[\frac{G}{T}\right] - [K] - [B_n] - BO_o \quad \text{(B-10)}$$

$$\left[\frac{C}{N}\right]_d = [P_t]_d + [G_t]_d - [Losses]_d + \left[\frac{G}{T}\right]_d - [K] - [B_n] - BO_o$$

$$= 17dBW + 40.435dBi - 217.138dB$$

$$+ 12.836dBK^{-1} — (-228.6dB) - 39.24dBHz - 0.6dB = 41.89dB$$

$$\left[\frac{C}{N}\right]_u = [P_t]_u + [G_t]_u - [Losses] + \left[\frac{G}{T}\right]_u - [K] - [B_n] - BO_i$$

$$= 23dBW + 49.93dBi - 220.753dB$$

$$+ 8.747dBK^{-1} — (-228.6dB) - 39.24dBHz - 1.1dBm$$

$$= 49.184dB$$

10- Cross- Polarization Discrimination (XPD):

For circular polarization, the polarization tilt angle (τ) =45°, rain attenuation A_{01d}=4.938dB, A_{01u}=7.06dB, and σ =10°, for exceeding 0.01% of the time.

$$XPD = 30logf - 10\,log(0.5 - 0.4697cos4\tau) - 40lo\,g(cos\theta) + 0.0052\sigma^2 - 12.8f^{0.19}.(lo\,g[A_{01}]) \quad \text{(B-11)}$$

$$XPD_{d_{rain}} = 30log12 - 10lo\,g(0.5 - 0.4697\cos(4 \times 45))$$

$$- 40lo\,g(cos25.7) + 0.0052 * 10^2 - 12.8 \times 12^{0.19} \times (\log 4.938)$$

$$= 32.375 - 0 - (-1.8095) + 0.52 - 14.234 = 20.47dB$$

$$XPD_{u_{rain}} = 30log15 - 10\log(0.5 - 0.4697\cos(4 \times 45)) - 40\log(cos31))$$

$$+ 0.0052 \times 10\text{^}2 - 12.8 \times 15\text{^}0.19 \times \log(7.06)$$

$$= 35.28 - 0 - (-2.677) + 0.52 - 18.175 = 20.3dB$$

$$Cice = XPD_{rain} \times \frac{0.3+0.1logp}{2} \quad \text{(B-12)}$$

$$Cice_d = 20.47 \times \frac{0.3 + 0.1log0.01}{2} = 1.0235dB$$

$$XPD_{01_d} = XPD_{rain} - Cice = 20.47 - 1.0235 = 19.447dB$$

$$Cice_u = 20.3 \times \frac{0.3 + 0.1log0.01}{2} = 1.015dB$$

$$XPD_{01_u} = XPD_{u_{rain}} - Cice_u = 20.3 - 1.015 = 19.285dB$$

11- Carrier to Interference ratio C/I:

$G(\theta) = 29 - 25\log\theta$ in dBi For $1° \leq \theta \leq 7°$ (B-13)

$$\left[\frac{C}{I}\right] = [\Delta EIRP_t] + [G_r] + [XPD_{01}] - (29 - 25log\emptyset)n - BO \quad \text{(B-14)}$$

Assuming that the interfering satellites have EIRP equal to that of the selected satellite, and there are two interfering satellites with 2° separation from the selected satellite, the symbol n is the number of interfering satellites which is in this case equal to 2.

$$\left[\frac{C}{I}\right]_d = [\Delta EIRP_t\,]_d + [G_r\,]_d + [XPD_{01}\,]_d - (29 - 25log2) \times 2 - OBO0$$

$$+ 40.435dBi + 19.447dB - 21.47 \times 2 - 0.6 = 16.342dB$$

Assuming that the interfering earth stations have the same Pt of the selected earth station, and the main earth station is separated from the two interfering earth station by 2°.

$$\left[\frac{C}{I}\right]_u = [\Delta P_t]_u + [G_r]_u + [XPD_{01}]_u - (29 - 25log2) \times 2 - IBO \quad \text{(B-15)}$$

$$= 0 + 42.37 + 19.285 - 21.47 * 2 - 1.1 = 17.615dB$$

12- Carrier to noise and interference ratio C/(N+I):

$$\frac{1}{\frac{C}{N+I}} = \frac{1}{\frac{C}{N}} + \frac{1}{\frac{C}{I}} \quad \text{(B-16)}$$

$$\left(\frac{C}{I}\right)_d = 10^{0.1\times16.342} = 43.072, \quad \left(\frac{C}{I}\right)_u = 10^{0.1\times17.615} = 57.743$$

$$\left(\frac{C}{N}\right)_d = 10^{0.1\times41.893} = 15463.22\,, \quad \left(\frac{C}{N}\right)_u = 10^{0.1\times49.184} = 82870.5$$

Downlink: $\frac{1}{\frac{C}{N+I}d} = \frac{1}{15463.22} + \frac{1}{43.072} = 0.0233$

$$\left(\frac{C}{N+I}\right)_d = \frac{1}{0.0815} = 42.955, \quad \left[\frac{C}{N+I}\right]_d = 10log42.955 = 16.33dB$$

Uplink: $\frac{1}{\left(\frac{C}{N+I}\right)u} = \frac{1}{82870.5} + \frac{1}{57.743} = 0.0173$

$$\left(\frac{C}{N+I}\right)_u = \frac{1}{0.1694} = 57.70, \quad \left[\frac{C}{N+I}\right]_u = 10log57.70 = 17.612dB$$

13- Total carrier to noise and interference ratio:

$$\frac{1}{\left(\frac{C}{N+I}\right)_{total}} = \frac{1}{\left(\frac{C}{N+I}\right)_d} + \frac{1}{\left(\frac{C}{N+I}\right)_u} \quad \text{(B-17)}$$

$$\frac{1}{\left(\frac{C}{N+I}\right)_{total}} = \frac{1}{42.955} + \frac{1}{57.70} = 0.0406, \quad \left(\frac{C}{N+I}\right)_{total} = 24.624$$

$$\left[\frac{C}{N+I}\right]_{total} = 10log24.624 = 13.91dB$$

B.2 Link Limitation

1- For $BER = 10^{-8}$ 8PSK, turbo ¾, F_s=25m/s, and R_b=16800b/s, the B_n will be equal to 7000Hz, plus the increase in C/N by 0.7918dB due to the reduction of B_n, and the target $\frac{E_b}{N_o} = 10.7dB$ [75, 122, 123, and 124].

Downlink:

$\left[\frac{C}{I}\right]_d = 16.34dB$, $\left[\frac{C}{N}\right]_d = 41.89dB + 0.792dB = 42.685dB$

$\left[\frac{C}{N+I}\right]_d = 16.332dB$, $\left[\frac{E_b}{N_o}\right]_d = 12.53\ dB$

Uplink:

$\left[\frac{C}{I}\right]_u = 17.615dB$, $\left[\frac{C}{N}\right]_u = 49.184 + 0.7918 = 49.976dB$

$\left[\frac{C}{N+I}\right]_u$ =17.612, $\left[\frac{E_b}{N_o}\right]_u = 13.81dB$

2- When F_s=25 for ten regions, R_b=168Kb/s, B_n=70KHz, with 8PSK and turbo ¾, and BER 10^{-9} the C/N values will decrease by 9.2dB from the original values at table 1, due to the increase in bandwidth, and the target is $\frac{E_b}{N_o} = 11dB$.

$\left[\frac{C}{N}\right]_d = 32.693dB$, $\left[\frac{E_b}{N_o}\right]_d = 13.026dB$, $\left[\frac{C}{N+I}\right]_d = 16.2425dB$

$\left[\frac{C}{N}\right]_u = 39.984dB$, $\left[\frac{E_b}{N_o}\right]_u = 17.59dB$, $\left[\frac{C}{N+I}\right]_u = 18.5747dB$

3- If the earth receiving antenna diameter was reduced from 1m to 50cm, for the original link budget, this will reduce the antenna gain by 6dB (Equation 6). This means that the figure of merit G/T and the C/I will both be reduced by 6dB each, BER 10^{-7}, and the target is [75]

$\left[\frac{E_b}{N_o}\right]_d = 6.5dB$. $\left[\frac{G}{T}\right]_d = 12.83 - 6 = 6.83dB$, this will eventually reduce the [C/N] by the same amount according to equation shown above.

$\left[\frac{C}{I}\right]_d = 10.34dB$, $\left[\frac{C}{N}\right]_d = 35.89dB$, $\left[\frac{C}{N+I}\right]_d = 10.33dB$, $\left[\frac{Eb}{No}\right]_d = 11.30dB$

Table B1: QPSK / BER / turbo performance

BER	Specification		Typical	
	Turbo 0.495	Turbo 0.793	Turbo 0.495	Turbo 0.793
1E-3	2.5 dB	3.3 dB	2.2 dB	3.0 dB
1E-4	2.7 dB	3.7 dB	2.3 dB	3.2 dB
1E-5	3.0 dB	4.1 dB	2.5 dB	3.4 dB
1E-6	3.2 dB	4.4 dB	2.6 dB	3.6 dB
1E-7	3.5 dB	4.8 dB	2.7 dB	3.8 dB
1E-8	3.7 dB	5.2 dB	2.9 dB	4.0 dB
1E-9	4.0 dB	5.6 dB	3.0 dB	4.2 dB
1E-10	4.2 dB	5.9 dB	3.2 dB	4.4 dB

4- In case of considering the latter for ten regions, BER 10^{-8} , B_n=84000Hz, R_b=67200b/s, the C/N will be reduced for further 10dB due to the increase in bandwidth, and the target is $\frac{E_b}{N_o} = 6.7dB$: [75]

$\left[\frac{C}{N}\right]_d = 25.893dB, \left[\frac{C}{N+I}\right]_d = 10.8dB, \left[\frac{E_b}{N_o}\right]_d = 11.77dB$

5- To decrease the antenna size in number 1, and the target is:

$\frac{Eb}{No} = 10.7dB\ , BER = 10^{-8}$

$\left[\frac{C}{N}\right]_d = 35.893dB, \left[\frac{C}{I}\right]_d = 10.342dB\ , \left[\frac{C}{N+I}\right]_d = 10.3299dB, \left[\frac{E_b}{N_o}\right]_d = 6.528dB$

Which is not sufficient, the downlink Pt has to be increased by ≥ 4dB

Table B2: 8PSK/BER/turbo performance [75]

BER	Specification		Typical	
	Turbo 0.495	Turbo 0.793	Turbo 0.495	Turbo 0.793
1E-3	NA	5.9 dB	2.2 dB	5.3 dB
1E-4	NA	6.3 dB	2.3 dB	5.6 dB
1E-5	NA	6.6 dB	2.5 dB	5.8 dB
1E-6	NA	6.9 dB	2.6 dB	6.1 dB
1E-7	NA	7.3 dB	2.7 dB	6.4 dB
1E-8	NA	7.7 dB	2.9 dB	6.7 dB
1E-9	NA	8.0 dB	3.0 dB	6.9 dB
1E-10	NA	8.4 dB	3.2 dB	7.1 dB

6- In case of considering reducing the size of the antenna, and having ten regions, 8PSK and turbo ¾, BER 10^{-8}, and the target is, $\frac{E_b}{N_o} = 11dB$: $\left[\frac{C}{N}\right]_d = 27.693dB$, $\left[\frac{C}{I}\right]_d = 10.342dB$, $\left[\frac{C}{N+I}\right]_d = 10.257dB$, $\left[\frac{E_b}{N_o}\right]_d = 6.455dB$.

In order to reduce the antenna size, the $\left[\frac{C}{N}\right]_d$; should be 14.8dB, which means that the Pt needs to be increased by 4.54dB.

Table B3: Link Budget Analysis, definitions and calculations

Link Budget Analysis Ku-Band system (15/12 GHz)				
Downlink	**Decibel (dB)**	**Uplink**	**Decibel(dB)**	**Definitions**
EIRP	56dBW	EIRP	71.5dBW	Effective isotropic radiate power
Pt	17dBW	Pt	23dBW	Transmission power
Lft	1.5dB	Lft	1.5dB	Transmission feeder loss
Lfr	0.5dB	Lfr	0.5dB	Receiving feeder loss
Lfsd	205.85dB	Lfsu	207.68dB	Free space loss
Gtd	40.44dBi	Gtu	49.93dBi	Transmission antenna gain
Gr	40.44dBi	Gru	42.37dBi	Receiving antenna gain
Ψd	-105.38dB	Ψu	-89.77dB	Saturation Flux Density
Pr	-120.7dBW	Pr	-106.9dBW	Receiving power
Nd	-165.6dBHz	Nu	-159.5dBHz	Noise power
Gt/T	12.84dBK^{-1}	Gt/T	8.75dBK^{-1}	Figure of Merit
BOo	0.6dBm	BOi	1.1dBm	Input and Output Back off
(C/N)d	41.89dB	(C/N)u	49.18dB	Carrier to Noise ratio
XPD01d	19.47dB	XPD01u	19.29dB	Cross − polarization discrimination
LAt01d	7.49dB	LAt01u	9.28dB	Atmospheric losses
(C/I)d	16.34dB	(C/I)u	17.62dB	Carrier to Interference ratio
(C/(N + I))d	16.33dB	(C/(N + I))u	17.61dB	Carrier to Noise and Interference
(Eb/No)d	17.30dB	(Eb/No)u	18.58dB	Bit energy/power to noise density
Downlink margin=13.8dB/ Uplink margin=15.08dB Total C/(N+I)= 13.913dB, Total LM= 11.38dB				**Link margin (LM)**

B.3 Satellite Communication Modelling

The satellite communication link's physical components and their duties were discussed in chapter 3. As shown in Figure 3-4, in order to transmit the data measurements provided by the PMU to the DG at a remote location, the data needs to go through several stages to be transmitted with the minimum error possible. These stages are [73, 74, 75, 78, 79, 85, and 121]:

1- ASCII Encoding: The frequency data measurements will be converted to the ASCII code, for example the power frequency of '49.93797' will be converted to ASCII as [32,52,57,46,57,51,55,57,54,55,13,0,0,0,0,0], and set the ASCII converter to a 16 characters as a representation of the power frequency measurement converted to ASCII code.

2- Converting integer to bits: In order for the measurement to be encoded and modulated later it needs to be converted from ASCII numbers to Bits. The measurement was converted to ASCII so that it would be possible to present the decimal numbers as integer (converting non-integer number to integer without

losing the fractional value). The number of bits needed will be 8 bits for every ASCII number (57 or 46 etc.), which will add up to 128 bits for every measurement.

3- FEC (BCH) Encoding: There are many encoding techniques that can be used such as, Turbo code, LCPD code, BCH code, Reed Solomon code, etc. The BCH is used in this model for encoding (only for technical reasons) and the encoding rate is (4/7) this means every 4 bit word when encoded the coded word will of 7 bits (3 extra bits added for encoding).

4- Scrambling: The scrambler will randomize the input data stream of bits, to prevent long strings of either binary 1 or 0. This process helps in modulation and data recovery processes, and it is also used in UTC time stamps by using the Manchester code.

5- QPSK Modulation: The safest and most efficient way to transmit a digital data through for up to 90000km (for geostationary satellites) of free space propagation path is to modulate the data into a radio frequency signal carrier and amplify it.

6- Up and Down converting the carrier signal's frequency: The block up converter (BUC) at the transmission station receive the analogue signal with low frequency at L-band level input from any satellite modem and converts it to a frequency within the satellite uplink. The uplink frequency is determined by the modem frequency, in this case it is 12GHz (Ku-band) for the reasons explained in Chapter3. The L-band input starts at the lower end point of 900-950MHz, and stretches from 500 to 1100MHz. the signal must be free of spurious signals that can cause poor performance or even cause the amplifier to fail. At the downlink station the Low Noise Blocker (LNB) usually down converts the frequency to L-band level and amplifies it before the demodulation process.

7- Amplifying the carrier signal: As shown in equation (B-6) and Table B3, most of the amount of energy losses that the signal suffers from occurs at the free space path. It is essential to amplify the carrier signal before transmitting and amplifies it again at the space station, in order to have enough bit energy to noise ratio maintains the data integrity and have the highest link availability.

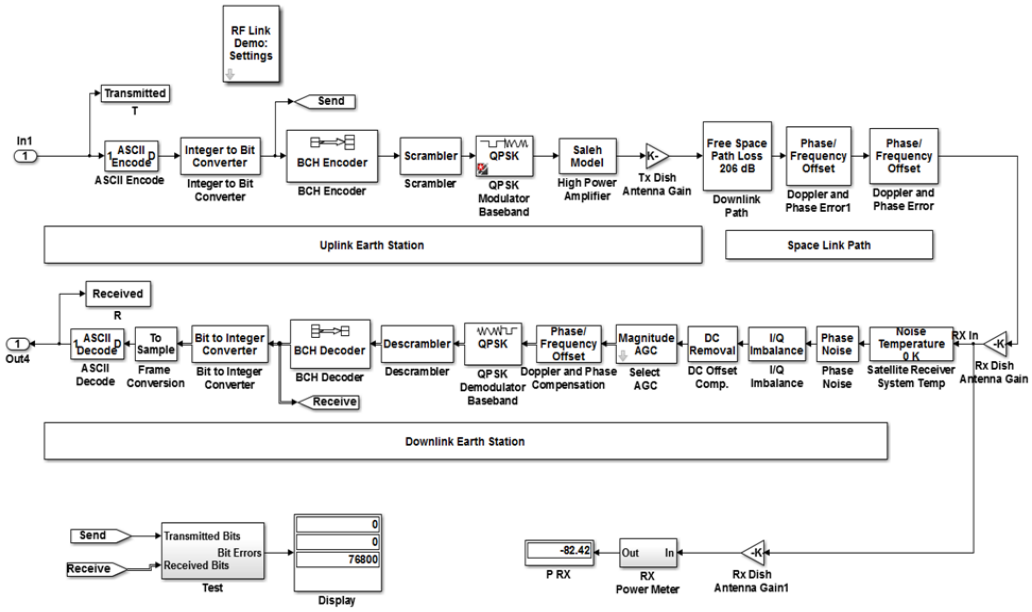

Figure B1: Satellite Communication Link Model

8- Transmitting antenna gain: As shown in equation (B-6) and Table B3, the antennas at the transmitting and receiving earth station also add extra gain to the signal of approximately 40dB from each antenna.

9- The space station: The space station usually has many transponders, and they're either transparent or regenerative type. The transparent type only converts the uplink frequency of the signal to the downlink frequency and amplifies the signal. While the regenerative type process the signal by filtering the signal from noise and isolate it from outer neighbouring signal related to the same satellite but different transponders and from other channels related to neighbouring satellites. After that it demodulates, descrambles, decodes, convert bits to integer and converts from the ASCII code to the original useful information and repeat the same process applied at the transmitting earth station. Usually most of the transponders are transparent and only some of the new satellites have regenerative transponders and they would add a lot to the cost of the link.

In Figure B1, the components that defines the free space path, uplink, downlink stations are presented. As explained above in point 9 it is assumed that the space transponder is of a transparent type. The focus in this model is on the processing of the data measurement, security and reliability of the transmission against power loss and noise effects.

APPENDIX C: CEM METHOD TEST RESULTS FOR 100 SETS OF FREQUENCY

C.1 Determination of Threshold value for the CEM TDE

C.1.1 The first set of frequencies, F_{l_1} and F_{r_1}:

(AD) Actual applied constant delay in samples (cycles)

(EE) Estimation error in samples (cycles)

(MEW) Measurement Estimation Window in minutes

(NA) Not Applicable (this means that the Delay Estimation Difference determined by equation (5-27) has exceeded the threshold, thereby, it will not be considered)

Table C1: CEM MEW of 3 minutes and three 60s estimations for a threshold of 0.5cycle

AD	CEM 1	CEM 2	CEM 3	CEM Average	EE
0	NA	NA	NA	NA	NA
5	NA	NA	NA	NA	NA
10	NA	NA	10.76	10.76	0.76
15	NA	NA	15.97	15.97	0.97
20	NA	NA	NA	NA	NA
25	NA	NA	NA	NA	NA
30	NA	NA	NA	NA	NA
35	NA	NA	NA	NA	NA
40	NA	NA	NA	NA	NA
45	NA	NA	NA	NA	NA
50	NA	NA	NA	NA	NA

Table C2: CEM MEW of 3 minutes and three 60s estimations for a threshold of 1cycle

AD	CEM 1	CEM 2	CEM 3	CEM Average	EE
0	0.50	NA	0.66	0.58	0.58
5	4.50	NA	5.56	5.03	0.03
10	9.50	NA	10.76	10.13	0.13
15	14.50	NA	15.97	17.27	2.27
20	19.50	NA	21.17	20.33	0.33
25	24.50	NA	26.37	25.44	0.44
30	29.50	NA	NA	29.50	-0.50
35	34.50	NA	NA	34.50	-0.50
40	39.50	NA	NA	39.50	-0.50
45	44.50	NA	NA	44.50	-0.50
50	49.50	NA	NA	49.50	-0.50

Table C3: CEM MEW of 3 minutes and three 60s estimations for a threshold of 1.5 cycles

AD	CEM 1	CEM 2	CEM 3	CEM Average	EE
0	0.50	NA	0.66	0.58	0.58
5	4.50	NA	5.56	5.03	0.03
10	9.50	NA	10.76	10.13	0.13
15	14.50	NA	15.97	15.24	0.24
20	19.50	NA	21.17	20.34	0.34
25	24.50	NA	26.37	25.44	0.44
30	29.50	NA	31.57	30.54	0.54
35	34.50	NA	NA	34.50	-0.50
40	39.50	NA	NA	39.50	-0.50
45	44.50	NA	NA	44.50	-0.50
50	49.50	NA	NA	49.50	-0.50

Table C4: CEM MEW of 3 minutes and three 60s estimations for a threshold of 2cycles

AD	CEM 1	CEM 2	CEM 3	CEM Average	EE
0	0.50	NA	0.66	0.58	0.58
5	4.50	NA	5.56	5.03	0.03
10	9.50	NA	10.76	10.13	0.13
15	14.50	NA	15.97	15.24	0.24
20	19.50	NA	21.17	20.34	0.34
25	24.50	NA	26.37	25.44	0.44
30	29.50	NA	31.57	30.54	0.54
35	34.50	NA	36.78	35.64	0.64
40	39.50	NA	NA	39.50	-0.50
45	44.50	NA	NA	44.50	-0.50
50	49.50	NA	NA	49.50	-0.50

Table C5: CEM MEW of 2 minutes and an four 30s estimations for a threshold of 1 cycle

AD	CEM 1	CEM 2	CEM 3	CEM 4	CEM Average	EE
0	0.50	NA	NA	9.07	4.79	4.79
5	4.50	2.48	1.46	NA	2.81	-2.19
10	9.50	6.73	7.03	NA	7.03	-2.97
15	14.50	10.21	NA	NA	12.36	-2.64
20	19.50	14.50	NA	NA	17.00	-3.00
25	24.50	19.40	NA	NA	21.95	-3.05
30	29.50	NA	NA	NA	29.50	-0.50
35	34.50	NA	NA	NA	34.50	-0.50
40	39.50	NA	NA	NA	39.50	-0.50
45	44.50	NA	NA	NA	44.50	-0.50
50	49.50	NA	NA	NA	49.50	-0.50

Table C6: CEM MEW of 2 minutes and four 30s estimations for a threshold of 2 cycles

AD	CEM 1	CEM 2	CEM 3	CEM 4	CEM Average	EE
0	0.50	1.57	4.11	13.48	4.92	4.92
5	4.50	2.48	1.46	13.70	5.54	0.54
10	9.50	9.50	7.03	NA	7.75	-2.25
15	14.50	10.21	12.60	NA	12.44	-2.56
20	19.50	14.50	NA	NA	19.50	-0.50
25	24.50	19.40	NA	NA	21.95	-3.05
30	29.50	25.89	NA	NA	27.70	-2.30
35	34.50	30.67	NA	NA	32.59	-2.41
40	39.50	NA	NA	NA	39.50	-0.50
45	44.50	NA	NA	NA	44.50	-0.50
50	49.50	NA	NA	NA	49.50	-0.50

Table C7: CEM MEW of 2 minutes and four 30s estimations for a threshold of 3 cycles

AD	CEM 1	CEM 2	CEM 3	CEM 4	CEM Average	EE
0	0.50	1.57	4.11	13.48	4.92	4.92
5	4.50	2.48	1.46	13.70	5.54	0.54
10	9.50	6.73	7.03	18.33	10.40	0.40
15	14.50	10.21	12.60	22.96	15.07	0.07
20	19.50	14.80	18.16	NA	17.49	-2.51
25	24.50	19.40	NA	NA	21.95	-3.05
30	29.50	25.89	NA	NA	27.70	-2.30
35	34.50	30.67	NA	NA	32.59	-2.41
40	39.50	35.46	NA	NA	37.48	-2.52
45	44.50	40.24	NA	NA	42.37	-2.63
50	49.50	45.21	NA	NA	47.36	-2.64

Table C8: CEM MEW of 2 minutes and four 30s estimations for a threshold of 4 cycles

AD	CEM 1	CEM 2	CEM 3	CEM 4	CEM Average	EE
0	0.50	1.57	4.11	13.48	4.92	4.92
5	4.50	2.48	1.46	13.70	5.54	0.54
10	9.50	6.73	7.03	18.33	10.40	0.40
15	14.50	10.21	12.6	22.96	15.07	0.07
20	19.50	14.80	18.16	27.59	20.01	0.01
25	24.50	19.40	NA	NA	21.95	-3.05
30	29.50	25.89	26.33	NA	27.24	-2.76
35	34.50	30.67	NA	NA	32.59	-2.41
40	39.50	35.46	NA	NA	37.48	-2.52
45	44.50	40.24	NA	NA	42.37	-2.63
50	49.50	45.21	NA	NA	47.36	-2.64

Table C9: CEM MEW of 1 minutes and six 10s estimations for a threshold of 2 cycles

AD	CEM 1	CEM 2	CEM 3	CEM 4	CEM 5	CEM 6	CEM Average	EE
0	0.50	0.48	2.35	NA	3.90	11.20	3.69	3.69
5	4.50	5.19	7.50	NA	1.77	0.00	3.79	-1.21
10	9.50	9.23	NA	NA	NA	18.31	12.35	2.35
15	14.50	15.08	NA	NA	NA	23.07	17.55	2.55
20	19.50	20.93	NA	NA	NA	27.84	22.76	2.76
25	24.50	NA	28.06	NA	NA	31.62	28.06	3.06
30	29.50	NA	NA	NA	NA	NA	29.50	-0.5
35	34.50	NA	NA	NA	34.42	41.94	36.95	1.95
40	39.50	NA	NA	NA	37.67	47.54	41.57	0.44
45	44.50	NA	NA	NA	40.92	53.15	46.19	1.19
50	49.50	NA	NA	NA	44.17	58.98	50.88	0.88

Table C10: CEM MEW of 1 minutes and six 10s estimations for a threshold of 3 cycles

AD	CEM 1	CEM 2	CEM 3	CEM 4	CEM 5	CEM 6	CEM Average	EE
0	0.50	0.48	2.35	NA	3.90	11.20	3.69	3.69
5	4.50	5.19	7.50	NA	1.77	15.04	6.80	1.80
10	9.50	9.23	12.10	NA	7.11	18.31	11.25	1.25
15	14.50	15.08	17.80	NA	12.02	23.07	16.49	1.49
20	19.50	20.93	22.85	NA	NA	27.84	22.78	2.78
25	24.50	27.66	28.06	NA	NA	31.62	27.96	2.96
30	29.50	32.72	32.72	NA	NA	39.27	33.55	3.55
35	34.50	35.26	NA	NA	34.42	41.94	36.53	1.53
40	39.50	40.53	NA	NA	37.67	47.54	41.31	1.31
45	44.50	NA	NA	NA	40.92	53.15	46.19	1.19
50	49.50	NA	NA	NA	44.17	58.98	50.88	0.88

Table C11: CEM MEW of 1 minutes and six 10s estimations for a threshold of 4 cycles

AD	CEM 1	CEM 2	CEM 3	CEM 4	CEM 5	CEM 6	CEM Average	EE
0	0.50	0.48	2.35	7.28	3.90	11.20	4.29	4.29
5	4.50	5.19	7.50	NA	1.77	15.04	6.80	1.80
10	9.50	9.23	12.10	NA	7.11	18.31	11.25	1.25
15	14.50	15.08	17.80	NA	12.02	23.07	16.49	1.49
20	19.50	20.93	22.85	NA	16.93	27.84	21.61	1.61
25	24.50	27.66	28.06	NA	NA	31.62	27.96	2.96
30	29.50	32.72	32.72	NA	NA	39.27	33.55	3.55
35	34.50	35.26	36.62	NA	34.42	41.94	36.55	1.55
40	39.50	40.53	NA	NA	37.67	47.54	41.31	1.31
45	44.50	46.09	NA	NA	40.92	53.15	46.17	1.17
50	49.50	51.94	NA	NA	44.17	58.98	51.15	1.15

Table C12: CEM MEW of 1 minutes and six 10s estimations for a threshold of 5 cycles

AD	CEM 1	CEM 2	CEM 3	CEM 4	CEM 5	CEM 6	CEM Average	EE
0	0.50	0.48	2.35	7.28	3.90	11.20	4.29	4.29
5	4.50	5.19	7.50	NA	1.77	15.04	6.80	1.80
10	9.50	9.23	12.10	NA	7.11	18.31	11.25	1.25
15	14.50	15.08	17.80	NA	12.02	23.07	16.49	1.49
20	19.50	20.93	22.85	NA	16.93	27.84	21.61	1.61
25	24.50	27.66	28.06	NA	21.84	31.62	26.74	1.74
30	29.50	32.72	32.72	NA	NA	39.27	33.55	3.55
35	34.50	35.26	36.62	NA	34.42	41.94	36.55	1.55
40	39.50	40.53	41.38	NA	37.67	47.54	41.32	1.32
45	44.50	46.09	46.33	NA	40.92	53.15	46.20	1.20
50	49.50	51.94	NA	NA	44.17	58.98	51.15	1.15

C.1.2 The second set of frequencies, F_{l_2} *and* F_{r_2}:

Table C13: CEM MEW of 3 minutes and three 60s estimations for a threshold of 0.5cycle

AD	CEM 1	CEM 2	CEM 3	CEM Average	EE
0	NA	NA	NA	NA	NA
5	NA	NA	NA	NA	NA
10	NA	NA	7.66	7.66	-2.44
15	NA	NA	12.64	12.64	-2.36
20	NA	NA	NA	NA	NA
25	NA	NA	NA	NA	NA
30	NA	NA	NA	NA	NA
35	NA	NA	NA	NA	NA
40	NA	NA	NA	NA	NA
45	NA	NA	NA	NA	NA
50	NA	NA	NA	NA	NA

Table C14: CEM MEW of 3 minutes and three 60s estimations for a threshold of 1 cycle

AD	CEM 1	CEM 2	CEM 3	CEM Average	EE
0	0.50	NA	NA	0.50	0.50
5	4.50	NA	2.68	3.59	-1.41
10	9.50	NA	7.66	8.58	-1.42
15	14.50	NA	12.64	13.57	-1.43
20	19.50	NA	17.62	18.56	-1.44
25	24.50	NA	NA	24.50	-0.50
30	29.50	NA	NA	29.50	-0.50
35	34.50	NA	32.27	33.39	-1.61
40	39.50	NA	NA	39.50	-0.50
45	44.50	NA	NA	44.50	-0.50
50	49.50	NA	NA	49.50	-0.50

Table C15: CEM MEW of 3 minutes and three 60s estimations for a threshold of 1.5 cycles

AD	CEM 1	CEM 2	CEM 3	CEM Average	EE
0	0.50	2.02	2.31	1.61	1.61
5	4.50	NA	2.68	3.59	-1.41
10	9.50	NA	7.66	8.58	-1.42
15	14.50	NA	12.64	13.57	-1.43
20	19.50	NA	17.62	18.56	-1.44
25	24.50	NA	22.85	23.68	-1.32
30	29.50	NA	NA	29.50	-0.50
35	34.50	NA	32.27	33.39	-1.61
40	39.50	NA	37.55	38.53	-1.47
45	44.50	NA	42.83	43.67	-1.33
50	49.50	NA	NA	49.50	-0.50

Table C16: CEM MEW of 3 minutes and three 60s estimations for a threshold of 2cycles

AD	CEM 1	CEM 2	CEM 3	CEM Average	EE
0	0.50	2.02	2.31	1.61	1.61
5	4.50	7.51	2.68	4.90	-0.1
10	9.50	NA	7.66	8.58	-1.42
15	14.50	NA	12.64	13.57	-1.43
20	19.50	NA	17.62	18.56	-1.44
25	24.50	NA	22.85	23.68	-1.32
30	29.50	NA	27.92	28.71	-1.29
35	34.50	NA	32.27	33.39	-1.61
40	39.50	NA	37.55	38.53	-1.47
45	44.50	NA	42.83	43.67	-1.33
50	49.50	NA	48.11	48.81	-1.19

Table C17: CEM MEW of 2 minutes and four 30s estimations for a threshold of 1 cycle

AD	CEM 1	CEM 2	CEM 3	CEM 4	CEM Average	EE
0	0.50	0.96	NA	2.32	1.26	1.26
5	NA	NA	NA	NA	NA	NA
10	NA	NA	2.97	NA	2.97	-2.03
15	NA	NA	7.93	NA	7.93	-7.03
20	NA	NA	12.89	NA	12.89	-7.11
25	24.50	NA	17.85	NA	21.18	-4.82
30	29.50	NA	22.81	NA	26.16	-3.84
35	35.00	NA	NA	NA	35.00	0.00
40	NA	NA	NA	NA	NA	NA
45	44.50	NA	NA	NA	44.50	-0.50
50	49.50	NA	NA	NA	49.50	-0.50

Table C18: CEM MEW of 2 minutes and four 30s estimations for a threshold of 2 cycles

AD	CEM 1	CEM 2	CEM 3	CEM 4	CEM Average	EE
0	0.50	0.96	7.46	2.32	2.81	2.81
5	4.50	4.04	2.32	2.81	3.42	-1.38
10	9.50	9.07	2.97	8.09	7.41	-2.59
15	14.50	14.06	7.93	13.20	12.42	-2.58
20	19.50	19.05	12.89	18.35	17.45	-2.55
25	24.50	24.04	17.85	NA	22.13	-2.87
30	29.50	29.03	22.81	NA	27.11	-2.89
35	34.50	34.03	29.02	33.97	32.88	-2.22
40	39.50	38.92	NA	38.79	39.07	-0.93
45	44.50	44.12	NA	43.62	44.08	-0.92
50	49.50	49.11	NA	48.44	49.31	-0.69

Table C19: CEM MEW of 2 minutes and four 30s estimations for a threshold of 3 cycles

AD	CEM 1	CEM 2	CEM 3	CEM 4	CEM Average	EE
0	0.50	0.96	7.46	2.32	2.83	2.83
5	4.50	4.04	2.32	2.81	3.42	-1.58
10	9.50	9.07	2.97	8.09	7.41	-2.59
15	14.50	14.06	7.93	13.20	12.42	-2.58
20	19.50	19.05	12.89	18.35	17.45	-2.55
25	24.50	24.04	17.85	23.23	22.41	-2.59
30	29.50	29.04	22.81	28.28	27.41	-2.12
35	34.50	34.03	29.02	33.97	32.88	-2.36
40	39.50	38.92	33.34	38.79	37.64	-2.36
45	44.50	44.12	37.66	43.62	42.48	-2.52
50	49.50	49.11	NA	48.44	49.31	-0.69

Table C20: CEM MEW of 2 minutes and four 30s estimations for a threshold of 4 cycles

AD	CEM 1	CEM 2	CEM 3	CEM 4	CEM Average	EE
0	0.50	0.96	7.46	2.32	2.83	2.83
5	4.50	4.04	2.32	2.81	3.42	-1.58
10	9.50	9.07	2.97	8.09	7.41	-2.59
15	14.50	14.06	7.93	13.20	12.42	-2.58
20	19.50	19.05	12.89	18.35	17.45	-2.55
25	24.50	24.04	17.85	23.23	22.41	-2.59
30	29.50	29.04	22.81	28.28	27.41	-2.12
35	34.50	34.03	29.02	33.97	32.88	-2.36
40	39.50	38.92	33.34	38.79	37.64	-2.36
45	44.50	44.12	37.66	43.62	42.48	-2.52
50	49.50	49.11	41.98	48.44	47.26	-2.74

Table C21: CEM MEW of 1 minute and six 10s estimations for a threshold of 2 cycles

AD	CEM 1	CEM 2	CEM 3	CEM 4	CEM 5	CEM 6	CEM Average	EE
0	0.50	NA	NA	1.07	0.66	4.54	1.69	1.69
5	4.50	NA	NA	4.08	5.46	0.46	3.63	-1.37
10	9.50	NA	NA	9.25	10.15	5.10	8.50	-1.50
15	14.50	NA	NA	NA	15.26	9.85	13.20	-1.80
20	19.50	2.52	NA	NA	20.06	15.18	14.32	-5.68
25	24.50	NA	NA	NA	24.34	20.52	23.12	-1.88
30	29.50	NA	NA	NA	29.63	25.85	28.33	-1.67
35	34.50	NA	NA	34.52	34.55	NA	34.52	-0.48
40	39.50	NA	NA	N	40.08	NA	39.79	-0.21
45	44.50	NA	NA	44.08	NA	NA	44.29	-0.71
50	49.50	NA	NA	48.90	NA	NA	49.20	-0.80

Table C22: CEM MEW of 1 minute and six 10s estimations for a threshold of 3 cycles

AD	CEM 1	CEM 2	CEM 3	CEM 4	CEM 5	CEM 6	CEM Average	EE
0	0.50	NA	2.40	1.07	0.66	4.54	1.83	1.83
5	4.50	NA	NA	4.08	5.46	0.46	3.63	-1.64
10	9.50	NA	NA	9.25	10.15	5.10	8.50	-1.50
15	14.50	7.17	NA	14.27	15.26	9.85	12.21	-2.79
20	19.50	2.52	NA	19.30	20.06	15.18	15.31	-4.69
25	24.50	2.12	NA	24.52	24.34	20.52	19.20	-5.80
30	29.50	NA	NA	29.32	29.63	25.85	28.58	-1.42
35	34.50	NA	NA	34.52	34.55	29.87	33.36	-1.64
40	39.50	NA	NA	38.92	40.08	35.82	38.58	-1.42
45	44.50	NA	NA	44.08	NA	41.78	43.45	-1.55
50	49.50	NA	NA	48.90	NA	47.73	48.71	-1.29

Table C23: CEM MEW of 1 minute and six 10s estimations for a threshold of 4 cycles

AD	CEM 1	CEM 2	CEM 3	CEM 4	CEM 5	CEM 6	CEM Average	EE
0	0.50	NA	2.40	1.07	0.66	4.54	1.83	1.83
5	4.50	NA	NA	4.08	5.46	0.46	3.63	-1.37
10	9.50	NA	NA	9.25	10.15	5.10	8.50	-1.50
15	14.50	7.17	NA	14.27	15.26	9.85	12.21	-2.79
20	19.50	2.52	NA	19.30	20.06	15.18	15.31	-4.69
25	24.50	2.12	NA	24.52	24.34	20.52	19.20	-5.80
30	29.50	NA	NA	29.32	29.63	25.85	28.58	-1.42
35	34.50	NA	NA	34.52	34.55	29.87	33.36	-1.64
40	39.50	NA	NA	38.92	40.08	35.82	38.58	-1.42
45	44.50	NA	NA	44.08	45.11	41.78	43.87	-1.13
50	49.50	NA	NA	48.90	NA	47.73	48.71	-1.29

Table C24: CEM MEW of 1 minute and six 10s estimations for a threshold of 5 cycles

AD	CEM 1	CEM 2	CEM 3	CEM 4	CEM 5	CEM 6	CEM Average	EE
0	0.50	NA	2.40	1.07	0.66	4.54	1.83	1.83
5	4.50	NA	6.79	4.08	5.46	0.46	4.26	-0.74
10	9.50	11.81	NA	9.25	10.15	5.10	9.16	-0.84
15	14.50	7.17	NA	14.27	15.26	9.85	12.21	-2.79
20	19.50	2.52	NA	19.30	20.06	15.18	15.31	-4.69
25	24.50	2.12	NA	24.52	24.34	20.52	19.20	-5.80
30	29.50	NA	NA	29.32	29.63	25.85	28.58	-1.42
35	34.50	NA	NA	34.52	34.55	29.87	33.36	-1.64
40	39.50	NA	NA	38.92	40.08	35.82	38.58	-1.42
45	44.50	NA	NA	44.08	45.11	41.78	43.87	-1.13
50	49.50	NA	NA	48.90	50.13	47.73	49.07	-0.93

C.1.3 The third set of frequencies, F_{l_3} *and* F_{r_3}:

Table C25: CEM MEW of 3 minutes and three 60s estimations for a threshold of 0.5 cycle

AD	CEM 1	CEM 2	CEM 3	CEM Average	EE
0	NA	NA	NA	NA	NA
5	NA	NA	2.67	2.67	-2.33
10	NA	NA	NA	NA	NA
15	NA	NA	NA	NA	NA
20	NA	NA	NA	NA	NA
25	NA	NA	NA	NA	NA
30	NA	NA	NA	NA	NA
35	NA	NA	NA	NA	NA
40	NA	NA	NA	NA	NA
45	NA	NA	NA	NA	NA
50	NA	NA	NA	NA	NA

Table C26: CEM MEW of 3 minutes and three 60s estimations for a threshold of 1cycle

AD	CEM 1	CEM 2	CEM 3	CEM Average	EE
0	0.50	NA	NA	0.50	0.50
5	NA	NA	2.67	2.67	-2.33
10	NA	NA	NA	NA	NA
15	NA	NA	NA	NA	NA
20	NA	NA	NA	NA	NA
25	NA	NA	NA	NA	NA
30	NA	NA	NA	NA	NA
35	NA	NA	NA	NA	NA
40	NA	NA	NA	NA	NA
45	NA	NA	NA	NA	NA
50	NA	NA	NA	NA	NA

Table C27: CEM MEW of 3 minutes and three 60s estimations for a threshold of 1.5 cycles

AD	CEM 1	CEM 2	CEM 3	CEM Average	EE
0	0.50	NA	7.96	4.23	4.23
5	4.50	NA	2.67	3.59	-1.41
10	9.50	NA	NA	9.50	-0.50
15	14.50	NA	NA	14.50	-0.50
20	19.50	NA	NA	19.50	-0.50
25	24.50	NA	NA	24.50	-0.50
30	29.50	NA	NA	29.50	-0.50
35	34.50	NA	NA	34.50	-0.50
40	39.50	NA	NA	39.50	-0.50
45	44.50	NA	NA	44.50	-0.50
50	49.50	NA	NA	49.50	-0.50

Table C28: CEM MEW of 3 minutes and three 60s estimations for a threshold of 2 cycles

AD	CEM 1	CEM 2	CEM 3	CEM Average	EE
0	0.50	NA	7.96	2.52	2.52
5	4.50	NA	2.67	4.25	-0.75
10	9.50	NA	NA	9.77	-0.23
15	14.50	NA	NA	14.74	-0.26
20	19.50	NA	NA	19.63	-0.37
25	24.50	NA	NA	24.70	-0.30
30	29.50	NA	NA	29.78	-0.22
35	34.50	NA	NA	34.86	-0.14
40	39.50	NA	NA	39.94	-0.06
45	44.50	NA	NA	45.02	0.02
50	49.50	NA	NA	50.10	0.10

Table C29: CEM MEW of 2 minutes and four 30s estimations for a threshold of 1 cycle

AD	CEM 1	CEM 2	CEM 3	CEM 4	CEM Average	EE
0	0.50	6.35	NA	6.03	4.29	4.29
5	4.50	NA	NA	11.25	7.88	2.88
10	9.50	NA	0.92	NA	5.21	-4.79
15	14.50	NA	NA	NA	14.50	-0.50
20	19.50	NA	NA	NA	19.50	-0.50
25	24.50	NA	NA	NA	24.50	-0.50
30	29.50	NA	NA	NA	29.50	-0.50
35	34.50	NA	NA	NA	34.50	-0.50
40	39.50	NA	NA	45.85	42.68	2.68
45	44.50	NA	NA	NA	45.06	0.06
50	49.50	NA	NA	NA	49.50	-0.50

Table C30: CEM MEW of 2 minutes and four 30s estimations for a threshold of 2 cycles

AD	CEM 1	CEM 2	CEM 3	CEM 4	CEM Average	EE
0	0.50	6.35	NA	6.03	4.29	4.29
5	4.50	NA	NA	11.25	7.88	2.88
10	9.50	14.69	0.92	16.26	10.63	0.63
15	14.50	NA	5.13	21.48	13.70	-1.30
20	19.50	NA	NA	NA	19.50	-0.50
25	24.50	28.02	NA	NA	26.26	1.26
30	29.50	NA	NA	NA	29.50	-0.50
35	34.50	NA	NA	NA	34.50	-0.50
40	39.50	NA	NA	45.85	42.68	2.68
45	44.50	NA	NA	NA	44.50	-0.50
50	49.50	NA	NA	58.90	54.20	4.20

Table C31: CEM MEW of 2 minutes and four 30s estimations for a threshold of 3 cycles

AD	CEM 1	CEM 2	CEM 3	CEM 4	CEM Average	EE
0	0.50	6.35	NA	6.03	4.29	4.29
5	4.50	10.74	NA	11.25	8.83	3.83
10	9.50	14.70	0.92	16.26	10.35	0.35
15	14.50	NA	5.13	21.48	13.70	-1.30
20	19.50	NA	NA	26.70	23.10	3.10
25	24.50	28.02	NA	NA	26.26	1.26
30	29.50	33.58	NA	NA	31.54	1.54
35	34.50	39.14	NA	NA	36.82	1.82
40	39.50	NA	NA	45.85	42.68	2.68
45	44.50	NA	NA	NA	44.50	-0.50
50	49.50	NA	NA	58.90	54.20	4.20

Table C32: CEM MEW of 2 minutes and four 30s estimations for a threshold of 4 cycles

AD	CEM 1	CEM 2	CEM 3	CEM 4	CEM Average	EE
0	0.50	6.35	NA	6.03	4.29	4.29
5	4.50	10.74	6.25	11.25	8.19	3.19
10	9.50	14.70	0.92	16.26	10.35	0.35
15	14.50	NA	5.13	21.48	13.70	-1.30
20	19.50	24.02	10.00	26.70	20.06	0.06
25	24.50	28.02	13.96	31.92	24.60	-0.40
30	29.50	33.58	NA	37.13	33.40	1.45
35	34.50	39.14	NA	NA	36.82	1.82
40	39.50	44.54	29.98	45.85	39.97	-0.03
45	44.50	NA	NA	NA	44.50	-0.50
50	49.50	NA	NA	58.90	54.20	4.20

Table C33: CEM MEW of 1 minutes and four 10s estimations for a threshold of 3 cycles

AD	CEM 1	CEM 2	CEM 3	CEM 4	CEM 5	CEM 6	CEM Average	EE
0	0.50	1.83	6.13	2.42	6.30	1.59	3.13	3.13
5	4.50	3.15	NA	6.68	11.41	6.83	6.51	1.51
10	9.50	8.12	NA	10.93	16.72	12.56	11.57	1.57
15	14.50	12.93	NA	15.19	NA	16.50	14.78	-0.22
20	19.50	17.91	19.54	18.86	NA	21.74	19.51	-0.49
25	24.50	22.88	26.16	23.90	NA	28.21	25.13	0.13
30	29.50	27.86	32.78	28.94	NA	32.41	30.30	0.30
35	34.50	32.83	39.40	NA	NA	36.60	35.83	0.83
40	39.50	37.81	45.36	NA	NA	NA	40.89	0.89
45	44.50	42.78	51.99	44.87	50.82	NA	46.99	1.99
50	49.50	47.76	58.61	50.11	NA	NA	51.50	1.50

Table C34: CEM MEW of 1 minutes and four 10s estimations for a threshold of 4 cycles

AD	CEM 1	CEM 2	CEM 3	CEM 4	CEM 5	CEM 6	CEM Average	EE
0	0.50	1.83	6.13	2.42	6.30	1.59	3.13	3.13
5	4.50	3.15	10.28	6.68	11.41	6.83	7.14	2.14
10	9.50	8.12	NA	10.93	16.72	12.56	11.57	1.57
15	14.50	12.93	NA	15.19	22.24	16.50	16.27	1.27
20	19.50	17.91	19.54	18.86	27.35	21.74	20.82	0.82
25	24.50	22.88	26.16	23.90	NA	28.21	25.13	0.13
30	29.50	27.86	32.78	28.94	NA	32.41	30.30	0.30
35	34.50	32.83	39.40	NA	NA	36.60	35.83	0.83
40	39.50	37.81	45.36	NA	NA	NA	40.89	0.89
45	44.50	42.78	51.99	44.87	50.82	NA	46.99	1.99
50	49.50	47.76	58.61	50.11	56.43	NA	52.48	2.48

Table C35: CEM MEW of 1 minutes and four 10s estimations for a threshold of 5 cycles

AD	CEM 1	CEM 2	CEM 3	CEM 4	CEM 5	CEM 6	CEM Average	EE
0	0.50	1.83	6.13	2.42	6.30	1.59	3.13	3.13
5	4.50	3.15	10.28	6.68	11.41	6.83	7.14	2.14
10	9.50	8.12	NA	10.93	16.72	12.56	11.57	1.57
15	14.50	12.93	NA	15.19	22.24	16.50	16.27	1.27
20	19.50	17.91	19.54	18.86	27.35	21.74	20.82	0.82
25	24.50	22.88	26.16	23.90	32.46	28.21	26.35	1.35
30	29.50	27.86	32.78	28.94	NA	32.41	30.30	0.30
35	34.50	32.83	39.40	32.47	NA	36.60	35.16	0.16
40	39.50	37.81	45.36	NA	NA	39.27	40.49	0.49
45	44.50	42.78	51.99	44.87	50.82	44.50	46.58	1.58
50	49.50	47.76	58.61	50.11	56.43	NA	52.48	2.48

C.2 CEM method tested on 100 sets of frequencies

Table C36: CEM for Frequency Set of 1-10 with a threshold of 1.5 cycles

AD	CEM 1	CEM 2	CEM 3	CEM 4	CEM 5	CEM 6	CEM 7	CEM 8	CEM 9	CM 10
0	0.75	2.84	2.52	4.41	0.90	3.31	0.90	7.06	3.74	8.54
5	7.09	4.26	4.25	3.20	5.19	7.97	4.82	6.36	7.44	6.05
10	10.13	9.15	9.77	8.07	10.21	12.83	10.50	8.94	10.31	9.08
15	17.27	13.87	14.74	16.25	15.21	17.81	13.66	9.55	14.53	12.06
20	20.33	18.80	19.63	19.50	20.21	22.73	16.02	13.20	19.60	15.12
25	25.44	23.93	24.70	22.89	25.23	27.51	18.97	18.29	24.52	18.10
30	30.54	29.61	29.8	27.69	29.65	24.37	23.44	23.41	29.72	21.73
35	34.50	33.9	34.86	34.33	34.62	37.33	34.38	28.46	37.33	26.70
40	39.50	39.05	39.94	39.29	39.60	42.44	39.87	33.58	40.19	36.80
45	44.50	43.67	45.02	42.93	44.63	47.37	44.50	41.81	47.28	41.71
50	49.50	51.68	50.10	49.50	49.52	53.48	49.56	47.78	49.53	46.50

Table C37: CEM for Frequency Set of 11-20 with a threshold of 1.5 cycles

AD	CEM 11	CEM 12	CEM 13	CEM 14	CEM 15	CEM 16	CEM 17	CEM 18	CEM 19	CEM 20
0	1.41	6.56	1.57	1.82	1.16	0.69	1.43	1.33	2.75	3.00
5	6.02	11.21	4.64	3.93	4.41	7.02	5.58	6.06	3.95	4.41
10	11.17	16.04	9.64	8.73	9.30	9.45	10.57	10.55	8.37	8.41
15	16.26	18.59	11.37	13.68	14.32	14.45	15.61	15.67	13.32	13.40
20	21.28	22.13	14.26	18.92	18.75	19.62	20.49	20.67	18.20	18.48
25	26.53	27.03	19.37	23.61	23.77	24.61	25.46	25.66	23.19	25.03
30	31.35	29.50	26.04	28.57	29.33	29.57	30.93	30.63	27.98	29.91
35	35.04	34.50	30.65	33.62	33.69	34.64	35.48	35.56	33.04	34.51
40	40.57	42.33	33.56	38.63	38.73	39.69	39.38	41.56	37.88	39.09
45	46.18	49.04	40.77	43.78	44.49	50.77	44.32	46.48	49.16	44.54
50	51.10	54.26	45.80	50.71	49.38	49.16	49.26	51.27	54.60	48.91

Table C38: CEM for Frequency Set of 21-30 with a threshold of 1.5 cycles

AD	CEM 21	CEM 22	CEM 23	CEM 24	CEM 25	CEM 26	CEM 27	CEM 28	CEM 29	CEM 30
0	2.99	8.84	0.73	3.30	2.20	1.89	3.48	1.10	9.67	2.23
5	5.01	5.68	5.46	5.56	3.84	5.50	5.99	3.95	14.39	3.27
10	10.67	7.53	10.47	10.41	8.26	9.12	10.23	8.94	19.43	8.14
15	15.56	9.35	15.46	15.72	13.15	14.05	14.88	13.98	24.48	13.11
20	19.83	11.13	20.21	18.42	19.56	19.10	17.51	18.98	25.82	18.02
25	23.55	15.38	25.52	23.32	23.23	23.93	24.73	24.00	33.24	23.54
30	29.35	29.50	30.52	28.34	28.30	28.99	27.36	29.01	28.83	28.51
35	34.71	34.50	35.25	33.47	33.31	34.04	32.46	33.83	33.52	33.46
40	39.50	35.85	40.58	38.55	38.41	38.88	39.40	44.03	32.40	38.22
45	44.50	44.50	45.29	45.15	44.59	43.93	44.39	43.71	37.64	44.66
50	49.50	49.50	50.63	47.76	48.44	48.97	49.36	52.73	42.87	47.64

Table C39: CEM for Frequency Set of 31-40 with a threshold of 1.5 cycles

AD	CEM 31	CEM 32	CEM 33	CEM 34	CEM 35	CEM 36	CEM 37	CEM 38	CEM 39	CEM 40
0	5.27	0.95	4.12	2.32	0.87	3.75	1.98	1.62	4.50	2.07
5	3.09	4.35	7.63	3.28	4.31	4.88	6.76	4.35	4.61	4.67
10	7.77	9.36	12.72	8.73	9.01	8.16	11.68	9.35	8.10	9.61
15	10.80	14.44	18.01	13.76	30.43	12.20	16.87	14.38	13.12	13.13
20	15.47	19.37	22.75	18.80	18.96	20.04	21.90	19.40	18.18	17.84
25	17.92	24.34	27.80	23.62	23.95	25.23	26.77	24.40	23.19	22.63
30	24.39	29.38	32.76	28.56	28.93	30.16	31.82	28.74	28.26	27.65
35	29.63	34.13	37.95	34.50	36.91	35.67	36.85	34.59	33.29	34.50
40	35.43	39.09	42.27	39.50	39.07	41.28	41.12	39.52	40.22	39.50
45	40.78	44.20	47.60	44.50	38.77	43.06	46.14	42.99	45.34	44.50
50	49.63	49.22	52.93	49.50	48.83	49.50	53.12	48.22	48.64	48.13

Table C40: CEM for Frequency Set of 41-50 with a threshold of 1.5 cycles

AD	CEM 41	CEM 42	CEM 43	CEM 44	CEM 45	CEM 46	CEM 47	CEM 48	CEM 49	CEM 50
0	2.64	3.28	0.89	1.28	1.05	1.57	4.70	0.84	0.57	1.44
5	4.42	6.45	5.59	4.99	13.54	4.51	3.08	4.23	10.05	5.88
10	8.16	11.45	10.56	10.01	15.87	7.40	6.19	9.04	10.05	10.85
15	12.67	16.46	15.52	14.87	14.72	14.45	12.74	14.03	15.08	15.84
20	18.30	21.46	20.51	19.76	20.81	19.37	19.50	19.02	20.01	20.81
25	23.27	26.50	25.35	24.68	23.87	24.35	22.85	24.01	24.99	25.79
30	28.23	31.16	30.21	29.61	29.37	29.22	29.50	29.00	30.06	30.76
35	33.34	36.13	34.50	34.64	34.27	34.23	33.24	33.83	35.10	35.73
40	37.74	41.19	39.50	40.52	39.36	39.23	38.23	38.93	40.14	40.61
45	43.37	46.53	44.50	44.55	34.96	44.25	43.22	43.94	45.18	45.62
50	48.33	50.07	50.75	49.46	49.53	49.15	48.21	48.96	50.13	50.64

Table C41: CEM for Frequency Set of 51-60 with a threshold of 1.5 cycles

AD	CEM 51	CEM 52	CEM 53	CEM 54	CEM 55	CEM 56	CEM 57	CEM 58	CEM 59	CEM 60
0	2.15	0.94	5.24	2.87	2.39	2.04	4.84	2.48	1.94	4.21
5	6.36	4.37	6.39	5.01	11.77	3.79	6.50	3.12	3.59	7.66
10	9.45	9.55	8.87	9.24	10.23	8.77	7.57	6.62	8.35	12.52
15	14.03	14.53	11.35	12.64	12.79	15.04	12.13	15.48	13.35	17.38
20	18.98	15.42	14.53	17.77	21.97	18.69	16.66	17.05	18.18	18.02
25	23.97	19.44	19.38	22.72	19.73	23.88	24.28	22.05	23.22	15.45
30	29.02	24.24	24.15	27.68	21.57	28.77	29.21	27.24	28.18	32.00
35	33.91	34.68	28.95	27.72	26.56	35.20	34.21	34.50	34.41	33.04
40	42.05	39.51	39.04	32.45	42.12	41.86	39.36	39.50	38.02	37.99
45	47.05	44.57	44.06	42.48	36.98	46.59	46.53	44.01	43.01	42.95
50	49.36	49.68	49.07	47.53	52.26	50.87	51.55	46.76	47.87	52.25

Table C42: CEM for Frequency Set of 61-70 with a threshold of 1.5 cycles

AD	CEM 61	CEM 62	CEM 63	CEM 64	CEM 65	CEM 66	CEM 67	CEM 68	CEM 69	CEM 70
0	5.81	3.66	4.63	3.97	0.71	1.47	1.00	4.03	3.04	0.72
5	8.93	4.92	4.56	4.96	5.14	3.75	4.35	6.50	6.14	10.26
10	13.64	10.54	8.28	9.99	10.23	6.64	9.13	11.37	11.10	15.11
15	18.36	15.38	13.19	15.00	15.16	11.76	14.97	17.10	16.07	14.50
20	19.02	20.54	18.25	20.01	20.15	15.71	19.81	22.06	21.14	19.50
25	23.97	24.51	23.30	25.00	25.09	20.54	24.82	29.19	26.12	24.50
30	29.05	32.74	27.02	30.01	30.11	27.79	29.74	31.41	31.23	29.50
35	33.98	34.16	32.12	35.06	35.26	32.80	34.81	36.63	36.29	34.50
40	39.02	37.32	39.50	43.71	40.09	36.97	38.52	41.85	41.19	39.50
45	44.01	44.50	44.02	45.07	45.07	40.88	43.65	50.21	46.14	44.50
50	49.84	51.28	49.19	50.02	50.05	49.50	51.77	55.37	51.35	49.50

Table C43: CEM for Frequency Set of 71-80 with a threshold of 1.5 cycles

AD	CEM 71	CEM 72	CEM 73	CEM 74	CEM 75	CEM 76	CEM 77	CEM 78	CEM 79	CEM 80
0	3.11	2.29	1.66	2.88	3.06	3.08	2.39	1.60	3.69	2.57
5	7.39	6.98	3.31	4.34	5.49	3.95	6.06	3.53	6.15	6.09
10	12.32	11.92	8.28	7.45	10.40	8.62	10.71	8.50	10.94	11.68
15	17.13	16.93	13.22	12.35	15.50	13.64	15.00	13.35	15.89	16.56
20	22.19	21.61	24.57	17.36	20.47	18.67	19.92	18.33	22.41	21.71
25	27.36	26.70	24.52	22.36	25.37	24.87	23.44	23.33	27.26	26.86
30	32.28	31.13	29.36	27.44	31.01	27.76	31.52	28.35	29.33	31.21
35	37.59	36.24	39.44	32.48	37.93	35.92	34.90	33.94	33.39	36.59
40	39.44	40.65	40.00	39.14	44.20	40.92	41.46	38.39	38.48	41.59
45	47.02	45.91	44.06	44.12	48.14	45.92	44.50	43.53	46.43	46.61
50	52.57	50.70	49.17	50.04	53.15	51.00	50.37	48.55	47.91	51.63

Table C44: CEM for Frequency Set of 81-90 with a threshold of 1.5 cycles

AD	CEM 81	CEM 82	CEM 83	CEM 84	CEM 85	CEM 86	CEM 87	CEM 88	CEM 89	CEM 90
0	4.95	1.51	4.95	2.46	2.08	5.40	4.43	1.94	4.57	3.16
5	4.92	4.52	6.54	4.20	5.76	9.26	4.24	8.27	9.49	7.28
10	6.01	8.74	9.54	9.06	8.78	14.27	8.11	7.84	14.09	12.27
15	12.53	13.58	12.57	13.97	11.93	19.30	14.46	12.20	18.90	18.24
20	17.43	18.28	16.67	18.72	15.90	24.21	19.50	17.84	15.96	23.14
25	22.56	23.20	21.69	23.73	20.86	29.40	24.59	22.83	22.92	27.99
30	27.89	27.93	30.07	28.73	25.85	34.46	29.62	27.48	31.24	32.44
35	32.44	32.96	36.09	33.70	29.49	33.51	34.51	32.57	34.50	38.21
40	37.39	37.83	40.32	40.02	39.48	44.11	37.50	37.67	39.50	43.18
45	43.04	43.65	45.42	44.98	45.78	43.48	44.82	42.76	29.19	47.60
50	47.93	48.86	50.61	49.50	49.50	48.46	47.24	47.85	32.40	53.79

Table C45: CEM for Frequency Set of 91-100 with a threshold of 1.5 cycles

AD	CEM 91	CEM 92	CEM 93	CEM 94	CEM 95	CEM 96	CEM 97	CEM 98	CEM 99	CEM 100
0	0.79	3.25	1.78	3.39	0.74	6.31	4.15	1.28	2.45	2.57
5	4.39	6.02	4.87	6.11	5.24	4.86	9.16	3.93	3.99	3.98
10	9.40	7.60	9.90	10.40	10.17	7.71	10.76	8.89	8.20	10.93
15	14.10	15.90	14.95	15.26	15.16	12.71	18.61	13.89	9.82	16.04
20	18.40	20.79	20.03	20.51	20.14	20.92	23.57	19.27	19.39	19.50
25	20.79	25.78	24.95	25.49	25.12	22.70	28.73	23.90	24.39	24.50
30	29.28	30.66	29.85	30.33	33.33	31.27	33.67	28.85	29.60	31.71
35	27.75	35.87	34.87	35.22	37.99	36.37	38.61	33.76	34.55	42.80
40	29.79	40.87	40.04	39.96	43.17	37.62	43.43	38.72	39.43	47.78
45	34.96	45.86	45.01	44.77	47.28	39.75	45.05	44.39	44.44	53.80
50	39.61	46.33	50.09	50.11	50.33	47.01	49.93	51.29	49.51	57.46